T.R.
ONDOKUZ MAYIS UNIVERSITY
INSTITUTE OF GRADUATE STUDIES
DEPARTMANT OFENVIRONMENTAL ENGINEERING

USE OF AMINE-MODIFIED CROSS-LINKED POLYMERS FOR CO_2 ADSORPTION

Master's Thesis

Huda Fahad Muttaır AL-BEHADILI

Supervisor

Prof. Dr. Bahtiyar ÖZTÜRK

This thesis was supported by Ondokuz Mayıs University Scientific Research Support Unit (BAPSİS) within the framework of the project titled "Development of Amine Modified Adsorbent for CO_2 Recovery" with code PYO.MUH.1908.22.061.

SAMSUN
2023

ACCEPTANCE AND APPROVAL OF THE THESIS

The study entitled **" USE OF AMINE-MODIFIED CROSS-LINKED POLYMERS FOR CO_2 ADSORPTION "** prepared by **Huda Fahad Muttaır AL-BEHADILI**, and supervised by **Prof. Dr. Bahtiyar ÖZTÜRK**, was found successful and unanimouslyaccepted by committee members asMasterthesis, following the examination on the date 4.1.2024.

	Title Name SURNAME University Department/Art	Final Decision
Chairman	Prof. Dr.Çetin ÇAKANYILDIRIM Hitit University Department of Chemical Engineering	☒ Accept ☐ Reject
Member	Prof. Dr. Bahtiyar ÖZTÜRK Ondokuz Mayıs University Department of Environment Engineering	☒ Accept ☐ Reject
Member	Assist. Prof. Dr. Hülya AYKAÇ Ondokuz Mayıs University Department of Environment Engineering	☒ Accept ☐ Reject

This thesis has been approved by the committee members that already stated above and determined by the Institute Executive Board.

.

Prof. Dr. Ahmet TABAK
Head of Institute of Graduate Studies

DECLARATION OF COMPLIANCE WITH SCIENTIFIC ETHIC

I hereby declare and undertake that I complied with scientific ethics and academic rules in all stages of my Master's Thesis, that I have referred to each quotation that I use directly or indirectly in the study and that the works I have used consist of those shown in the sources, that it was written in accordance with the institute writing guide and that the situations stated in the article 3, section 9 of the Regulation for TÜBİTAK Research and Publication Ethics Board were not violated.

Is Ethics Committee Necessary?

Yes ☐ (If it necessary, please add appendices.)

No ☒

08 /01/ 2024
Huda Fahad Muttaır AL-BEHADILI

DECLARATION OF THE THESIS STUDY ORIGINALITY REPORT

Thesis Title :USE OF AMINE-MODIFIED CROSS-LINKED POLYMERS FOR CO_2 ADSORPTION

As a result of the originality report taken by me from the plagiarism detection program on 5 /12 /2023 for the thesis titled above;

Similarity ratio : % 19

Single resource rate : % 1 has been released.

08 /01/ 2024
Prof. Dr. Bahtiyar ÖZTÜRK

ÖZET

CO_2 ADSORPSİYONU İÇİN AMİNLE MODİFİYE EDİLMİŞ ÇAPRAZ BAĞLI POLİMERLERİN KULLANILMASI

Huda Fahad Muttaır AL-BEHADILI
Ondokuz Mayıs Üniversitesi
Lisansüstü Eğitim Enstitüsü
Çevre Mühendisliği Ana Bilim Dalı
Yüksek Lisans, Ocak/2024
Danışman: Prof. Dr. Bahtiyar ÖZTÜRK

Bu tez çalışması bir gaz karışımından CO_2 yi gidermek için amin ile modifiye edilmiş hidrojellerin kullanılabilirliğnin incelenmesini kapsamaktadır. Bu kapsamda kimyasal yapılarında C=O-C, C=NH-C ve SO_3H olan beş ayrı hidrojel sentezlenmiş ve bu hidrojellerin CO_2 tutma kapasitelerini artırmak için yapılarına monoethanol amin (MEA) ve dietilentriamin (DETA) emdirilerek modifiye edilmişlerdir. Elde edilen sonuçlardan DETA ile modifiye edilmiş hidrojellerin MEA ile modifiye edilmiş olanlara göre daha fazla CO_2 tutuğu, yapısında –NH grubu bulunan (C=NH-C) hidrojellerin CO_2 tutmada daha iyi performans gösterdiği anlaşılmıştır. CO_2'nin hidrojellere adsorplanması Langmuir izotermine uymuştur. Bu durum CO_2 nin hidrojel yapısına tek tabaka oluşturacak şekilde tutunduğunu göstermektedir. Ancak, amin ile CO_2nin kimyasal reaksiyon verdiği göz önüne alındığında bu adsorpsiyon prosesinde adsorbent üzerinde bir adsorbate tabakası oluştuğundan söz etmenin uygun olmayacağıdır. Elde edilen sonjuçlardan en fazla CO_2 tutma işlemini DETA ile modifiye edilmiş P(AMPSA) nın gösterdiği (113.64 mg CO_2/g-adsorbent) ve genel olarak DETA ile modifiye edilmiş hidrojelere CO_2 adsorpsiyonunda elde edilen düşük Lanmuir katsayısının (K_L) bu hidrojelleerin daha düşük bir enerji harcayarak rejenere edilebileceğini göstermektedir.

Anahtar Sözcükler: CO_2 adsorpsiyonu, hidrojel, MEA, DETA

ABSTRACT

USE OF AMINE-MODIFIED CROSS-LINKED POLYMERS FOR CO_2 ADSORPTION

Huda Fahad Muttaır AL-BEHADILI
Ondokuz Mayıs University
Institute of Graduate Studies
Department ofEnvironmental Engineering
Master,January/2024
Supervisor Prof. Dr. Bahtiyar ÖZTÜRK

This thesis involves examining the usability of amine-modified hydrogels to remove CO_2 from a gas mixture. In this context, five different hydrogels with C=O-C, C=NH-C and SO_3H in their chemical structures were synthesized and they were modified by impregnating monoethanol amine (MEA) and diethylenetriamine (DETA) to increase the CO_2 capture capacity of these hydrogels. From the results obtained, it was understood that hydrogels modified with DETA captured more CO_2 than those modified with MEA, and hydrogels with –NH groups in their structure (C=NH-C) showed better performance in capturing CO_2. The adsorption of CO2 to the hydrogels obeyed the Langmuir isotherm. This shows that CO_2 adheres to the hydrogel structure to form a single layer. However, considering the chemical reaction between amine and CO_2, it would not be appropriate to say that an adsorbate layer is formed on the adsorbent in this adsorption process. Among the results obtained, DETA-modified P(AMPSA) showed the highest CO_2 capture (113.64 mg CO_2/g-adsorbent) and in general, the low Langmuir coefficient (K_L) obtained in CO_2adsorption to DETA-modified hydrogels indicates that these hydrogels have a lower regeneration energy consumption..

Keywords: CO_2 adsorpsiyonu, hidrojel, MEA, DETA

ACKNOWLEDGEMENT

I would like to thank all the people who contributed to this journey with their encouragement and support. Firstly, I am very grateful to my supervisor (Prof. Dr. Bahtiyar ÖZTÜRK),for his continuous guidance, support, and encouragement throughout the process of this thesis and provided me the opportunity to work under her supervision. I learned a lot from your inspiring ideas, broad knowledge, and attitudes towards scientific research. Without your help and guidance, this message will not be finished in time.I would like to express my sincere gratitude to Assistant Professor Dr. Kutalmış GÖKKUŞ who synthesized the adsorbents. I would like to express my sincere gratitude to Prof.Dr. Emre Burcu ÖZKARAOVA, Prof. Dr. Feryal AKBAL and Prof. Dr. Gülfem BAKAN for their guidance, thank you very much for spending your valuable time in my learning.I would also like to express my gratitude to Assistant Professor Dr. Hülya AYKAÇ ÖZEN for teaching and helping me while starting my studies here. I would also like to thank my colleagues and friends that I met during my studies and residency. Thank you for all the happy moments and good situations.

I would like to express my great gratitude to my family. I would not have achieved anything without the moral and material support and constant encouragement, especially my mother, who supported me at every step. Thank you, mom. Without you, I wouldn't be here today.

Huda Fahad Muttaır AL-BEHADILI

CONTENTS

ACCEPTANCE AND APPROVAL OF THE THESIS i
DECLARATION OF COMPLIANCE WITH SCIENTIFIC ETHIC ii
DECLARATION OF THE THESIS STUDY ORIGINALITY REPORT ii
ÖZET iii
ABSTRACT iv
ACKNOWLEDGEMENT v
CONTENTS vi
SYMBOLS AND ABBREVIATIONS vii
FIGURES LEGENDS viii
TABLES LEGENDS ix
1. INTRODUCTION 1
2. LITERATURE SURVEY 4
2.1 Global Warming 4
2.2 Greenhouse Gases (GHGs) and Their Main Sources 5
2.2.1 Carbon dioxide (CO_2) 5
2.2.2 Methane (CH_4) 8
2.2.3 Nitrous oxide (N_2O) 10
2.2.4 Water vapor 11
2.2.5 Chlorofluorocarbons (CFCs) 12
2.3 Impact of Global Warming 12
2.4 International Progress for Reduction and Control of Global Warming 15
2.5 CO_2 Capture Processes 23
2.5.1 Pre-combustion Processes 25
2.5.2 Oxy-fuel Combustion Processes 26
2.5.3 Post-combustion processes 27
2.6 Adsorbents for CO_2 Capture 40
2.6.1 Activated carbon 41
2.6.2 Zeolites 43
2.6.3 Metal–organic frameworks 45
2.6.4 Modified Adsorbents 46
2.7 Adsorption Isotherms 53
3. MATERIALS AND METHODS 56
3.1 Chemicals Used 56
3.2 Synthesis of Poly (2-hydroxyethyl methacrylate) Hydrogel, P(HEMA) 58
3.3 Synthesis of Poly (N-hidroksietilmetakrilat) Hydrogel, P(N-HEA) 59
3.4 Synthesis of Poly (2-acrylamido-2-methylpropane sulfonic acid) Hydrogel, P(AMPSA) 60
3.5 Synthesis of Poly (3-Sulfopropyl methacrylate potassium salt) Hydrogel, P(3-SPMP) 61
3.6 Synthesis of Poly (Acrylic acid) Hydrogel, P(AAc) 62
3.7 Modification of Hydrogels Using Amines 63
3.8 Characterization of Amin-Modified Hydrogels 64
3.8.1 SEM Imaging 64
3.8.2 TGA Analysis 64
3.8.3 FTIR Analysis 65
3.9 Gas Adsorption 66
4. RESULTS AND DISCUSSION 71
4.1 Characterization of Adsorbents 71
4.1.1 Scanning Electron Microscopy (SEM) Analysis 71
4.1.2 Thermogravimetric Analysis (TGA) 74
4.1.3 Fourier Transform Infrared Spectroscopy 75

4.2 CO_2 Adsorption on Hydrogels 80
4.2.1 CO2 Adsorption on P(HEMA) 80
5. CONCLUSION 91
REFERENCES.. 92
CIRCULUM VITEA 115

SYMBOLS ANDABBREVIATIONS

Aac	: Acrylic Acid
Acnfs	: Activated Carbon Fibers
ACs	: Activated Carbons
ADS-17	: Macroporous Resin
Ags	: Aerogels
AMPSA	: 2-Acrylamido-2-Methylpropane Sulfonic Acid
AP	: Amino-Propyl
APS	: Ammonium Peroxodisulfate
APTES	: 3-Aminopropyltrimethoxysilane
ASU	: Air Separation Unit
CCS	: Carbon Capture and Storage
Cfcs	: Chlorofluorocarbons
CH_4	: Methane
Cnfs	: Carbon Nanofibers
Cnts	: Carbon Nanotubes
CO_2	: Carbon Dioxide
D101	: Macroporous Resin
DEA	: Diethanolamine
DETA	: Diethylenetriamine
DIPA	: Diisopropanol Amine
DMA	: Dimethylamine,
DT	: Diethylene-Triamine
ED	: Ethylene-Diamine
EDA	: Ethylenediamine
EIA	: The Energy Information Administration
EOA	: Ethanolamine
E-Snts	: Ethane-Silica Nanotubes
FTIR	: Fourier Transform Infrared Spectroscopy
GO	: Graphite Oxide
Gofs	: Graphene Organic Frameworks
GSC	: Gas Sorption Cell
GWP	: A Global Warming Potential
H_2O	: Water Vapor
HEMA	: 2-Hydroxyethyl Methacrylate

HP-20	: Highly Porous Resin
HPPN	: Hierarchial Porous Polymer Networks
Htcs	: Hydrotalcides
IEA	: The International Energy Agency
IGCC	: Integrated Gasification Combined Cycle Power Plants
IPCC	: The Intergovernmental Panel On Climate Change
IR	: Infra-Red
KP-CP2	: Kyoto Protocol
MBA	: N.N’-Methylenebisacrylamide
MDEA	: Methyldiethanolamine
MEA	: Monoethanolamine
MF	: Melamine-Formaldehyde
MF/PAM	: Melamine/Polyacrylamide
Mg/DOBDC	: Magnesium Dioxybenzenedicarboxylate
Mofs	: Metal Organic Frameworks
MPEG	: Methoxypolyethylene Glycol
Mwcnts	: Multi-Walled Carbon Nanotubes
N_2O	: Nitrous Oxide
Nm	: Nanometers
N-NEHA	: N-Hydroxyethyl Acrylamide
O_3	: Ozone
Ocs	: Organic Compounds
Ops	: Organic Polymers
P(3-SPMP)	: Poly (3-Sulfopropyl Methacrylate Potassium Salt) Hydrogel
P(Aac)	: Poly (Acrylic Acid) Hydrogel
P(AMPSA)	: Poly (2-Acrylamido-2-Methylpropane Sulfonic Acid) Hydrogel
P(HEMA)	: Poly (2-Hydroxyethyl Methacrylate) Hydrogel
P(N-HEA)	: Poly (2-Acrylamido-2-Methylpropane Sulfonic Acid) Hydrogel
PAN	: Polyacrylonitrile
PANI	: Polyaniline
PEHA	: Pentaethylenehegzaamine
PEI	: Polyethyleneimine
PEPA	: Polyethylene Polyamine
Ponfs	: Polyolefin Nanofiber
Ptnts	: Protonated Titanate Nanotubes

QELROS	: Quantified Emissions Limitation And Reduction Obligations
SEM	: Scanning Electron Microscope
Snts	: Silca Nanotubes
SPMP	: 3-Sulfopropylmethacrylate Potassium Salt
TEA	: Triethanolamine
TEMED	: Tetramethylethylene Diamine
TEPA	: Tetraethylene-Pentamine,
TGA	: Thermogravimetric Analysis
UNFCCC	: The United Nations Framework Convention On Climate Change
X-5	: Macroporous Resin
XAD-4	: Polystyrene

FIGURES LEGENDS

Figure 2.1 Showing radiation absorption and emission by greenhouse gases. 5
Figure 2.2 Sources of the main CO_2 emissions are broken down. 6
Figure 2.3 Main sources of CO_2 Emission 6
Figure 2.4 Atmospheric CO_2 concentration and fossil fuel consumption. 7
Figure 2.5 Atmospheric CH_4 concentration. 9
Figure 2.6 Methane emissions in last 40 years. 9
Figure 2.7 Main sources of NO_2 emissions of nitrogen oxides 11
Figure 2.8 Sea-level rise from 1870 to 2001. 13
Figure 2.9 Show the effect of global warming all over the world as sources 14
Figure 2.10 Main combustion CO_2 capture technologies. 25
Figure 2.11 Process diagrams for membrane carbon capture. 32
Figure 2.12 A typical CO_2 absorption-stripping process. 34
Figure 2.13 Process diagrams for the cryogenic carbon capture. 35
Figure 2.14 Schmatic representation of physical and chemical adsorption of a CO_2 molecule by an adsorbent. 39
Figure 2.15 Precursors for producing porous carbon used to capture CO_2. 42
Figure 2.16 The structure of box-like zeolite. 44
Figure 2.17 Schematic illustration of basic components of a MOF and their arrangement in the lattice system. 45
Figure 2.18 Graphical representation of IUPAC classification of adsorption types .. 55
Figure 3.1 Representation of Hydrogel preparation. 56
Figure 3.2 Schematic representation of the synthesis of PHEMA hydrogel. 59
Figure 3.3 Schematic representation of the synthesis of P (N-HEA) hydrogel. 60
Figure 3.4 Schematic representation of the synthesis of P(AMPSA) hydrogel. 61
Figure 3.5 Schematic representation of the synthesis of P(3-SPMP) hydrogel. 62
Figure 3.6 Schematic representation of the synthesis of P(AAc) hydrogel. 63
Figure 3.7 SEM device. 64
Figure 3.8 TGA device 65
Figure 3.9 FTIR device. 66
Figure 3.10 Schmatic drawing of gas adsorption cell (GSC). 67
Figure 3.11 GSC used for gas adsorption. 68
Figure 3.12 Microbalance. 68
Figure 3.13 Vacuum pump. 69
Figure 3.14 Pressure calibration for GSC. 70

Figure 4.1 SEM pictures of P(HEMA) ... 72
Figure 4.2 SEM pictures of P(N-HEA). ... 72
Figure 4.3 SEM pictures of P(AAc) ... 73
Figure 4.4 SEM pictures of P(3-SPMP). ... 73
Figure 4.5 SEM pictures of P(AMPSA). ... 73
Figure 4.6 TGA curves of hydrogels impregnated with MEA and DETA. ... 75
Figure 4.7 FTIR spectrum of P(HEMA) loaded with DETA. ... 76
Figure 4.8 FTIR spectrum of P(NHEA) loaded with DETA. ... 77
Figure 4.9 FTIR spectrum of P(AAc) loaded with DETA. ... 77
Figure 4.10 FTIR spectrum of P(3-SPMP) loaded with MEA. ... 78
Figure 4.11 FTIR spectrum of P(AMPSA) loaded with MEA. ... 79
Figure 4.12 FTIR spectrum of P(AMPSA) loaded with DETA. ... 79
Figure 4.13 Adsorption isotherms for CO_2 adsorption onto P(HEMA) impregnated with MEA and DETA. ... 81
Figure 4.14 Langmuir plot of CO_2 adsorption on MEA and DETA impregnated P(HEMA). ... 82
Figure 4.15 Adsorption isotherms for CO_2 adsorption onto P(NHEA) impregnated with MEA and DETA. ... 84
Figure 4.16 Langmuir plot of CO_2 adsorption on MEA and DETA impregnated P(NHEA). ... 85
Figure 4.17 Adsorption isotherms for CO_2 adsorption onto P(AAc) ... 86
Figure 4.18 Langmuir plot of CO_2 adsorption on MEA and DETA impregnated P(AAc). ... 86
Figure 4.19 Adsorption isotherms for CO_2 adsorption onto P(3-SPMP) ... 87
Figure 4.20 Langmuir plot of CO_2 adsorption on MEA and DETA impregnated ... 88
Figure 4.21 Adsorption isotherms for CO_2 adsorption onto P(AMPSA) ... 88
Figure 4.22 Langmuir plot of CO_2 adsorption on MEA and DETA impregnated P(AMPSA). ... 89

TABLES LEGENDS

Table 2.1 International Conference 16
Table 2.2 Comparison of CO_2 capture systems 28
Table 2.3 Modified adsorbents for CO_2 capture. 47
Table 2.4 Types of chemicals used for adsorbent modification................................ 52
Table 4.1 Langmuir constants for adsorption of amine impregnated hydrogels........ 90

1. INTRODUCTION

Global warming is the rise in the average temperature of the Earth's roof since the middle of the 20th century. Because of the increase in the concentration of greenhouse gases (GHGs) such as water vapor, methane, ozone, carbon dioxide, chlorofluorocarbons (CFCs), and nitrous oxide (Al-Ghussain, 2019; Sulukan et al., 2023). Global warming can cause some negative effects, have a variety of effects on our quality of life. The issue of global warming caused by greenhouse gas emissions has attracted great attention as it is undoubtedly the most serious environmental and economic threat of our time (Kumar and Pooja, 2020; Xue et al., 2017). Carbon dioxide (CO_2) is one of the major greenhouse gases (GHG). CO_2 emissions come from a variety of sources, including anthropogenic CO_2 emissions caused by human activity and natural sources and causes such as wildfires (Gür, 2022). Industrial activities account for over 61% of worldwide CO_2 emissions (electricity and heat generation and other industries (Benhelal et al., 2013). The combustion of fossil fuels is the most significant source of anthropogenic CO_2 contributing to the rise in atmospheric concentrations since the industrial revolution (Koornneef et al., 2011). Carbon dioxide become a global issue in the last few decades because greenhouse effect (Ohashi et al., 2011). As a result of the greenhouse effect average temperature of the atmosphere increases parallel with the concentrations of atmospheric greenhouse gases. By 2100, the atmosphere could contain up to 570 ppmv of CO_2, resulting in a 1.9 °C rise in mean global temperature and a 3.8 m rise in mean sea level (Park et al., 2018). This increase in temperature causes some unexpected catastrophic phenomena such as sea level rise, ice melting, long forest fire, flooding......etc (Saravanan et al., 2021). Because of this negative effect of CO_2, is an emission reduction has become a more important researcher's subject.

Increasing rather than reducing the use of fossil fuels in industry and energy production processes causes CO_2 emissions to increase, thus necessitating their effective capture order to reduce CO_2 emissions. The United Nations Framework Convention on Climate Change (UNFCCC), Intergovernmental Panel on Climate Change (IPCC), Kyoto Protocol, and Paris Agreement all identify CO_2 capture as one of the promising technologies to fight global warming (Chai et al., 2022). It is anticipated that industrial CO_2 emissions would be reduced by 50% by 2050 thanks to carbon capture and storage (CCS), which is seen as a major technology to reduce emissions from energy and carbon-intensive industries (Wei et al., 2020), such as power plants and biorefineries (Xue et al., 2017; Middleton et al., 2020). Indicated that the carbon capture technology is the most effective future technology for reducing greenhouse gas emissions.

Three main methods are recommended to reduce the CO_2 emissions of industrial processes burning fossil fuels: pre-combustion control, oxy-combustion and post-combustion control. Pre-combustion carbon capture is the process of removing carbon dioxide from fossil fuels or biomass fuels before the combustion process is finished. Typically, it is used in natural gas power plants and the gasification of coal, natural gas, and biomass (Olabi et al., 2022). In pre-combustion capture, a fuel is heated with oxygen or air, and occasionally steam, to produce synthesis gas (syngas) also referred to as fuel gas (Songolzadeh et al., 2014). After CO_2 is captured from the synthesis gas containing H_2 and CO_2, H_2 is sent to the combustion chamber and the resulting combustion product is water vapor. In the oxy-combustion process, pure oxygen is used instead of air in the combustion process, resulting in a flue gas containing more than 80% CO_2, which is necessitates straightforward CO_2 purification (Olajire, 2010). Since pre-combustion and oxygen combustion technologies are expensive and difficult to apply to large combustion processes, CO_2 removal from flue gas, that is, post combustion control, has become the most commonly applied CO_2 removal process in reducing the CO_2 emissions of combustion processes. The processes of removing CO_2 from flue gas are generally absorption, adsorption, cryogenic separation and membrane separation processes. The most widely used technique for capturing CO_2 after combustion is absorption, with amine-based or ammonia-based absorption processes accepting the most attention (Lloret et al., 2017). There are several disadvantages to this technology for post-combustion applications. Include high energy needs for sorbent regeneration (releasing carbon dioxide from solutions can use up to 40% of a power plant's energy output), Evaporation and corrosion problems that cause mine losses. Amines decompose at a relatively low temperature, especially in the presence of oxygen in the flue gas, and thermal and chemical degradation of amines in the presence of oxygen (Zhao et al., 2018). One of the studies carried out to reduce these disadvantages and to increase CO_2 removal from flue gas streams was to popularize the use of modified adsorbents, especially amine-modified.

Adsorption is one of the most promising technologies for the capture of CO_2. The main advantage of adsorption is the low cost (as it is less energy-intensive in the desorption process), less volatile degradation and corrosive properties, and the variety of adsorbents that can be used to avoid the drawbacks of aqueous amine systems and offer potential energy savings with lower capital (Abuelnoor et al., 2021). High CO_2 adsorption capacity, quick adsorption/desorption kinetics, high CO_2 selectivity, mild regeneration conditions, stability during extensive adsorption-desorption cycling, tolerance to the presence of moisture and other impurities in the feed, cheap cost and a long lifetime are all desirable characteristics of an adsorbent (Nie et al., 2018). Adsorbents for CO_2 capture can be divided into various categories based on their chemical makeup, structural features, or the type of adsorption mechanism they use, such as physical vs. chemical. Many studies have been done recently for adsorptive CO_2 capture using a variety of solid adsorbents, such as zeolitic imidazolate frameworks (ZIFs), zeolites, porous silicates, clays, ashes, hydrotalcite, aerogels, and resins. Activated carbons (ACs), activated carbon fibers (ACFs), carbon nanotubes (CNTs), alkali metal oxides (AMOs), metal-organic frameworks (MOFs), covalent organic frameworks (COFs), porous polymer networks (PPNs). Physical adsorbents have a lower CO_2 adsorption capacity than chemical absorbents despite saving significantly more energy (Zhao et al., 2018).

In this study, cross-linked polymeric adsorbents were produced and the adsorption of CO_2 from its CO_2-N_2 mixture was examined. In this study, cross-linked polymeric adsorbents were produced and their capacity to capture CO_2 from the CO_2-N_2 mixture was examined. The adsorption process was carried out using an adsorption cell operating according to the constant volume variable pressure method. The results obtained from the study were evaluated in terms of the CO_2 capture capacity of the adsorbents used and the factors affecting this process.

2. LITERATURE SURVEY

2.1 Global Warming

The term "global warming" refers to the gradual rise in average Earth's temperature caused by the buildup of greenhouse gases in the atmosphere. One of the most urgent issues is global warming issues facing the modern world in the 21st century (Kumar et al., 2012; Al-Ghussain., 2019; Kumar and Pooja., 2020 Koohestanian and Shahraki, 2021). The increase in the average temperature of our Earth's atmosphere is not due to more energy coming from the sun to a unit area per unit time, because the heat is trapped in the atmosphere. Some gases, which we call greenhouse gases (GHGs), trap heat in the atmosphere. Common greenhouse gases whose concentration in the atmosphere began to increase rapidly after the industrial revolution are water vapor (H_2O), methane (CH_4), ozone (O_3), carbon dioxide (CO_2), chlorofluorocarbons (CFCs), and nitrous oxide (N_2O) (Kweko et al., 2018; Kumar and Pooja., 2020; Sulukan et al., 2023). Greenhouse gases, consisting of three or more atoms, absorb some of the infra-red rays reflected from the earth to the atmosphere and prevent these rays spreading from the earth's atmosphere into space (Figure 2.1). As a result, it causes an increase in the average temperature of the atmosphere surrounding our world (Jain, 1993).

The greenhouse effect is a natural process that is tens of millions of years old. It is an important factor in a variable affecting Earth's surface temperature. The greenhouse effect was initially identified by Joseph Fourier in 1827, confirmed experimentally by John Tyndall in 1861, and identified by Svante Arrhenius in 1896. Indeed, The existence of life as we know it would be unthinkable without the greenhouse effect because of the drastically lower average world temperature (Kweku et al., 2018).

Excessive rainfall and consequent floods and landslides, melting of glaciers and rise in sea level, drought and decrease in agricultural production, forest fires, etc. are caused by global warming which is one of the biggest problems humanity needs to solve. To reduce the problems caused by global warming, it is necessary Greenhouse gas emissions must be decreased to lessen the issues brought on by global warming and keep the average atmospheric temperature increase below 2ºC compared to a pre-industrial age. When it comes to greenhouse gas emission control, the first thing that comes to mind is CO_2 emission control because CO_2 is the gas that is most emitted into the atmosphere from our daily activities such as domestic, industrial, and transportation and from many natural sources.

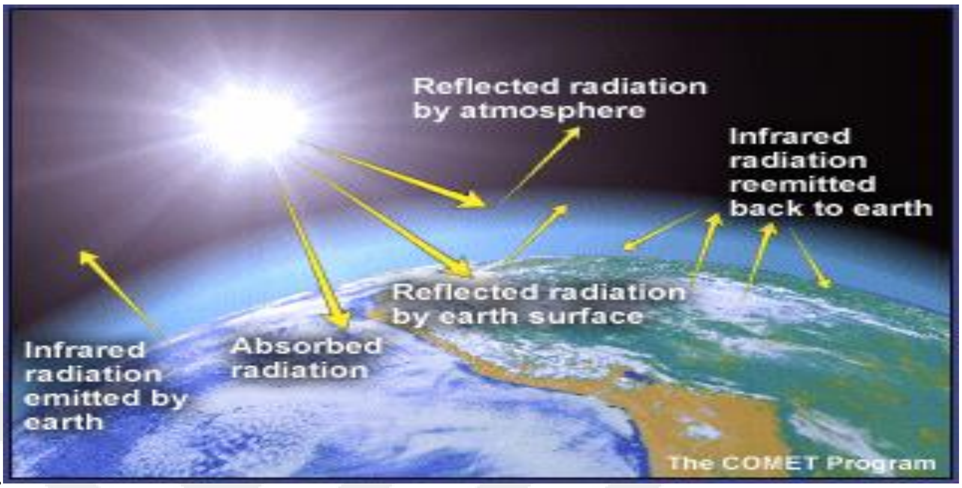

Figure 2.1 Showing radiation absorption and emission by greenhouse gases.

2.2 Greenhouse Gases (GHGs) and Their Main Sources

2.2.1 Carbon dioxide (CO_2)

Carbon dioxide (CO_2) is one of the greenhouse gases, and it is the most significant human greenhouse gas because of its capacity to persist in the atmosphere for centuries (Zeleňák et al., 2018; Nie et al., 2018; Zhang et al., 2020; Min et al; 2022). In the period from 1990 to 2018, CO_2 emissions accounted for 64% of all anthropogenic greenhouse gas (GHG) emissions, primarily as a result of the burning of fossil fuels and industrial processes, according to the IPCC's Sixth Assessment Report (Hatta et al., 2023). CO_2 emissions come from various sources, including anthropogenic CO_2 emissions caused by human activity and natural sources and causes such as wildfires. Wildfires are another significant source of CO_2 emissions, (Gür, 2022). Many businesses, including energy, transportation, manufacturing, fuel, power, and agriculture, have contributed to an increase in CO_2 concentrations in the atmosphere (Saravanan et al., 2021). Anthropogenic CO_2, which is released primarily through the combustion of fossil fuels, is one of the main causes of global warming. Due to their affordability and wide availability, fossil fuels are currently being used more and more as a source of energy, especially in developing nations (Sher et al., 2020). Facilities such as power plants and the cement industry, which use large amounts of fossil fuels, are the processes that release the most CO_2 into the atmosphere (Figure 2.2).

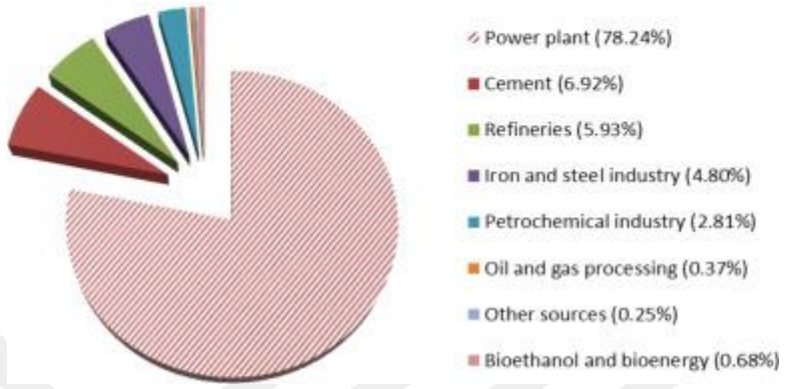

Figure 2.2 Sources of the main CO_2 emissions are broken down.

Electricity and heat production are the primary sources of CO_2 emissions, accounting for 42% of total CO_2 emissions globally (Figure 2.3) (Koohestanian and Shahraki, 2021).

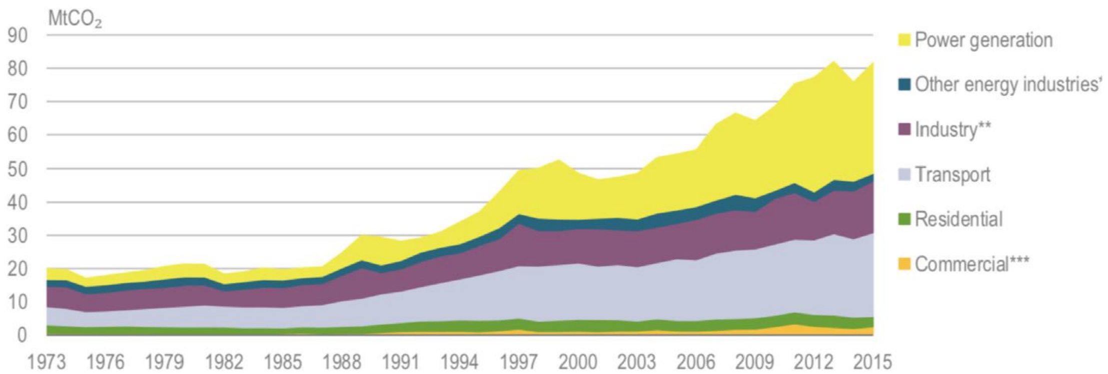

Figure 2.3 Main sources of CO_2 emission.

For example, the cement sector emits 5% of total anthropogenic CO_2 emissions (Sayari et al., 2011; Middleton et al., 2020). As a result of human activity, the earth's atmosphere has been warming noticeably, and this trend is anticipated to continue as industrialization takes hold in the twenty-first century. Environmental CO_2 emissions are mostly caused by the quick advancement of modern civilization. This rapid progress has led to global warming, an environmental problem that requires urgent action. CO_2, which constitutes 55% of anthropogenic greenhouse gas emissions, is the greenhouse gas that creates the most environmental problems, and is responsible for the change of the hydrological cycle and vegetation in the world and the occurrence of severe weather events (George et al., 2021). CO_2 emissions at this rate have raised various alarms, including urban haze, health concerns, and acid rain (Sher et al., 2020).

The stability of CO_2 is reflected in its average residence time, which is less than 10 years, or specifically around 3 years in the troposphere. This indicates the time it takes for a CO_2 molecule to be removed from the atmosphere or troposphere. Residence duration is the amount of time a molecule spends in the troposphere on average before being reused by another biological process on the planet's surface or disintegrating in the stratosphere (Raghuvanshi et al., 2006). In parallel with the increasing energy consumption, especially in the 20th century, the concentration of CO_2 in the atmosphere increased, reaching an average of 414 ppm (as of October 2021); this corresponds to a 47.86% increase compared to the pre-industrial revolution epoch (280 ppm) (Figure 2.4) (Chai et al., 2022).

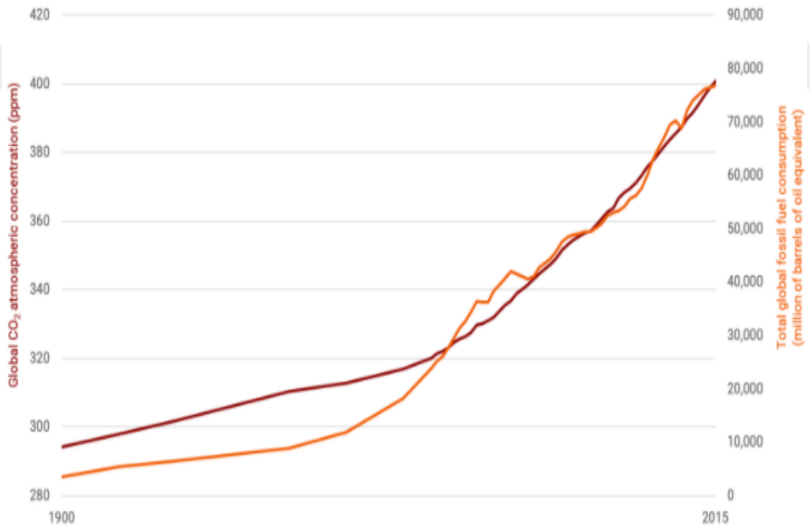

Figure 2.4 Atmospheric CO_2 concentration and fossil fuel consumption.

The average global temperature increased between 0.6 and 1 °Cthroughout the same time period (Koohestanian and Shahraki, 2021). This alarming increase in the amount of CO_2 in the atmosphere and therefore in temperature may have serious environmental consequences.

According to the Energy Information Administration (EIA), there will be a 57% rise in energy use by 2030 (Köne and Büke, 2010). Approximately five Gt of carbon are released into the atmosphere year as a result of the combustion of fossil fuels. The earth's surface temperature is expected to rise by 1.5- 4 °C due to high CO_2 emissions in the next 30–40 years, according to scientists estimate (Raghuvanshi et al., 2006). Stabilizing atmospheric CO_2 levels is imperative to prevent irreversible damage. This involves: Reducing fossil fuel use by embracing alternative sources like biofuels. Promoting reforestation for enhanced carbon sequestration. Implementing separation methods for CO_2 removal to curtail daily emissions, particularly from power plants and refineries (Fatıma et al.,, 2022).

2.2.2 Methane (CH_4)

The second-most important greenhouse gas is CH_4 after CO_2 according to reports, with human activity accounting for about 18% of its overall production. Methane accounts for a significant share of global greenhouse gas emissions, with one-third of the total emissions originating from this potent gas. This substantial contribution to emissions is primarily linked to various sources, including agriculture and the energy sector, highlighting the importance of addressing methane emissions to mitigate climate change (Conrad, 2009; Tiwari et al.,2020; Wallenius et al., 2021). Although methane is far less common than carbon dioxide (CO_2) Because it absorbs thermal infrared radiation in the atmosphere far more efficiently, it has a global warming potential (GWP) that is 86 times greater over 20 years and 28 times greater over a 100-year time horizon (Benson et al ., 2012). Methane is produced by burning fossil fuels and natural seeps, pyrogenic (produced by burning biomass and biofuels), thermogenic (found in lakes, agriculture, waste/landfill, and permafrost), and mixed (found in hydrates and geological sources) (Saunois et al., 2016). Methane levels in the atmosphere have reached about 2.5 times their pre-industrial levels. This increase signifies a substantial rise in atmospheric methane concentrations since the industrial era. The current trajectory indicates that methane levels continue to ascend (Figure 2.5 and 2.6) (IEA, 2021).

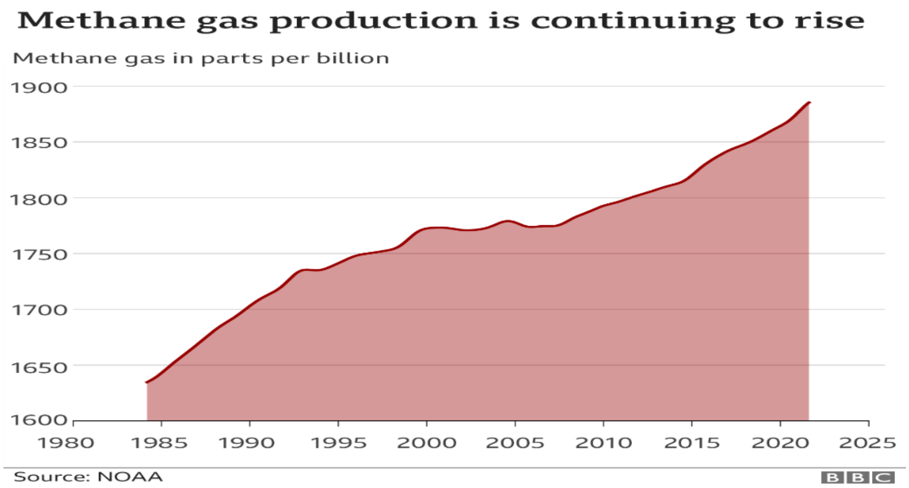

Figure 2.5 Atmospheric CH_4 concentration.

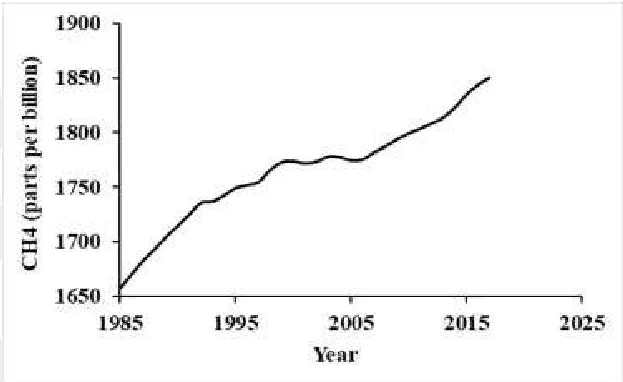

Figure 2.6 Methane emissions in last 40 years.

Wetlands are the main natural source of the significant greenhouse gas methane (CH_4), which accounts for around one-third (80-110Tg yr1) of worldwide emissions (Bhullar et al., 2014). Littoral zones are the main locations where CH_4 is emitted from wetlands because helophytes there generate a conduit for methane synthesis via the sediment-root-stem-atmosphere continuum. 90% of the methane emission in natural wetlands is thought to be caused by the thick emergent macrophyte plants (Benson et al .,2012). Several processes release methane into the atmosphere, including microbial metabolism, incomplete combustion of biomass, and the Earth's crust (thermogenic). Methanogenic archaea play a crucial role in producing biogenic methane during the decomposition of organic matter in oxygen-depleted conditions. In oxic (oxygen-rich) oceans, the production of methane by cyanobacteria and other phytoplankton is reduced (Wallenius et al., 2021). Anthropogenic sources contributing to significant methane emissions include: Sewage systems, Landfills, Ruminant intestines (livestock digestion), Rice fields (Conrad, 2009).Wetlands are the main natural source of the significant greenhouse gas methane (CH_4), which accounts for around one-third (80-110 Tg yr1) of worldwide emissions (Bhullar et al., 2014).

2.2.3 Nitrous oxide (N_2O)

Nitrous oxide (N_2O) is indeed a potent greenhouse gas, playing a significant role in stratospheric ozone depletion and contributing to approximately 6% of the enhanced global warming effect. In grassland ecosystems, the primary sources of N_2O emissions include the deposition of livestock excreta, the application of nitrogen-rich manure, and the use of mineral nitrogen fertilizers. These agricultural activities release N_2O into the atmosphere, emphasizing the importance of sustainable farming practices to mitigate greenhouse gas emissions and address environmental concerns (Prokopiou et al., 2018; Dangal et al., 2019; Timilsina et al.,2020). Agriculture is the most important anthropogenic source of emissions (together with industry, biomass burning, and indirect emissions through reactive N). Microbial sources account for the majority of global N_2O production. N_2O is produced by bacteria and archaea via nitrification and denitrification. Under aerobic conditions, nitrification is the primary source of N_2O (Prokopiou et al., 2018 Approximately 40% of global nitrous oxide (N_2O) emissions stem from human activities. These activities include the burning of fossil fuels, agricultural practices, industrial processes, and wastewater management. The diverse sources of N_2O contribute significantly to its release into the atmosphere, impacting climate change and environmental health. The data depicting global N_2O emissions by industry in 2010 emphasizes the substantial role of human-related sources in the overall N_2O emission profile (Figure 2.7).

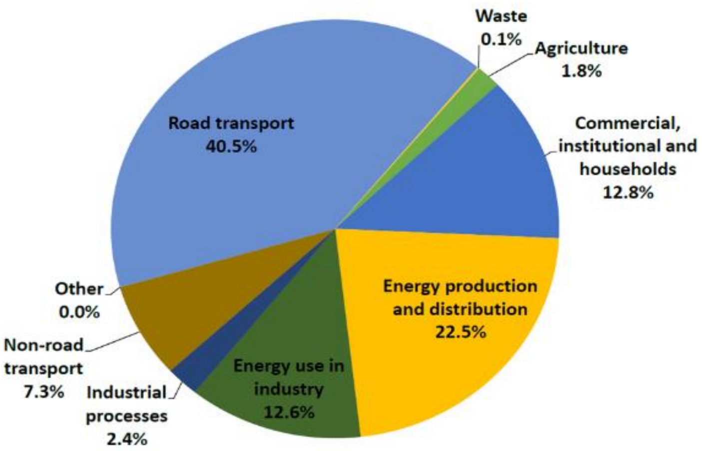

Figure 2.7 Main sources of NO_2 emissions of nitrogen oxides

Nitrous oxide (N_2O) exhibits a residence time in the atmosphere of approximately 114 years. It undergoes elimination as part of the nitrogen cycle, facilitated by specific bacteria, or gets destroyed through chemical reactions or exposure to ultraviolet light. Importantly, N_2O possesses a warming potential nearly 300 times greater than carbon dioxide (CO_2) on a 1-to-1 basis. Despite its potent warming effect, the concentration of N_2O in the atmosphere is considerably lower than that of CO_2 (Al-Ghussain, 2019).

2.2.4 Water vapor

Water vapor is the most significant natural greenhouse gas. Water vapor concentration varies greatly depending on location, season, and time (Martins et al., 2019; Mikhaylov et al., 2020). Water vapor (H_2O) is the most abundant short-lived GHG in the atmosphere involved in all major atmospheric processes, from global climate to micrometeorology. In the context of climate change, water vapor serves as the primary resource for the natural greenhouse effect (Al-Ghussain., 2019 ; Chen et al., 2023). Water vapor plays a significant role in the environmental feedback loop and global warming. The heat added to the atmosphere is dependent on the amount of water vapor introduced. A stable equilibrium exists due to water vapor's limited lifetime, but rising temperatures upset this balance, contributing to global warming. Notably, water vapor has the potential to amplify warming, potentially doubling the effect caused by carbon dioxide (Al-Ghussain., 2019). Additionally, water vapor can directly contribute to global warming by raising the likelihood of clouds by increasing the amount of water vapor in the atmosphere as temperatures rise (Schneider et al., 2010).

2.2.5. Chlorofluorocarbons (CFCs)

Chlorofluorocarbons (CFCs) are man-made chemicals and are the main factor contributing to the Antarctic ozone hole. These compounds have a lifespan in the atmosphere of between 50 and 500 years (Wang et al., 2021). These are commonly used in refrigeration, aerosol production, air conditioning, plastic foam manufacture (as a foam-blowing agent in the creation of polystyrene foam), cleaning, and other applications. These are also employed as solvents and in the manufacture of inhalers (Das et al., 2023). CFC levels in the atmosphere increased considerably over the next decades as a result of the rapid increase in manufacturing and the stability of these gases in the troposphere. The principal sink for CFCs is photocatalytic interactions with ozone in the stratosphere. CFC levels in the atmosphere have been measured internationally since 1978. Based on estimates of CFC production and release, as well as their atmospheric lifetimes, a reconstruction of the CFC atmospheric history during the period 1930-1978 may be built (Lee et al., 2002). Chlorofluorocarbons (CFCs) became prevalent in the mid-20th century, primarily employed as refrigerants and propellants. Their usage has significantly decreased since the discovery of their role in depleting the life-saving stratospheric ozone layer (Das et al., 2023).

2.3 Impact of Global Warming

The effects of Global Warming can have a variety of effects on our quality of life. The most significant impact is on the climate, often known as climate change (Xue et al., 2017). This causes severe effects like climate change, extreme weather, ocean warming, and the acidification of the ocean extinction of some animal and plant species, expansion of the desert area, and population migration, as well as frequently occurring extreme events such as heat waves and cold spells (Williams, 2013; Sulukan et al., 2023) Sea level rise, which is linked to the loss of coastal lands, and extreme weather events like drought, hurricanes, and floods will all be problems brought on by global warming, which poses a serious threat to life as we know it (Koohestanian and Shahraki, 2021). Sea level rises continuously depending on the polar ice melting which is also a consequence of global warming (Figure 2.8).

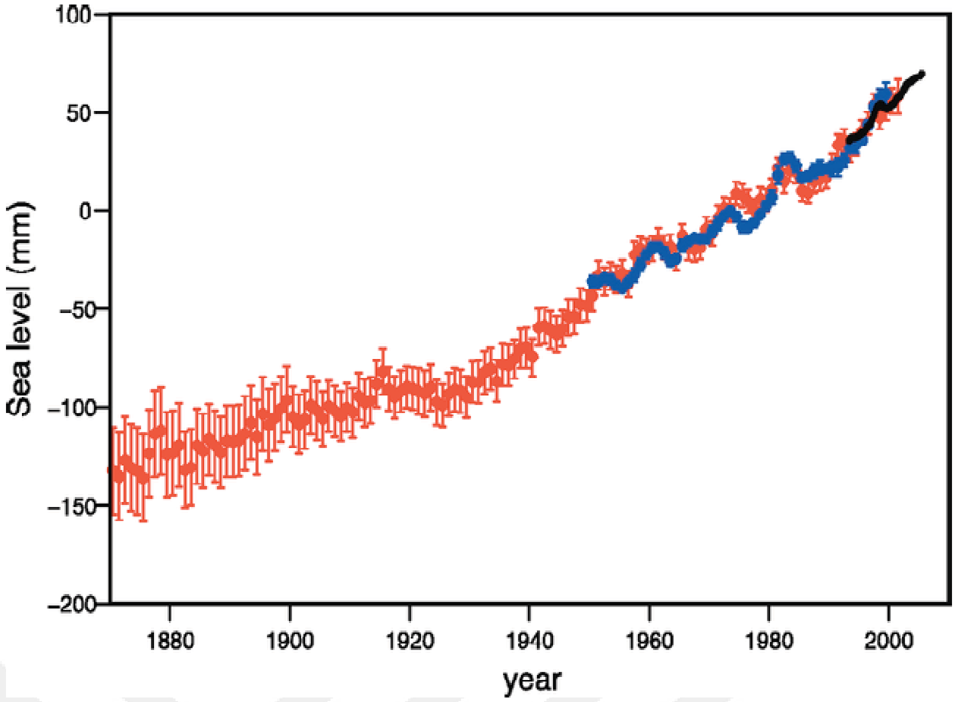

Figure 2.8 Sea-level rise from 1870 to 2001.

Warming has had a negative influence on ecosystems, human society, and the economy all across the world, which is primarily due to changes in climate extremes (Zhang and Zhou, 2020). Global warming causes a unique air circulation pattern to intensify, resulting in heat waves. Heat waves can kill more people in a shorter period than practically any other type of weather event (Kumar and Pooja, 2020).

Global warming, driven by human-caused greenhouse gas emissions, significantly influences precipitation patterns. The complex interplay of rising temperatures and atmospheric changes results in both drought and heavy precipitation events. Increased temperatures lead to more evaporation and surface drying, contributing to the severity and duration of droughts. The rise in water vapor may not necessarily translate into more rainfall due to complex atmospheric dynamics. Global warming disrupts traditional precipitation patterns, causing uneven distribution. Dry regions may experience intensified droughts, while wet areas face an elevated risk of flooding. The alteration of precipitation patterns is attributed to the release of greenhouse gases, primarily from human activities, contributing to the broader issue of climate change. This complex relationship between global warming and precipitation underscores the need for continued efforts to mitigate climate change and adapt to its impacts (Trenberth,. 2011).

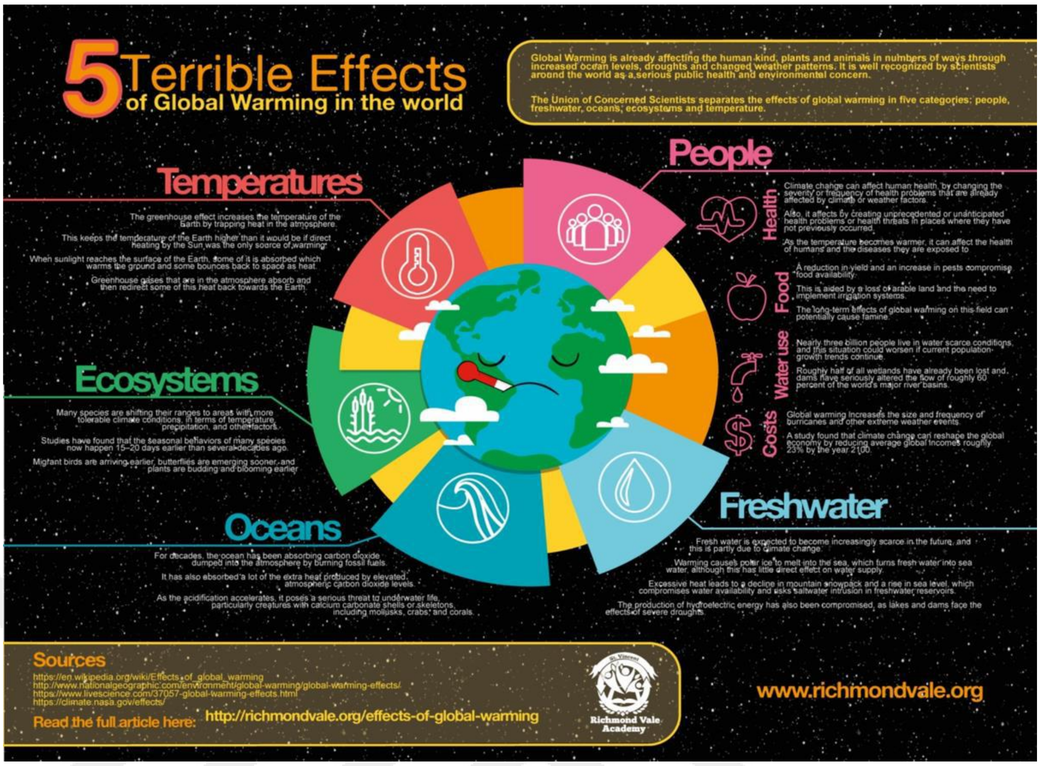

Figure 2.9 Show the effect of global warming all over the world as sources .

The general effects of global warming in the world have been summarized in Figure (2.9). Global warming plays a crucial role in shaping the dynamics of tropical storms and hurricanes. The interaction between rising temperatures and atmospheric changes significantly impacts the formation and intensity of these weather phenomena. The temperature of the sea surface and air humidity are critical factors in tropical storm formation. Global warming contributes to increased sea surface temperatures and higher atmospheric humidity, creating favorable conditions for the initiation of tropical storms. Since 1980, the temperature of the surface saltwater has risen by 0.3 °C, while air humidity has risen by around 4% (Saravanan et al., 2021). As a result, our planet's water cycle is accelerating. At the same time, both precipitation and evaporation rates are rising globally (Manabe, 2019). Aquatic ecosystems have faced severe impacts due to global warming, with aquatic species being particularly affected.The majority of aquatic species are poikilothermic, meaning their body temperature is dependent on the external environment. This makes them highly vulnerable to temperature changes caused by global warming.

The physiological and biochemical processes of these creatures can degrade as a result of variations in body temperature brought on by shifts in external temperatures (Sulukan et al., 2023).

2.4 International Progress for Reduction and Control of Global Warming

Environmentalists are now very concerned about the issues related to the release of greenhouse gases and the declining environmental quality. The increase in greenhouse gases has a detrimental effect on the ecosystem and the climate, which is why this is a cause for concern. This is what motivated many nations to sign the Kyoto Protocol and other international agreements (Anomohanran.,2011**)**. GHG reduction is critical for all nations because the problem is global in scope and no one country or group of countries can provide a solution. This is why international and regional cooperation is more desired and has been strongly urged in the worldwide community of atmospheric sanity. In this effort, the United Nations Framework Convention on Climate Change (UNFCCC) has lately been developed to address the global climate challenge. This was carried out as an international accord involving many countries from various regions to reduce the harmful concentration of anthropogenic GHGs in the atmosphere (Usman.,2012). Table (2.1) shows major international meetings concerning the global warming.

Table 2.1 International Conference

Place	Conference	Time	Result Conclusions and Recommendations
Geneva, Switzerland	The first World Climate Conference	1979	The first meeting of the WHO was about carbon neutrality. The meeting supported the relationship between health and climate change. In conclusion, It provided a dire warning that there are intolerable health risks associated with climate change in the absence of mitigation and adaptation (Neira et al.2014).
Villach, Austria	Villach Conference	1985	A multinational panel of scientists (participating in their individual capacities) came to the conclusion in Villach in 1985 that "in the first half of the next century a rise of global mean temperature would occurs which is greater than any in man's history." Also suggested by these experts was that "scientists and policymakers should start working actively together to explore the effectiveness of alternative policies and adjustments." ((Agrawala, 1998).
Bellagio, Italy	Bellagio Conference	1987	The impacts on natural ecosystems and human society, as well as the rate and amount of sea

			level rise, temperature changes, and ambient concentrations of particular greenhouse gases, should all be subject to restrictions, the stabilization of emissions of greenhouse gases, the enhancement of sinks for greenhouse gases, and the equitable distribution of greenhouse gas emission reduction measures among the various actors (Agrawala, 1998).
Toronto, Canada	Toronto Conference	1988	“Calling for a 20 percent reduction in global CO_2 emissions by 2005, as well as for the formulation of an international convention on the matte" (Campa, 2021).
Noordwijk	Noordwijk Conference	1989	"For the long-term safeguarding of our planet and maintaining its ecological balance, joint effort and action should aim at limiting or reducing emissions and increasing sinks for greenhouse gases to a level consistent with the natural capacity of the planet. Such a level should be reached within a time frame sufficient to allow ecosystems to adapt naturally to climate change, to ensure that food production is not threatened and permit economic

			activity to develop in a sustainable and environmentally sound manner" (Leemans and Vellinga, 2017).
	Second World Climate Conference	1990	After lengthy negotiations, it adopted a final proclamation that lacked any targets. It did, however, embrace a few of the UNFCCC's later guiding principles. Climate change was also listed as a "common concern of humanity"(Leemans and Vellinga, 2017).
	The first IPCC report	1990	" concluded that there was no evidence of a human influence on the climate at this time, but concluded that it is unlikely that observations will reveal the increasing greenhouse effect with certainty until at least ten years”(Knutson et al., 2017).
Brazil	the Rio de Janeiro	1992	The 1992 UN Conference's conclusions urged nations and organizations to promote public engagement and awareness by making information widely available (Ewing, 2011; Aragón-Pérez, 2019).
Berlin Germany	The first Conference of the Parties (COP1)	1995	By highlighting the need for a treaty on reducing greenhouse gas emissions and restating that Germany was committed to

			achieving a 25% reduction in CO_2 emissions from 1990 levels by the year 2005, he displayed leadership. A reduction protocol for the period after the year 2000 was not approved by the COP. Unresolved problems included the Rules of Procedure and the continuation of current commitments after the year 200 (Hermann, 1995).
	The second IPCC report	1996	“The balance of evidence suggests a discernible human influence on climate” (Knutson et al., 2017).
Japan	Kyoto Protocol	1997	The KP established legally-binding targets for 37 high-income countries and the European Union (EU), mandating them to reduce their greenhouse gas emissions by an average of 5% below 1990 levels between 2009 and 2012. It did away with the requirement that developing countries fulfill their GHG mitigation commitments (Leggett, 2020).
	The third IPCC report	2001	“the balance of evidence suggests a discernible human influence on climate” (Knutson et al., 2017).
Bali	Bali Climate Conference	2007	The United Nations Framework Convention on Climate Change

			(UNFCCC)'s next phase of discussions was officially launched during the Bali Climate Conference, which represented a turning point in the intergovernmental response to climate change. Developing nations concurred that they will go above and beyond their current UNFCCC commitments as part of these negotiations. Second, the USA, which abandoned the Kyoto Protocol in 2001, consented to negotiate fresh commitments that will guarantee "comparability of efforts" with the Kyoto parties already in place. The Bali Action Plan has a 2009 deadline, with the results being delivered to the Conference of the Parties' (15th) meeting in Copenhagen in December of that year (Depledge, 2009).
	The fourth IPCC report	2007	“Most of the observed increase in global average temperatures since the mid-20th century is very likely due to the observed increase in anthropogenic greenhouse gas concentrations” (Knutson et al., 2017).

Denmark	Copenhagen Consensus (COP-15)	2009	keeping the average global temperature at 2°C or below (Ares et al., 2012).
Cancún, Mexico		2010	The ultimate objective determined by the United Nations Framework Convention on Climate Change (UNFCCC) is to achieve “stabilization of greenhouse gas concentrations in the atmosphere at a level that would prevent dangerous anthropogenic interference with the climate system. Such a level should be achieved within a time frame sufficient to allow ecosystems to adapt naturally to climate change, to ensure that food production is not threatened, and to enable economic development to proceed in a sustainable manner”(Ewing, 2011; Gao et al., 2017).
South Africa	The Durban conference	2011	Delegates in Durban decided to begin a work plan to find ways to close the gap between the current emission reduction commitments made by nations for 2020 and the target of limiting global warming to 2 °C. But it's unclear how exactly that will be accomplished. Additionally, some of the major issues in the current commitment period have not been adequately

			resolved (Fuhr et al., 2012).
Qatar	The Doha climate conference (COP-18)	2012	Governments reached a consensus on the technical details of the Kyoto Protocol's second commitment period (KP-CP2), which is scheduled to run from 2013 to 2020 (Morel et al., 2012).
	RİO+20	2012	Attention was drawn to the gap between countries' promises to reduce greenhouse gases by targeting 2020 and an increase of 1.5 or 2 degrees in the world's average temperature.
	The fifth IPCC report	2013	"It is extremely likely that more than half of the observed increase in global average surface temperature from 1951 to 2010 was caused by 16 the anthropogenic increase in greenhouse gas concentrations and other anthropogenic forcings together." (Knutson et al., 2017).
Paris, France		2015	195 nations agreed on a strategy to cut back on greenhouse gas emissions, with the goal of keeping the rise in global temperature to well below 2°C over the pre-industrial era. This means that, given the rise in temperature by 0.6 °C by the end of the 20th century, future warming will be less than 1.4 °C)

			(Anderson et al., 2010; Lima and Gupta, 2013).
Fiji	The 23rd Conference of the parties (COP 23)	2017	The conference placed a lot of emphasis on increasing the bar for climate protection and drafting regulations to carry out the Paris Agreement (Obergassel et al., 2018).
Poland	Katowice Conference	2018	The choice has been made to put the Paris Agreement into effect (Obergassel et al., 2018).

2.5 CO_2 Capture Processes

After it was determined that the main gas responsible for global warming is CO_2, controlling the emission of this gas has become an important issue that remains on the agenda all over the world (Nie et al., 2018). The Intergovernmental Panel on Climate Change (IPCC) estimates that 64% of all anthropogenic greenhouse gas (GHG) emissions between 1990 and 2018 were mostly caused by the burning of fossil fuels and industrial activities (Hatta et al., 2023). Although member states of the United Nations Environmental Convention on Climate Change (UNFCCC) promised to reduce CO_2 emissions to combat climate change in Paris in 2016, CO_2 emissions still continue to increase worldwide. According to a report by the International Energy Agency (IEA), the annual CO_2 generation in 2018 increased by an average of 2.4% annually, reaching 33.5 Gt due to greater energy demand. According to predictions, the rise in CO_2 would cause the average global temperature to rise by about 3.2 °C by the year 2100, having a substantial impact on the planet and human activity (Raftery et al., 2017). There are several strategies for reducing CO_2 emissions, including increasing the use of renewable energy sources like solar and wind energy (O’Ryan et al., 2020), using natural gas instead of coal as fuel (Wilson and Staffell, 2018) putting laws in place to limit overall CO_2 emissions (Hashmi and Alam, 2019), CO_2 can be used as a raw material (Baena-Moreno et al., 2019), and utilizing a carbon capture and storage (CCS) strategy (Benhelal et al., 2013). The purpose of carbon capture is to use CO_2 instead of traditional raw materials in a variety of industrial processes in order to both reduce and profit from emissions to the atmosphere (Baena-Moreno et al., 2019). Carbon Capture and Storage (CCS) stands as a pivotal technology in addressing CO_2 emissions from large-scale fossil fuel systems, particularly in power stations. Projections indicate a substantial potential reduction of up to 50% in industrial CO_2 emissions by 2050, primarily driven by the widespread adoption of CCS technology. This technology is recognized as a major solution to curbing emissions from energy and carbon-intensive industries, playing a crucial role in achieving global emission reduction goals (Gaurina-Međimurec et al., 2018;Wei et al., 2020; Middleton et al., 2020). This technology involves capturing CO_2 emissions at their source, preventing them from entering the atmosphere and contributing to global warming. By implementing carbon capture strategies, industries can significantly reduce their carbon footprint, contributing to a more sustainable and environmentally conscious future (Xue et al., 2017). The United Nations Framework Convention on Climate Change (UNFCCC), Intergovernmental Panel on Climate Change (IPCC), Kyoto Protocol, and Paris Agreement all identify CO_2capture as one of the promising technologies to fight global warming (Chai et al., 2022). Today, there are several widely used and commercially available methods for extracting CO_2 from a gaseous mixture. These methods are typically utilized as a purification step in a variety of industrial processes, mostly in the extraction of oil and gas. The physical and chemical characteristics of the gaseous stream being processed (flow rate, pressure, temperature, CO_2 content, contaminants present, etc.) are typically taken into account when choosing a procedure. Many industrial processes, including those that produce hydrogen and ammonia as well as natural gas, have made extensive use of CC procedures to remove CO_2 (Olabi et al., 2022). CO_2 collection faces a number of challenges because of the wide range of emission sources and their diverse characteristics, compositions, volumes, and spatial and temporal distributions, in addition to the different material and technological options for removing CO_2 from flue streams (Gür, 2022).

The three main methods for capturing CO2 from fossil fuel-based power plants are as follows: (1) pre-combustion, (2) post-combustion, (3) oxy-fuel combustion stages of these three systems are shown schematically in Figure (2.10).

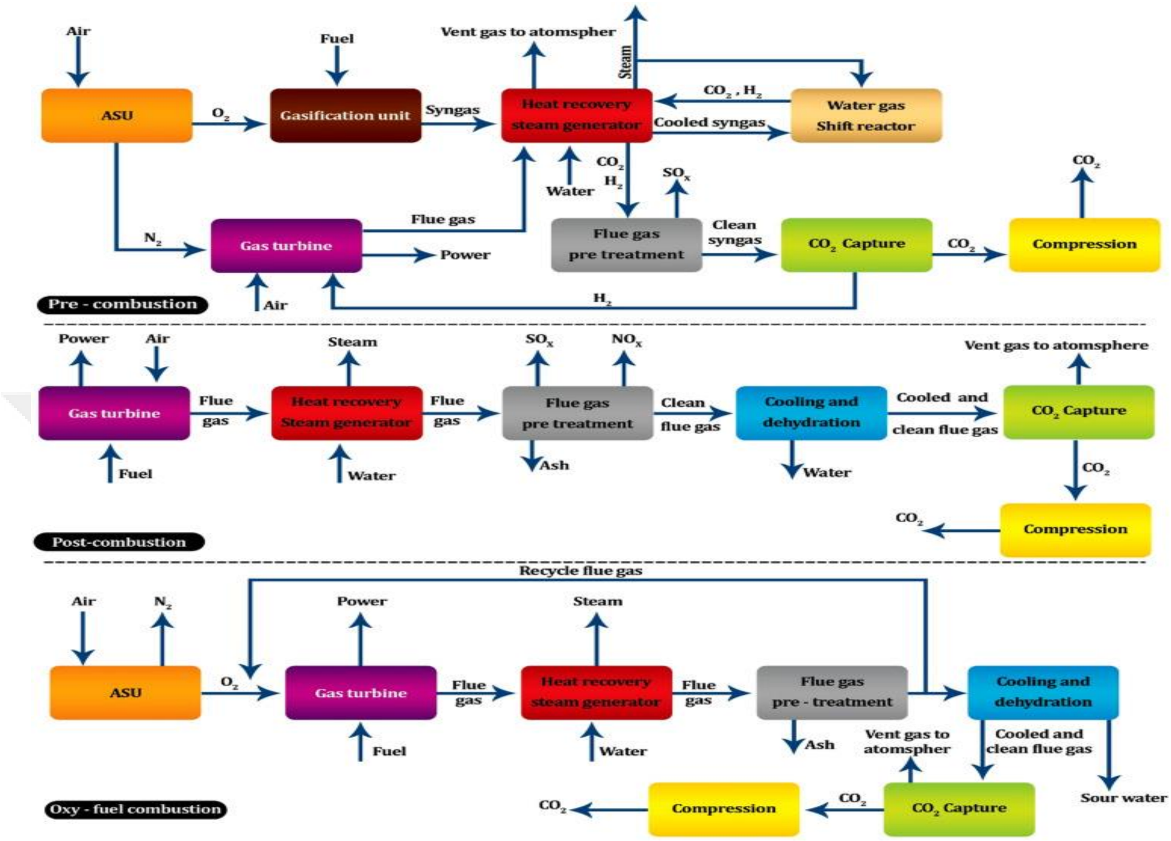

Figure 2.10 Main combustion CO_2 capture technologies.

2.5.1 Pre-combustion Processes

Pre-combustion carbon capture is a process designed to extract carbon dioxide (CO_2) from fossil fuels before they undergo combustion. This method plays a crucial role in mitigating greenhouse gas emissions associated with the burning of fossil fuels or biomass fuels before the combustion process is finished. Typically, it is used in natural gas power plants and the gasification of (coal, natural gas, and biomass) (Olabi et al., 2022). Pre-combustion capture creates synthesis gas, also known as fuel gas, by heating a fuel with oxygen, air, and sometimes steam (Songolzadeh et al., 2014). Consists mostly of hydrogen and carbon monoxide as its gaseous fuel constituents. After particle impurities from the syngas are removed, carbon monoxide is converted to carbon dioxide (CO_2) in a two-stage shift reactor by reaction with steam (H_2O). This results in the combination of CO_2 and hydrogen. A stream of virtually pure hydrogen is then left behind after the CO_2 is removed using a chemical solvent, such as the widely used commercial product Selexol (which employs a glycol-based solvent), and is burned in a combined cycle power plant to provide electricity (Rubin, 2012). This system is generally used in coal-fired integrated gasification combined cycle power plants (IGCC) as well as for liquid and gaseous fuels. The typical reaction for IGCC is shown in the equations below (Olajire, 2010).

$2C + O_2 + H_2O \rightarrow H_2 + CO + CO_2$

$C + H_2O \rightarrow H_2 + CO$

$CO + H_2O \rightarrow CO_2 + H_2$

2.5.2. Oxy-fuel Combustion Processes

In oxy-fuel combustion, oxygen (O_2) is utilized to fuel combustion rather than air. This mostly removes CO_2, H_2O, O_2, and a few other contaminants while also removing a sizeable part of the nitrogen N_2 present in traditional flue gas, i.e., 67–77 vol% (Olabi et al., 2022). Some CO_2 rich flue gas is recycled into the combustor in order to lower the extraordinarily high flame temperature that arises from fuel burning in pure oxygen. The flame temperature is lowered to that of an ordinary air-blown combustor as a result. One advantage of oxygen-blown combustion is that the flue gas has a CO_2 level of more than 80%, meaning that simple CO_2 purification is all that is required (Olajire, 2010). The oxy-fuel combustion process (CC) breaks down fossil fuels in pure oxygen to produce flue gas that is nitrogen-free and only contains CO_2 and water. The flue gas condensation process eliminates NOx emissions and produces a stream of pure CO_2 (Wilberforce et al., 2021). High capital costs and a significant electric power consumption to separate oxygen from the air are the main drawbacks of oxy-fuel combustion (Koohestanian and Shahraki, 2021).

2.5.3. Post-combustion processes

After combustion, CO_2 is separated from flue gas according to the post-combustion capture principle. Flue gas often contains oxygen as well as inert gases like nitrogen, argon, and water that dilute the CO_2 content (8-15% CO_2). Expensive technology like syngas separation, hydrogen turbines, or fuel cells are not necessary for post-combustion capture. The most crucial method for reducing CO_2 emissions is post-combustion capture since it is flexible and doesn't need altering the combustion cycle. The power plant can continue to run even if the capture plant stops (Songolzadeh et al., 2014). After burning the fossil fuel, post-combustion capture takes CO_2 out of the flue gas. Currently, the principal coal used in all coal-fired power plants burns directly to produce electricity. So for already-existing coal-fired power facilities, post-combustion capture is a more practical option (Akeeb et al., 2022). Most of the hot combustion gases that exit the boiler are nitrogen (from the air) and smaller amounts of water vapor and CO_2 produced by the hydrogen and carbon in the fuel. Coal impurities further produce sulfur dioxide, nitrogen oxides, and particulate matter (fly ash) as byproducts of coal burning. These controlled air pollutants along with other trace species like mercury need to be removed in order to meet applicable emission limitations. Sometimes more pollution removal especially of SO_2 is required to create a clean enough gas stream for upcoming CO_2 capture (Rubin et al., 2012). The removal method via absorption with an amine solution is the most commonly utilized CO_2 collection technology in the post-combustion system. The primary benefit of integrating post-combustion CO_2 capture devices into current power plants is the avoidance of modifying the combustion process. One may argue that the downside of this system is the high energy required for the use of strong chemicals and their regeneration in post-combustion systems, even though the amount of CO_2 in the flue gas is relatively lower than other gases (Olajire, 2010).

Table 2.2 Comparison of CO_2 capture systems.

Capture technology	Advantages	Disadvantages
Pre-combustion	• The procedure makes it possible to produce fuel without carbon and to capture CO_2under high pressure. • You can use a variety of hydrocarbon fuels, including biomass, coal, natural gas, and petroleum. • Syngas, the main byproduct of pre-combustion capture, can be used as a feedstock for the synthesis of various chemical compounds or in coupled cycles to generate energy. • Process for separating carbon dioxide that uses less energy since there is less gas volume, more pressure, and more carbon dioxide concentration • For the AGR process, more commercially available technologies are offered; • Fewer resources are needed	• Mequired additional expense for the production of syngas • More expensive in contrast to alternative approaches • Gas must be cooled in order to extract CO_2. • Loss of efficiency in the water-gas shift segment • Though not as much as during post-combustion capture, sorbent regeneration results in a significant energy loss. • Heat transfer issue related to the temperature variation in syngas • Hydrogen-fueled gas turbine application results in decreased efficiency • H_2/ CO_2separation is expensive and difficult.

	(in comparison to post-combustion capture); • Production of synthesis gas and hydrogen as a substitute for fuel • Typically higher CO_2 concentrations than for post-combustion collection Possibility of lowering compression costs/loads.	• The procedure's limitations include high expense and higher risk.
Oxy-fuel Combustion	• A high level of CO_2 (over 80% v/v) in the output stream • Easy separation of exhaust gases and a high flame temperature. • NOx emissions disappear when nitrogen is absent. • Very little pollution emissions • The use of chemicals on the premises is not necessary. • A broad range of coal fuel compatibility • Compared to post-combustion collection systems, refit is easier and simpler • Air separation technology	• Approximately pure O_2 is necessary • Substantial energy input required to separate air. • To remove oxygen from the air, it is expensive and requires a lot of electricity. • In pure oxygen, combustion is challenging. • Carbon dioxide compression and the energy-intensive air separation unit (ASU) result in a net loss in power output. • Air-tight installation is necessary to prevent

	is well developed. • It's a well-known technology to separate air. • A extremely high-purity CO_2 stream can be created using the procedure. Once trace impurities have been removed, the stream can be purified more quickly than with other CO_2 removal processes. • Decreased NO_X production • Intensifying the convective and radiative heat transfers • There is no need for additional substance or solvent while applying capturing.	air leaks (or carbon dioxide leaks brought on by over pressurized operation). • Potential corrosion issue • The control of oxygen and its impact on the boiler raise many risk and safety concerns.
Post-combustion	• Causing the existing power plant's original setup to alter as little as possible • Its upkeep is controllable and does not halt operation. • Advanced technologies • Retrofit to designs of current power plants • Additional NOx and SOx removal • It is very easy to integrate into established plants; highly compatible with	• increased NO_X production • Regeneration of solvent results in an energy penalty. • The detrimental state of flue gases. • Diminished solvent • energy-intensive carbon dioxide compression necessary • Most sorbent technologies aren't as

	retrofitting existing power plants (allowing the continuation of common power generation technologies, such as pulverized coal). • Specified procedure	reliable when it comes to high-performance demands. • Large amounts of water consumed • Process performance is significantly impacted by low CO_2 load

(Olajire, 2010; Rubin et al., 2012; Songolzadeh et al., 2014; Theo et al., 2016; Mukherjee et al., 2019; Koohestanian and Shahraki, 2021; Olabi et al., 2022).

The advantages and disadvantages of CO2 capture systems are given in Table (2.2).The various post-combustion CC technologies included membrane separation, cryogenic separation, adsorption, and absorption (Song et al., 2019; Akeeb et al., 2022).

2.5.3.1 Membrane Separation

Membrane separation technology is the best for recovering CO_2 while using less energy. Membranes are used in the pressure-driven process of gas separation. Flue gas pressure is low, which results in low driving force (low CO_2 content and low pressure) for membrane processes in post-combustion. When the feed mixture's CO_2 concentration rises, membrane methods offer improved separation performance (Songolzadeh et al., 2014). Can use membranes to filter out other flue gas constituents while letting only CO_2 flow through (Figure 2.11).

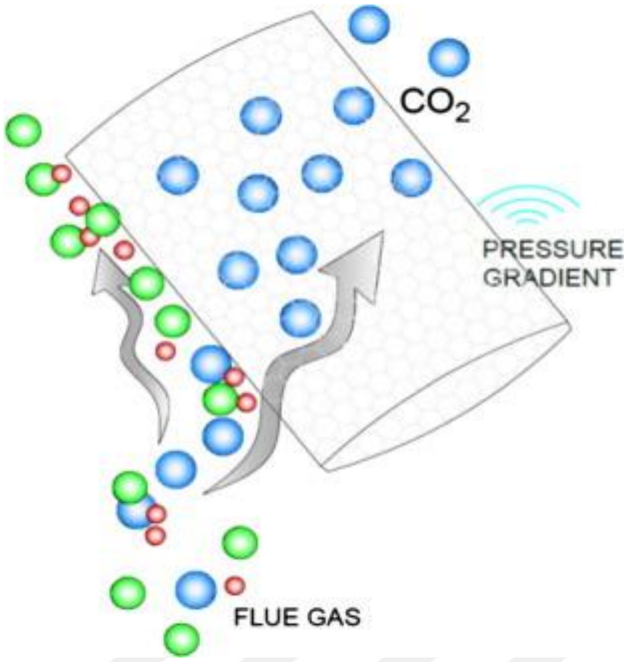

Figure 2.11 Process diagrams for membrane carbon capture.

Other gases like oxygen from nitrogen and carbon dioxide from natural gas have also been separated using this method (Leung et al., 2014). Membranes are semi-permeable barriers that can separate substances by a variety of methods, including (molecular sieving, ionic transport, solution/diffusion, and adsorption/diffusion). They are composed of a variety of materials, both porous and non-porous, including organic (polymeric) and inorganic (carbon, zeolite, ceramic, or metallic). In order to remove one or more gases from a feed mixture and produce a particular gas-rich permeate, membranes function as filters. Characteristics of a membrane affect its performance: selectivity, or the membrane's predilection to pass one species of gas over another, and permeability, or the flow of a specific gas through the membrane (Olajire, 2010; Sreedhar et al., 2017). Low initial and running expenses are one benefit of membrane separation. Little material is needed to coat the membrane, and extra facilities like huge pretreatment containers and solvent storage are not required. Replacement of the membrane is the main maintenance expense for a membrane separation machine. The membrane's simplicity and dependability, which allow it to operate unattended for extended periods of time, are further benefits. Due to the gas not remaining and reacting with the membrane, there is no saturation and no need for frequent shutdown and startup (Akeeb et al., 2022).

2.5.3.2 Absorption

The most well-known and widely used CO2 collecting technology is absorption using amine-based solutions. A chemical solvent collects CO_2 and then releases it when heated. The regeneration and absorption sections work at temperatures of around 40 and 120 °C, respectively (Bernhardsen and Knuutila, 2017). However, there are several disadvantages to this technique, such as the high energy consumption of amine regeneration (which can account for 25% to 33% of a power plant's output), amine losses due to equipment corrosion, and the thermal and chemical degradation of amines (Ooi et al., 2020). Other drawbacks include corrosion, amine losses by evaporation, amine degradation with temperature and time, and toxicity of solvents employed in absorption operations (Budzianowski, 2016). There are some advantages of the absorption process including solvent regeneration, minimal energy usage, and high holding capacity (Leung et al., 2014). Aqueous monoethanolamine (MEA) mixtures are the main post-combustion CO_2 capture technology. Additionally employed in post-combustion CO_2 capture techniques are diethanolamine (DEA), methyldiethanolamine (MDEA), and potassium carbonate (K_2CO_3). Compared to other aqueous alkanolamines, MEA is inexpensive, has a high absorption capacity, and requires less heat for regeneration (Leung et al., 2014). In this method, after the flue gas is cooled, it comes to the absorption column, where it comes into contact with the CO_2 selective solvent and is separated from other flue gas components. Afterwards, carbon dioxide gas is separated by desorption process as seen with the help of heating from carbon dioxide rich solution. In this way, high-purity carbon dioxide is stored, and the regenerated solvent is sent to the absorption column for reuse (Yurata et al., 2019). Temperature and pressure must be considered for the absorption process of CO_2 in the flue gas. Since the flue gas released after the combustion process is generally above 100ºC, the temperature of the flue gas must be lowered in order to perform the absorption process. This can only be done with direct water contact in a cooler. Thus, it is ensured that large particles such as ash in the flue gas are removed (Akeeb et al., 2022). It has been found that amine-based solvents absorb CO_2 gas well. It is therefore the most experienced solvent currently being utilized in CO_2 absorption. Lean amine is used to absorb CO_2 gas in an absorber column, where the flue gas first passes. The CO_2 loaded amine (or rich amine) is then passed to a stripper, where the amine solvent is recovered through heating (Figure 2.12).

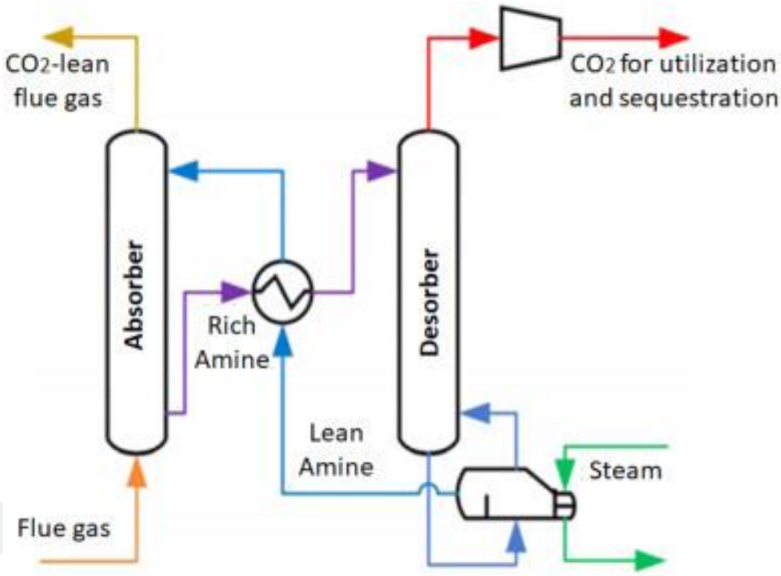

Figure 2.12 A typical CO_2 absorption-stripping process.

The N, O, and C atoms that make up the amine-based solvents have a high electron density.Based on how many hydrogen atoms were attached to the nitrogen atom (Ooi et al., 2020).

2.5.3.3 Cryogenic separation

This separation process, which involves multiple compression stages carried out at low temperatures and high atmospheric pressure, is primarily used on a commercial scale to remove CO_2 from the gaseous mixture stream. It involves compressing and cooling the CO_2 containing gas combination, which entails lowering the temperature of the gases to a very low level (below -73.3 °C) so that the CO_2 can separate and freeze off at various rates to quicken the phase transition of CO_2 and other substances that could be extracted by distillation later on. This technique utilizes the properties of condensing and de-sublimation of different components of the gaseous mixture to separate CO_2 in its concentrated form. The technique has the advantage of allowing for the liquid recovery of pure CO_2 (Olajire, 2010; Sreedhar et al., 2017; Gautam and Mondal, 2023). The supply gas is initially cooled using pre-coolers and heat exchangers before being cooled to a low temperature. After cooling, the feed gas is sent to the distillation column, which is equipped with several vapor-liquid contact devices (such trays or packing materials). The top and bottom products are the two main divisions of the component steam that comes from the distillation column. Through a partial condenser, the top-level methane separation is removed. The distillation column's base is where condensed CO_2 is collected. The reboiler, which generates vaporization heat, recycles a portion of the rich CO_2 stream to the distillation column. Following more separation of the remaining CO_2 stream, the purified CO_2 product is eventually removed from the separator (Figure 2.13) (Song et al., 2019).

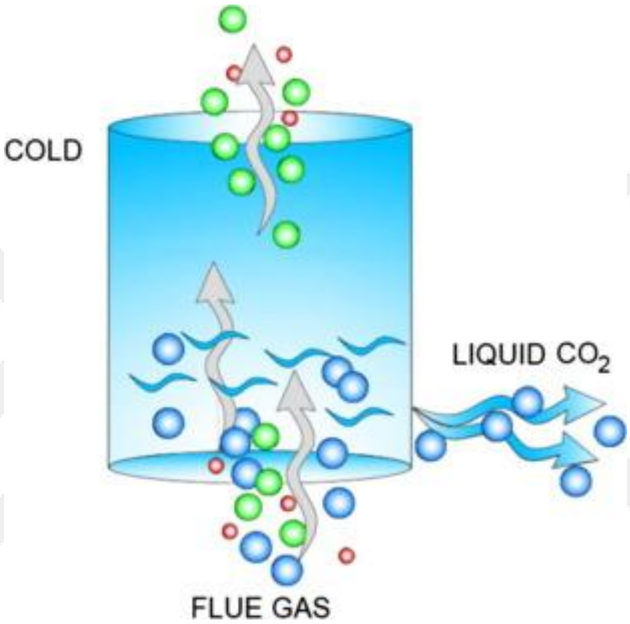

Figure 2.13 Process diagrams for the cryogenic carbon capture.

The advantages of cryogenic separation can be summed up as follows (Zanganeh et al., 2009; Song et al., 2012):

(1) Since liquid CO_2 is directly created, it is relatively simple to transfer or store for use in enhanced oil recovery.

(2) There are no solvents or other components in this method, making it rather simple.

(3) The cryogenic separation is simply scaled up for industrial use.

2.5.3.4. Adsorption

Adsorption, which is defined as the adhesion of atoms, ions, or molecules from a liquid, gas, or dissolved solid to a surface, is the process of extracting one or more components from a gaseous mixture using a suitable solid particle containing many active sites. Put differently, the stickiness of atoms, ions, or molecules on a solid surface is referred to as "adsorption". Desorption is the process of removing the atom, ion or molecule attached to the adsorbent surface from the surface, which is also called regeneration of the adsorbent (Raganati et al., 2021). Adsorption differs from absorption in that the absorbent material, whether it be a solid or a liquid, is used to absorb the absorbent solute (gas). Adsorption takes place on the surface, whereas absorption involves the entire material volume (Ben-Mansour et al., 2016; Gautam and Mondal, 2023). Adsorption of CO_2 gas is the phenomenon of its interaction with the active sites on adsorbents and adhesion to these sites by physical or chemical mechanisms (Wilberforce et al., 2019). When the flue gas mixtures containing CO_2 come into contact with an absorbent bed in packed column, The CO_2 sticks to the surface because it is drawn to it. After equilibrium is attained, desorption can be used to extract carbon dioxide into its pure form, and the regenerating adsorbent can then be recycled back for further usage. Applying a low pressure (as in pressure swing adsorption, or PSA) or low temperature (as in temperature swing adsorption, or TSA) separates the adsorbed CO_2 from the adsorbent in order to replenish the adsorbent (Theo et al., 2016).

One of the most promising techniques for post-combustion CO_2 capture from flue gases is adsorption, which offers potential energy savings with lower startup and operating costs while avoiding the problems of aqueous amine systems (Majchrzak-kuc and Wawrzy, 2016). The creation of very particular CO_2 adsorbent materials is essential to the success of this strategy (Ammendola et al., 2017). Adsorption techniques are gaining traction as a potential substitute for other separation methods among the various process technology solutions used to extract CO_2 from exhaust fumes. In contrast to conventional separation techniques, adsorption processes employ novel solid sorbents that have the ability to reversibly extract CO_2 from flue gas streams (Samanta et al., 2012). Among the possible CO_2 capture systems, adsorption employing solid material is chosen due to having numerous potential advantages, such as being less expensive and running costs, possessing corrosive properties, less volatile degradation, and versatility in adsorbent use, reduced energy for regeneration (the reusable nature of adsorbents), better capacity, selectivity, ease of handling, low energy requirement, regulated waste generation. Adsorbents must have low affinity for moisture and contaminants, high CO_2 uptake capacity from flue gas streams at ambient conditions, strong CO_2/N_2 selectivity, regeneration capability, and high specific surface area per unit mass, good mechanical and thermal durability for numerous cycles of adsorption-desorption, appropriate pore size distribution, considerable adaptability, and ease of use (Shafeeyan et al., 2010; Samanta et al., 2012; Majchrzak-kuc and Wawrzy, 2016; Borhan et al., 2019; Abuelnoor et al., 2021). For this kind of adsorption technology to be successful, adsorbents must have the required qualities, such as high adsorption capacity, high CO_2 selectivity, durability, and relatively rapid sorption and desorption kinetics (Samanta et al., 2012). The kind and size of the targeted adsorbate also determine the appropriate adsorbent. In order to create materials with higher performance, researchers are still trying to create new and advanced adsorbents and study the adsorption kinetics and thermodynamics (Fatıma et al., , 2022).

2.5.3.4.1 Chemical adsorption

Chemisorption is known as a subclass of Adsorption that is propelled by a reaction of chemicals at the surface that is exposed. In this adsorption, the adsorbate is strongly bonded to the adsorbent surface, usually by covalent bond. In chemisorption, the adsorption efficiency of the adsorbate increases with temperature. This adsorption process is quite selective as the adsorbate adheres to the surface with a chemical bond, and since the enthalpy of bond formation is high, the bond is difficult to break, meaning the regeneration of the adsorbent is difficult.

Metal compounds make up the majority of chemical adsorbents. The two kinds of metal compounds used for CO_2 adsorption are metal salts and metal oxides. Numerous metals have been studied, including metal salts (like lithium silicate and lithium zirconate), metallic lithium oxides (like Li2ZrO3, Li4SiO4, etc.), metal oxides (like CaO, MgO, etc.), and alkaline earth metal oxides (like magnesium oxide and calcium oxide) (Songolzadeh et al., 2012; Songolzadeh et al., 2014). One mole of the metal compound and one mole of CO_2 can generally result in a reversible reaction. Metal oxides (like CaO) at 923 K are converted into metal carbonates (like $CaCO_3$) at 1123 K by a series of cycles in a carbonation reactor, which regenerates the sorbent and produces a concentrated stream of CO_2 suitable for storage (Dou et al., 2010). In most chemical adsorption processes used in carbon capture, chemicals interact with one another to create CO_2 based molecule structures, which are then heated to a sufficient temperature to regenerate the collected CO_2. Most of the electricity needed in CCS is used during this process, which is regeneration. Consequently, it is necessary to create effective CO_2 capture materials and technologies that can significantly lower operation expenses by lowering regeneration costs (Ben-Mansour et al., 2016).

Chemical adsorbents can be divided into three primary groups: alkali metal oxides, carbonates, and porous materials containing amine functionalization. They include, but are not limited to, amine, potassium, sodium, and lithium-based sorbents (Wilberforce et al., 2019). CO_2 molecules can be adsorbed on the surface of these adsorbents by forming a chemical bond, primarily a covalent bond. Adsorbents used for chemical adsorption are generally produced by modifying a porous support material with a basic chemical. Amines, which have been used for a long time for absorptive capture of CO_2 in natural gas, have begun to be used in the modification of adsorbents to increase their CO_2 adsorptive capture capacity. Modification of porous support materials with a basic chemical to capture CO_2 will be discussed in a later section.

Benefits of this technology include good performance even in the presence of moisture, robust mechanical strength, and high CO_2 absorption capacity at low CO_2 partial pressure. Although this technology has many advantages, it also has several drawbacks, such as high regeneration energy requirements, poor cycle capacity because of amine degradation, amine vaporization during high-temperature operation, corrosion from regeneration, and high operating costs (Gautam and Mondal, 2023). Physical adsorption is primarily constrained by the low selectivity of CO_2, thus grafting or chemical coating can be applied to the porous adsorbent's surface. It is accomplished by integrating some fundamental chemicals with basic groups that are effective at trapping acidic CO_2 gas molecules into their structures (Ben-Mansour et al., 2016).

2.5.3.4.2. Phyical adsorption

Van der Waals forces cause the carbon dioxide gas molecules in physical adsorption (physisorption) to cling to the surface in the absence of surface-level chemical interactions. Physical adsorption occurs quickly and may be monolayer/multilayers, lower gas selectively, lower adsorption energy and desorption temperature and reversible while chemical adsorption occurs with monolayer coverage, higher gas selectivity, higher adsorption/desorption temperatures and irreversible. How an adsorbate adhare to the adsorbent surface with a physical or chemical bond is shown representatively in (Figure 2.14).

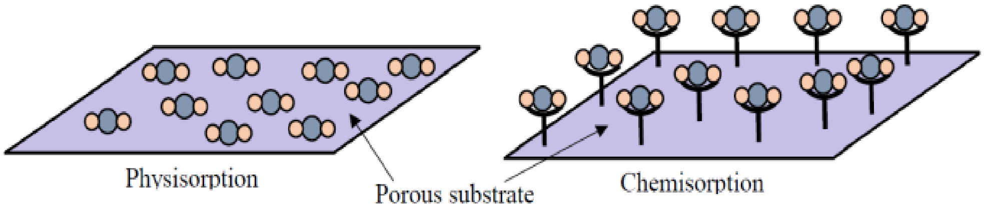

Figure 2.14 Schmatic representation of physical and chemical adsorption of a CO_2 molecule by an adsorbent.

Physical adsorption may be reversible if the adsorption and desorption of the gas molecules can be seen under the effects of pressure and temperature. When CO_2 adsorption is done at room temperature, physical adsorption is preferred, and the adsorption process is directly influenced by the adsorbent's texture (Ben-Mansour et al., 2016). The volume and size of the pores play a crucial role in physical adsorption. Cavities less than two nanometers (nm), mesopores between two and fifty nm, and macropores larger than fifty nm are referred to as micropores. The CO_2 is more selectively adsorbed by the micropores. An ideal, hypothetical adsorbent would generally have rapid adsorption and desorption kinetics, a substantial adsorption capacity, full regeneration capabilities, chemical and thermal stability, and a broad yet changeable range of operating conditions (Lua and Guo, 2001; Ogungbenro et al., 2017). Adsorption utilizing chemical adsorbents requires more energy than adsorption utilizing physical adsorbents, which include carbonaceous and non-carbonaceous materials. The reason for the reduced energy penalty for carbon dioxide regeneration is that no new bonds are formed between the carbon dioxide and the adsorbent surface (Ali et al., 2020).. Reduced CO_2 adsorption at low pressure, moisture restricting the adsorption capacity, and decreased CO_2 capture at high temperature are some drawbacks of physical adsorption (Gautam and Mondal, 2023).

Significant energy savings are a benefit of physical adsorption. These physical adsorbents, however, also have drawbacks, including low impurity tolerance and low CO_2 uptakes. The entering gas stream must also be totally dried for these adsorbents because water might reduce their adsorption capability and hasten their breakdown (Nie et al., 2018). Adsorbent preparation is less expensive, adsorbent renewal is easy and uses less energy, and physical adsorption is more effective for high-pressure activities, to name a few advantages.

2.6. Adsorbents for CO_2 Capture

Various materials have been produced and used as adsorbents to capture carbon dioxide in gas streams. In addition to the first used adsorbents such as activated carbon and zeolites, especially in the last two decades, various metal organic frameworks (MOFs), porous polymers and metal oxides have been produced and tested to capture CO_2. The number of research articles published on carbon capture by adsorption in the last 20 years is summarized in (Figure 2.15).

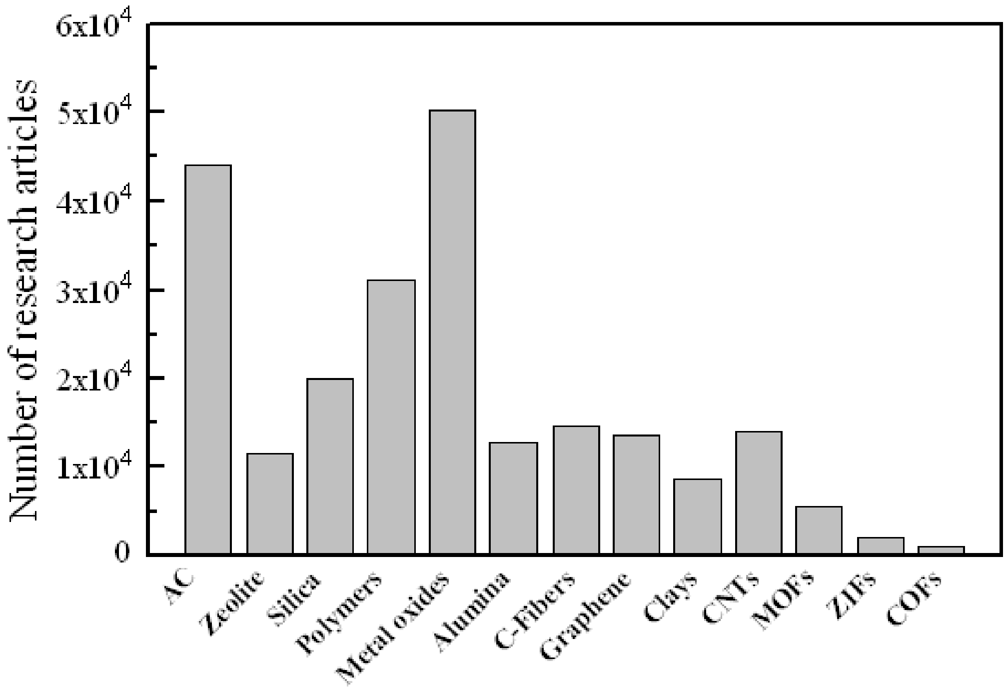

Figure 2.15 Research articles published in international journals between 2003-2023.

(Search in Science Direct with keywords of CO_2 capture and each solid adsorbent indicated in the figure")

2.6.1 Activated carbon

Activated carbon is an example of various carbon-based adsorbents (Nie et al., 2018). And it is the most frequently studied material in the literature and is widely used as an adsorbent in a variety of industrial applications, including gas purification, water treatment, and air pollution control. One of the best sorbents for separating/capturing CO_2 is activated carbon. Activated carbons are generally made from beginning materials such coal, lignite, wood, and peat that are high in carbon content but low in inorganic content (Lua and Guo, 2001).

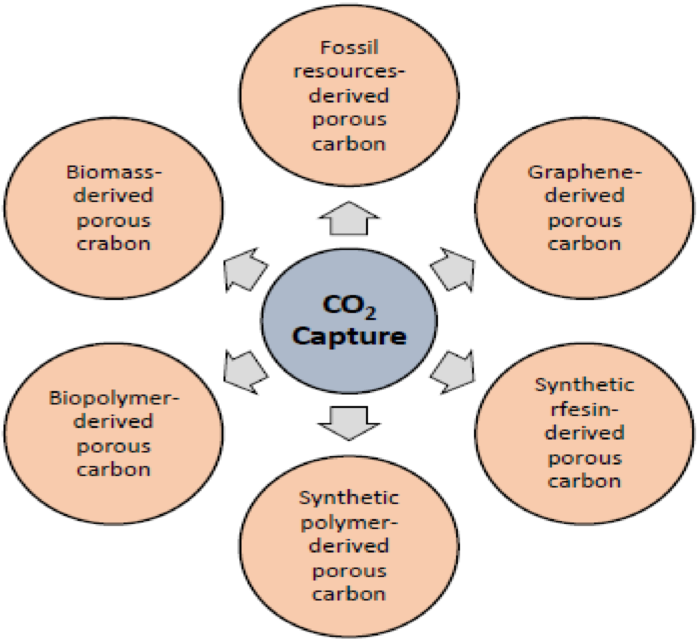

Figure 2.15 Precursors for producing porous carbon used to capture CO_2.

(Figure 2.15) shows precursors to synthesize activated carbon. The two primary steps in the conventional process of making activated carbon are (i) carbonization in an inert atmosphere at temperatures below 900 °C, and (ii) physical or chemical activation of the pre-carbonized product. The pyrolysis of raw materials in an anoxic, high-temperature environment, where the volatile components separate and the raw material develops pits and cracks, is referred to as "carbonization". The two most significant variables influencing the pyrolysis characteristics of the carbonization process are temperature and preheating rates (Jiang et al., 2019). With the pyrolysis process, a semi-coke material with native porosity and fixed carbon is produced (Ayinla et al., 2019). During the carbonization process, the bulk of the non-carbon components, such as H, O, and N, are mainly removed from the precursor materials as gases and tars, leaving behind a hard carbon skeleton. The succession of physical and chemical changes performed to the carbonized material to improve its pore structure, pore volume, specific surface area, and surface chemical characteristics is known as the "subsequent activation process (Sethia and Sayari, 2015; Kleszyk et al., 2015; Ayinla et al., 2019; Tian et al., 2021).After the activation stage, modified activated carbon with sufficient porosity, active substance and surface area is obtained. As a result of the activation process carried out using different precursors, functional groups are attached to the activated carbon surface and as a result, an activated carbon with increased carbon retention capacity is produced (Ge et al., 2022; Ge et al., 2023). They tend to be hydrophobic, have a large surface area, a high capacity to adsorb CO_2, and are thermally stable (Davini, 2002; Shafeeyan et al., 2010; Kleszyk et al., 2015; Ammendola et al., 2017). Another benefits of them are simple regeneration, low desorption temperature (<300 K), low cost, resistance to moisture and high mechanical strength (Montagnaro et al., 2015; Ogungbenro et al., 2017;Nie et al., 2018). The primary drawbacks of activated carbon include its poor CO_2 adsorption at relatively low CO_2 partial pressure because of its inert surface chemistry, its sharply declining adsorption capacities at high temperatures, and its heightened vulnerability to contaminants in the flue gas, such as NOx, SOx, and H_2O (Theo et al., 2016 ; Nie et al., 2018). Another disadvantage is that their CO_2 retention efficiency is low in the presence of moisture and low CO_2 concentrations (Ben-Mansour et al., 2016).

2.6.2. Zeolites

Zeolites can be created in the lab and are common natural minerals having microporous crystalline aluminosilicate skeletons. MnO Al_2O_3 $xSiO_2$ yH_2O is the empirical molecular formula for zeolites, where represents the valence of the cation and x and y are integers. They are composed of silicate [SiO_4] and aluminate [AlO_4] tetrahedrons connected by oxygen atoms, as seen in Figure(2.16). The range of their molecular sizes is 0.1–2.0 nm (Ghasemi et al., 2018).

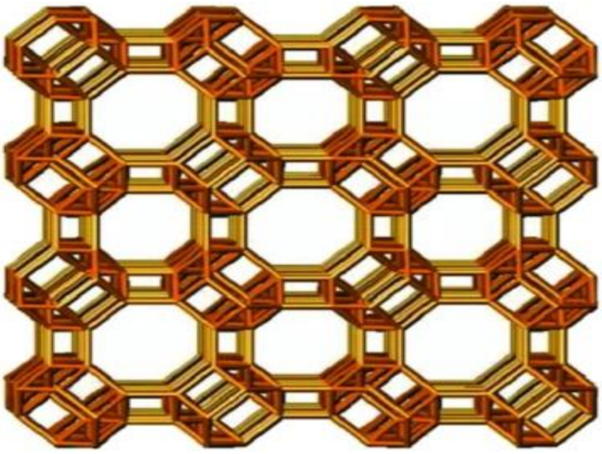

Figure 2.16 The structure of box-like zeolite.

Zeolites are divided into two groups natural and artificial. Analcime, chabazite, clinoptilolite, heulandite, natrolite, phillipsite, stilbite, mordenite, epistilbite, leumantite, neutralite, erionite, faujasite, ferrierite, gismondin, gonardite, harmatome, tomsonite, and warakite are the most prevalent naturally occurring zeolite minerals (Eroglu et al., 2017). Over 150 different varieties of synthetic zeolites have been created, while more than 60 different types of zeolites that exist naturally have been identified.

Zeolites are porous materials whose three-dimensional structure is composed of tetrahedra of SiO_4 and AlO_4. The molar ratio of silica to alumina, or Si/Al ratio, is used to characterize the characteristics of zeolites. Zeolites with a high ion exchange capacity are utilized in water softening, even if their silica content (Si/Al ratio of 2) is low. Low-silica zeolites can be converted into high-silica zeolites (Si/Al ratios of up to several thousand) by substituting silica for aluminum. It has been found that high-silica zeolites are efficient adsorbents for the removal of emerging organic compounds (OCs), such as N-nitrosamines and MTBE (Jiang et al., 2020). Zeolites have a unique capacity to molecularly sieve, which has been extensively used in separation technologies. The cationic structure of zeolite creates an electron field that interacts with a gas having a large quaternary moment, such as CO_2, and is helpful for adsorption. Porosities, electron field intensities, and alkalinities all have an impact on the adsorption properties of zeolites. Water vapor both enhances zeolites' stability and has a severe negative impact on their ability to adsorb CO_2. Zeolites are frequently limited as physical adsorbents at low temperatures. The majority of zeolites have flawless CO_2 adsorption kinetic and may reach an equilibrium state for adsorption in a matter of minutes. They are also mechanically stable enough to be formed into pellets and have good cycle stability. However, the performance of CO_2 capture is greatly influenced by temperature and pressure. Zeolites need a high temperature for regeneration (over 573 K), hence the process can use a lot of energy. Additionally, it's important to lower the high price of zeolite materials (Nie et al., 2018).

2.6.3. Metal–organic frameworks

Metal organic frameworks (MOFs) materials have two or three-dimensional porous structures made of metal centers or metal clusters joined by organic linkers, and they are crystallized (Anbia and Hoseini, 2012; Zou et al., 2021). Frequently, these substances consist of many metal-ligand connections that create three-dimensional organic-inorganic hybrid networks (Batten et al., 2013). MOFs are cage systems formed by connecting metal ions and clusters to each other with organic linkers and aligning them in different directions (Figure 2.17). Due to the coordination bonds in their structures, MOFs are also referred to as coordination networks or coordination polymers.

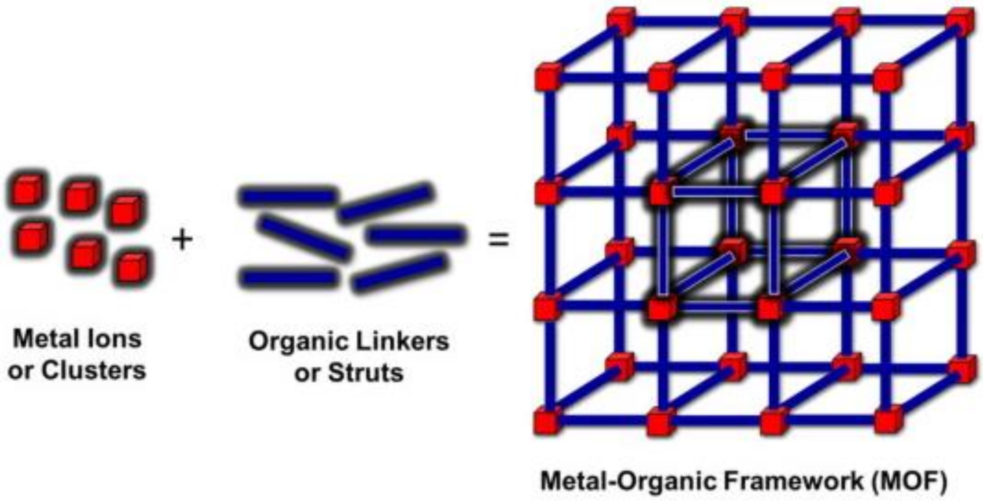

Figure 2.17 Schematic illustration of basic components of a MOF and their arrangement in the lattice system.

Their porous structures, large surface areas, chemical functionality and outstanding thermal stability offer MOFs the opportunity to be used in gas separation, gas purification, catalysts, water purification, conductive solids and supercapacitors (Farrusseng, 2011; Anbia and Hoseini, 2012).It was demonstrated that a number of MOFs and composites are effective CO_2 adsorbents (Ghanbari et al., 2020). At high pressures, MOFs can hold 10-12 times as much CO_2 as a single empty container. Other molecules can collect and store CO_2 once it has been absorbed by MOFs through their pores and channels (Younas et al., 2020). For CO_2 adsorption, the MOF's pores must be compatible with the kinetic diameter of the CO_2 molecules, which is the first important parameter to consider. Another requirement is that MOFs having polar pores (-OH, -N = N-, -NH2, and -N = C (R) -) have a better capacity for CO_2 adsorption because CO_2 molecules have quadrupole moments. So it is possible to greatly increase the CO_2 adsorption capacity and selectivity of these exceptional adsorbents by developing the MOF structure based on these requirements (Ghanbari et al., 2020).

2.6.4. Modified Adsorbents

Due to the physical adsorption of CO_2 onto adsorbents via van der Waals attraction, which results in lower adsorption capacities, researchers concentrated on altering the surface chemistry of the porous materials by adding basic sites, like amines, that can interact strongly with acidic CO_2. Grafting, impregnation and direct condensation methods are frequently applied modification processes to increase the CO_2 capture capacity of porous support materials. Although amines are the most preferred chemicals in CO_2 capture, they are difficult to use in direct condensation due to their high boiling points. The surface of porous support materials has to form aminal, amide, imide, and imidazole linkages in order for amine monomers to polymerize with them (Xu and Heidin, 2014). Grafting and impregnation are widely used procedures to insert organic molecules containing amino groups on the supports for CO_2 collection, in contrast to direct condensation. Only on mesoporous high surface area supports can grafting and surface polymerization of an adsorbent surface be accomplished (Gebald et al., 2010). The density of nitrogen in the grafted chemical and the existence of OH groups that can make covalent connections with amine species on the solid surface determine how successful dry and wet grafting techniques are (Wang et al., 2011; Aziz et al., 2012; Fusco et al., 2018; Vieira et al.

2018; Zhang et al., 2019). Physical impregnation loads a significant amount of amine into the support, but during the course of prolonged operations, amine leaches out of the impregnated support. The impregnated amine needs to have a high boiling point and the adsorption process needs to be carried out at a low operating temperature in order to stop the amine leaching (Sanz-Perez et al., 2018). Following the literature a summary of modified porous supports materials and the most used chemicals for the modification are given in Table (2.3) and Table (2.4) respectively.

Table 2.3 Modified adsorbents for CO_2 capture.

Types of porous materials	Modified adsorbents	Reference
Silicates	Silica gel	(Chen and Bhattacharjee, 2017; Sakpal et al. 2012 ; Zhanget al. 2012 ;Martin et al. 2016; Zhao et al. 2012; Wang et al. 2012)
	Silica aerogel	(Linneen et al. 2013)
	SBA-12	(Zelenak et al. 2008)
	SBA-15	(Cecilia et al.2020 ; Haydari-Gorji et al. 2011; Ji et al. 2016; Jing et al. 2014 ; Liu et al. 2010; Liu et al. 2017; Mamonovetal. 2018; Sanz-Perez et al. 2013; Sanz-Perez et al.2016; Tang et al. 2017; Ullah et al. 2015; Vilarrasa et al. 2015; Wang et al. 2017; Wei et al. 2017; Yan et al. 2011; Zhang et al. 2013; Zhang et al. 2018; Zhao et al. 2013; Watabe et al. 2013; Yildiz et al. 2019)
	SBA-16	(Wei et al. 2008 ; Liu et al. 2017

		; Wu et al. 2018)
	MCM-41	(Ahmed S. et al. 2016; Frachi et al. 2005; Fujiki et al. 2015; Haydari-Gorji et al. 2011; Haydari-Gorji et al. 2011; Heydari-Gorji et al. 2011; Ji et al. 2016 ; Kim et al. 2008; Le et al. 2014; Liu Et al. 2015 ; Mello et al. 2011; Rao et al. 2018; Sanz et al. 2015 ; Teng et al. 2017; Wang et al. 2015; Wang et al. 2015; Xu et al. 2002; Xu et al. 2003; Yildiz et al. 2019)
	MCM-48	(Huang et al. 2003; Nigar et al. 2016 ; Heo et al. 2016)
	KIT-6	(Liu et al. 2010 ; Kishor et al. 2015; Mei et al.2018; Lin et al. 2017; Liu et al.2018; Wei et al. 2018)
	Nanoporous silica	(Chen and Bhattacharjee, 2017; Kim and Ko 2018)
	Mesoporous silica	(Babaie et al.2014 ; Alkhabbaz et al. 2014; Al-Marri et al. 2017 ; De Avila et al. 2016 ;Hou et al. 2018 ; Jiao et al. 2014 ; Jiao et al. 2016 ; Kim et al. 2008 ; Kishor et al.2016; Knowles etal. 2005 ; Knowles and Chaffee 2016 ; Lee et al. 2013; Sanz-Perez et al. 2018; Vu et al. 2018 ; Watabe et al. 2013; Wang et al. 2015 ;Ma et al. 2014)

	Macroporous silica	(Radu et al. 2016)
	Silica foam	(Deng etal. 2019; Feng et al. 2013 ; Feng et al. 2013 ; Han et al. 2015; Jung et al. 2017 ; Liu et al. 2010; Liu et al. 2013; Liu et al. 2015; Liu et al. 2016; Ma et al. 2014; Yan et al. 2011; Subagyono et al. 2011 ; Zhao et al. 2019)
	Monolitic silica	(Maresz et al. 2020)
	Hollow silica	(Bae 2017)
Clays	Bentonite	(Wang et al. 2013; Gomez-Pozuelo et al. 2019; Chen et al. 2013; Nousir et al. 2019 ; Vilarrasa-Garcia et al. 2017b; Horri et al. 2019)
	Montmorillonite	(Gomez-Pozuelo et al. 2019; Roth et al. 2013 ;Wang et . 2014; Stevens et al. 2013)
	Sepiolite	(Gomez-Pozuelo et al. 2019; İrani et al. 2014 ;Liu et al. 2018)
	Saponite	(Gomez-Pozuelo et al. 2019)
	Palygorskite	Gomez-Pozuelo et al. 2019; Ma et al. 2017)
	Kaolinite	(Wang et . 2014)
Ashes	Fly ash	(Sarmah et al. 2013;Guo et al. 2019)
Hydrotalcites	HTCs	(Hanif et al. 2014)
Aerogels	AGs	(Kong et al. 2016 ; Linneen et al. 2013 ; Linneen et al. 2013 ;Zang et al. 2019)

	GOFs	(Haque et al. 2017)
MOFs	MIL-101	(Li et al. 2019; Li et al. 2016; Lin et al. 2013; Sun et al. 2018; Yoo et al. 2018; Zhang et al. 2017)
	HKUST-1	(Martinez et al. 2016)
	IRMOF-3	(Ullah et al. 2019)
	MIL-53 (Al)	(Martinez et al. 2016;Abid et al. 2018)
	MIL-53	(Mamonov et al.2018)
	ZIF-8	(Martinez et al. 2016 ;Mamonov et al.2020)
	Zn-MOF	(Bien et al. 2018)
	UiO66 (Zr)	(Yu and Balbuena 2015)
	UiO-66-NH_2 (Zr)	(Zhu, et al. 2019)
	Mg/DOBDC	(Andirova et al. 2015)
Zeolites	Y-type	(Su et al. 2010; Lee et al. 2012 ;Thakkar et al. 2017; Kim et al. 2016)
	13X	(Karka et al. 2019; Bezerra et al. 2011; Chen et al. 2015)
	4A	Panda et al. 2019; Wang and Yang 2019)
	5A	(Lie etal. 2016)
	ZMF-5	(Thakkar et al. 2017 ; Lee et al. 2015 ; Lin et al. 2017 ;Wang et al. 2018)
	SAPO-34	(Thakkar et al. 2017)
Porous	OPs	(Sanz-Perez et al. 2019; Kong et al. 2019)
	HPPN	(Mane et al. 2018)

polymers	MF/PAM	(Yin et al. 2018)
Activated carbons	ACs	(Adelodun et al. 2016; Bezerra et al. 2011; Lee et al. 2013; Lewcka 2017 ; Mahurin et al. 2014 ;Tseng et al. 2015 ;Wang and Guo 2016 ;Wang et al. 2015; Wang et al.2013; Wei et al. 2017 ; Yaumi et al. 2018; Shafeeyan et al. 2011; Tang et al. 2013 ; Gholidoust et al. 2017 ;Khalil et al. 2013)
	ACNFs	(Bai et al. 2015; Chiang et al. 2017 ; Chiang et al.2019;Abbasi etal.2019)
Nanotubes	CNTs	(Deng and Park 2019 ; Kommalapati et al. 2020)
	MWCNTs	Fatemi et al.2011; Gui et al. 2013 ; Liu et al. 2014 ;Khalil et al. 2013)
	PTNTs	(Guo et al. 2016)
	SNTs	(Yao et al. 2013)
	E-SNTs	(Yao et al. 2013)
Nanofibers	CNFs	(Abbasi et al. 2019a)
	PONFs	(Abbasi et al. 2019b)
Resins	MF	(Yin et al. 2017)
	HP20	(Chen et al. 2013)
	D101	(Yang et al. 2019)
	XAD-4	(Liu et al. 2017; Jo et al. 2015)
	X-5	(Yang et al. 2019)
	ADS-17	(Yang et al. 2019)
	PAN	(Liu et al. 2018)

Oxides	γ-Al_2O_3	(Chaikittisilp et al. 2011)
	TiO_2	(Ma et al. 2013; Ma et al. 2014; Kapica-Kozar et al. 2017)
	SiO_2	(Lai et al. 2020)
	GO	(Zhao etal. 2012; Hong et al. 2013)
	MgO	(Kasikamphaiboon and Khunjan 2018)

Table 2.4 Types of chemicals used for adsorbent modification.

Adsorption modification compounds	Types of chemical	Reference
Aminating compounds	PEI	(Wang et al. 2014 ; Vilarrasa-Garcia et al. 2015 ; Kishor et al. 2016 ; Liu et al. 2015; Ma et al. 2014; Le et al. 2014 ; Rao et al. 2018; Yang et al. 2019 ; Deng et al. 2019;Lee et al. 2015)
	TEPA	(Wang et al. 2015 ; Vilarrasa-Garcia et.al. 2017b ; Martinez et al. 2016 ; Jiao et al. 2014; Linneen et al. 2013 ; Liu et al. 2013; Liu Et al. 2015; Wei et al. 2017)
	MEA	(Sarmah et al. 2013)
	DEA	(Franchi et al. 2005 ;Sarmah et al. 2013)
	DIPA	
	EDA	(Liu Et al. 2015)
	TEA	(Wei et al. 2017)
	DETA	(Liu Et al. 2015 ; Ma et al. 2014)
	APTES	(Wang et al. 2015 ; Lai et al. 2020;Rao

		et al. 2018)
	APTMS	(Ma et al. 2014)
	PEHA	(Liu et al. 2015)
	MEPEG	(Wnag et al. 2019)
	PEPA	
	NH_4OH	(Ullah et al 2015)
	PANI	(Yoo et al. 2018)
Grafting compounds	AP	(Sanz-Perez et al. 2013)
	ED	(Calleja et al. 2011)
	DT	(Calleja et al. 2011:135)

2.7. Adsorption Isotherms

Adsorption isotherm is a graphic representation of the equilibrium between adsorbent and adsorbate at constant temperature. The simplest of this equilibrium model is the Langmuir isotherm, in which the adsorbate molecules form a monocoverage on the flat and homogeneous adsorbent surface and these molecules do not interact with each other. The mathematical representation of Langmuir isotherm can be seen in Equation 1.

$$q_e = \frac{K_L.P_e.q_m}{1+K_L.P_e} \quad (2.1)$$

q_e is the quantity of gas adsorbed on the surface of the adsorbent (mg/g), q_m represents the maximum adsorption capacity (monolayer coverage (mg/g), K_L is the Langmuir constant represents the affinity (sorption/desorption) of binding sites and related to the adsorption energy and Pe is the equivalent pressure of adsorbate gas (kPa). The constants (K_L and q_{max}) in the equation are found using the linearized Langmuir equation below.

$$\frac{P_e}{q_e} = \frac{1}{K_L.q_m} + \frac{P_e}{q_m} \quad (2.2)$$

Using Equation 2, $1/K_L.q_m$ is calculated from the intercept of the line and $1/q_m$ is calculated from the intercept by plotting P_e/q_e against P_e. The Langmuir model can also be linearized as follows;

$$\frac{1}{q_e} = \frac{1}{K_L.P_e.q_m} + \frac{1}{q_m} \quad (2.3)$$

Here a plot of $1/q_e$ versus $1/P_e$ should give a straight line with intercept $1/q_m$ and slope $1/K_L.q_m$.

If the adsorbates adhere to a heterogeneous surface with both monolayer and multilayer, the Freundlich model given in Equation 4 below may be more suitable for this type of adsorption.

$$q_e = K_F . q_e^{1/n} \qquad (2.4)$$

In Equation 4, K_F is the Freundlich constant and n is the Freundlich isotherm exponent. To find the value of the constants in the Freundlich isotherm, its linearized form below is used.

$$log q_e = log K_F + \frac{1}{n} . log P_e \qquad (2.5)$$

The intercept and slope of a log-log plot of Eq. 5 give $logK_F$ and 1/n, respectively.

In some cases, the adsorbate adheres to the adsorbent surface in a multilayer manner. It is assumed that the Langmuir model is valid in each layer and there is no transition between layers. This multilayer adsorption model is expressed by the Brunauer-Emmett-Teller isotherm given in Equation 6.

$$q_e = \frac{K_B . P_e . q_m}{(P_s - P_e) . \left\{1 + (K_B - 1) . (\frac{P_e}{P_s})\right\}} \qquad (2.6)$$

Here P_s is the saturation pressure, K_B is the BET constant related to the binding intensity of the adsorbate. The linearized form of the BET isotherm model is,

$$\frac{P_e}{(P_s - P_e) . q_e} = \frac{K_B - 1}{K_B . q_m} . \frac{P_e}{P_s} + \frac{1}{K_B . q_m} \qquad (2.7)$$

A plot of $P_e/[(P_s-P_e).q_e]$ versus P_e/P_s gives a straight line with slope $(K_B-1)/(K_B.q_m)$ and intercept equal to $1/(K_B.q_m)$

It is also possible for adsorbates to adhere to the adsorbent surface in other ways. In Figure (2.18) below, the IUPAC (International Union of Pure and Applied Chemistry) classification of isotherms belonging to adsorption types is shown graphically.

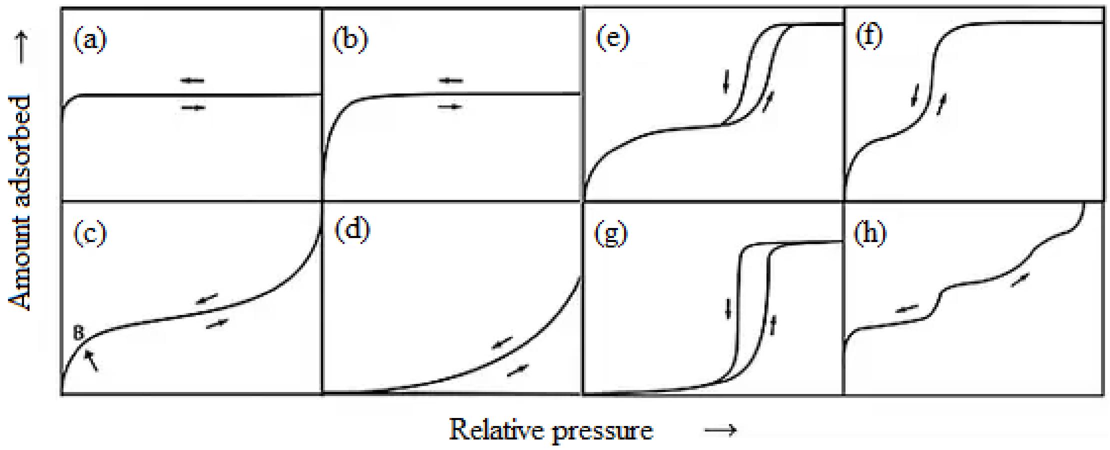

Figure 2.18 Graphical representation of IUPAC classification of adsorption types

Each type of adsorption isotherms above represents the pore size and surface character of the material. Adsorption of microporous materials such as zeolite (a), adsorption on partially microporous materials such as activated carbons (b), adsorption non nonporous materials such as nonporous silica and magnetic powder (c), adsorption on nonporous materials and materials which have weak interaction with adsorbate (for example graphite/water) (d), adsorption on mesoporous materials such as mesoporous silica and alumina (e), adsorption on mesoporous materials with pore diameters smaller than 4 nm (e.g. MCM-41) (f), adsorption on porous materials and materials that have the weak interaction with adsorbate (e.g. activated carbon/water) (g), and homogenous surface materials such as graphite/Kr and NaCl/Kr (h).

3. MATERIALS AND METHODS

In this study, different polymeric hydrogels were produced and used to capture CO_2 from the CO_2/N_2 gas mixture. Hydrogels are three-dimensional long polymer chains formed as a result of the monomers, which are the backbone of the polymeric structure, being made reactive by an initiator and the reactive monomers being cross-linked to each other with a crosslinker (Figure 3.1).

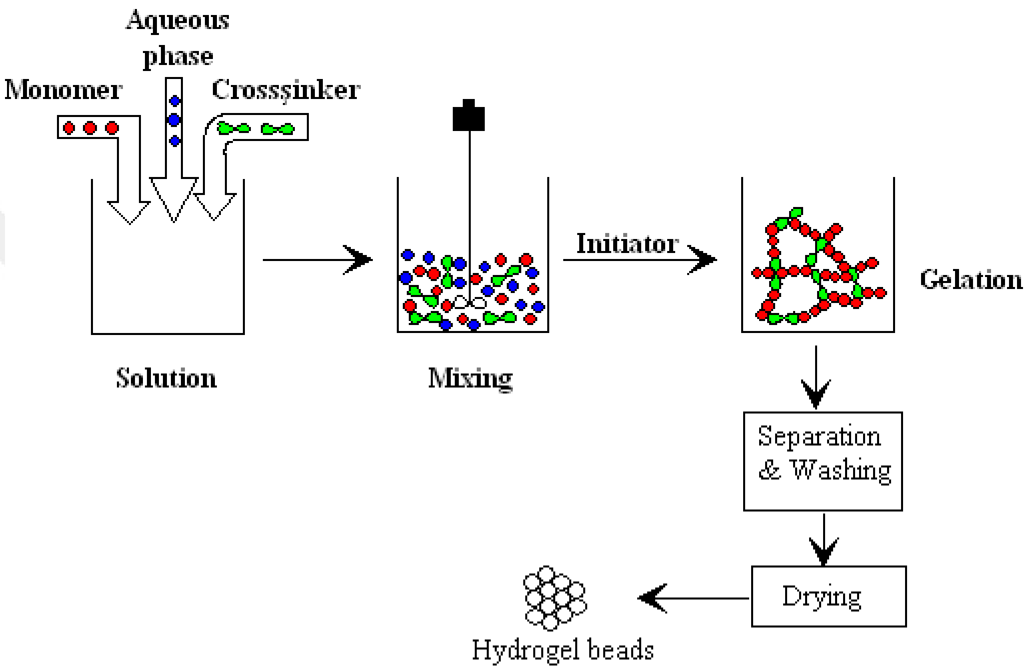

Figure 3.1 Representation of Hydrogel preparation.

3.1 Chemicals Used

The following chemicals used in this study were purchased from Sigma Aldrich and used without any pretreatment.

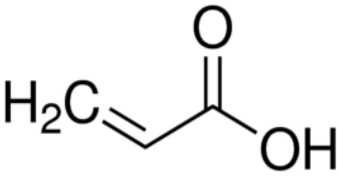

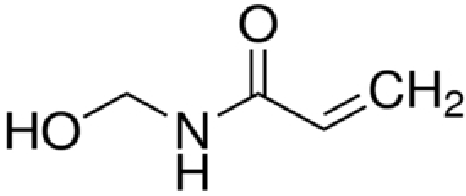

Acrylic acid (AAc) N-Hydroxyethyl acrylamide (N-NEHA)

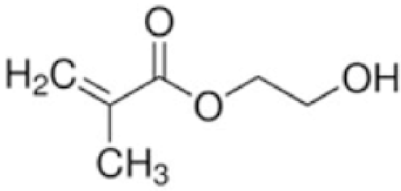

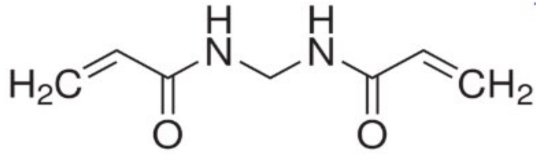

2-hydroxyethyl methacrylate (HEMA) N.N’-methylenebisacrylamide (MBA)

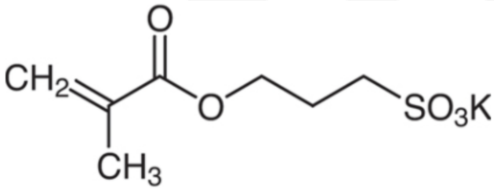

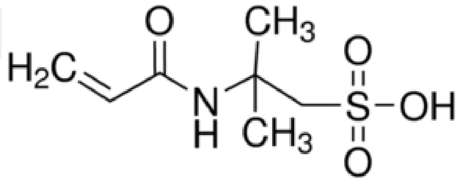

3-Sulfopropylmethacrylate potassium salt (SPMP) 2-Acrylamido-2-methylpropane sulfonic acid (AMPSA)

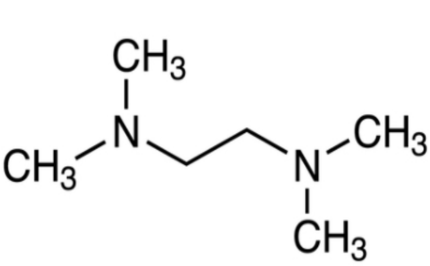

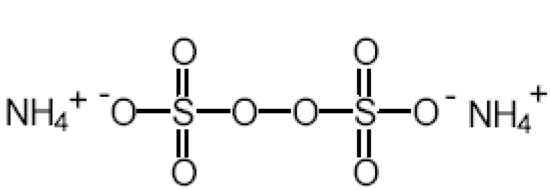

Tetramethylethylene diamine (TEMED) Ammonium peroxodisulfate (APS)

TEMED is a tertiary amine that is used to catalyze the formation of free radicals from ammonium persulfate or riboflavin. Such TEMED generated free radicals cause the compounds acrylamide and bis-acrylamide to polymerize and form the gel matrix polyacrylamide.

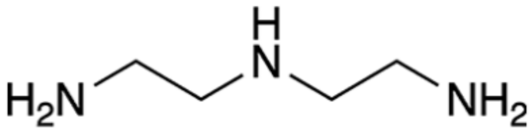

Diethylenetriamine (DETA)

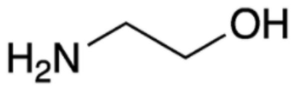

Ethanolamine (EOA)
Monoethanolamine (MEA)

3.2 Synthesis of Poly (2-hydroxyethyl methacrylate) Hydrogel, P(HEMA)

PHEMA hydrogel is obtained by connecting HEMA monomers to each other with MBA cross-linker. First, 4 mL HEMA, 12.7 mg MBA and 0.025 mL distilled water were placed in a vortex tube and this mixture was mixed with a magnetic stirrer at 200 rpm for 1 hour at room temperature. Then, 30μL TEMED was added to the mixture and then vortexed for 1 minute. 112.9 mg APS was added to this vortexed mixture and vortexed again for another 2 minutes. This last mixture was transferred to a plastic pipette with a diameter of 6 mm and one end closed, and after the transfer process, the other end of the pipette was also closed. The pipette tube was placed in the shaker and the gelation reaction was allowed to occur by shaking at 70 rpm for 24 hours at room temperature. The pipette containing the gel was cut to a length of 1 cm, the gels inside were taken out and washed with distilled water for 2 days. Finally, the gels were dried in the fume hood for 24 hours to take their final form (Figure 3.2).

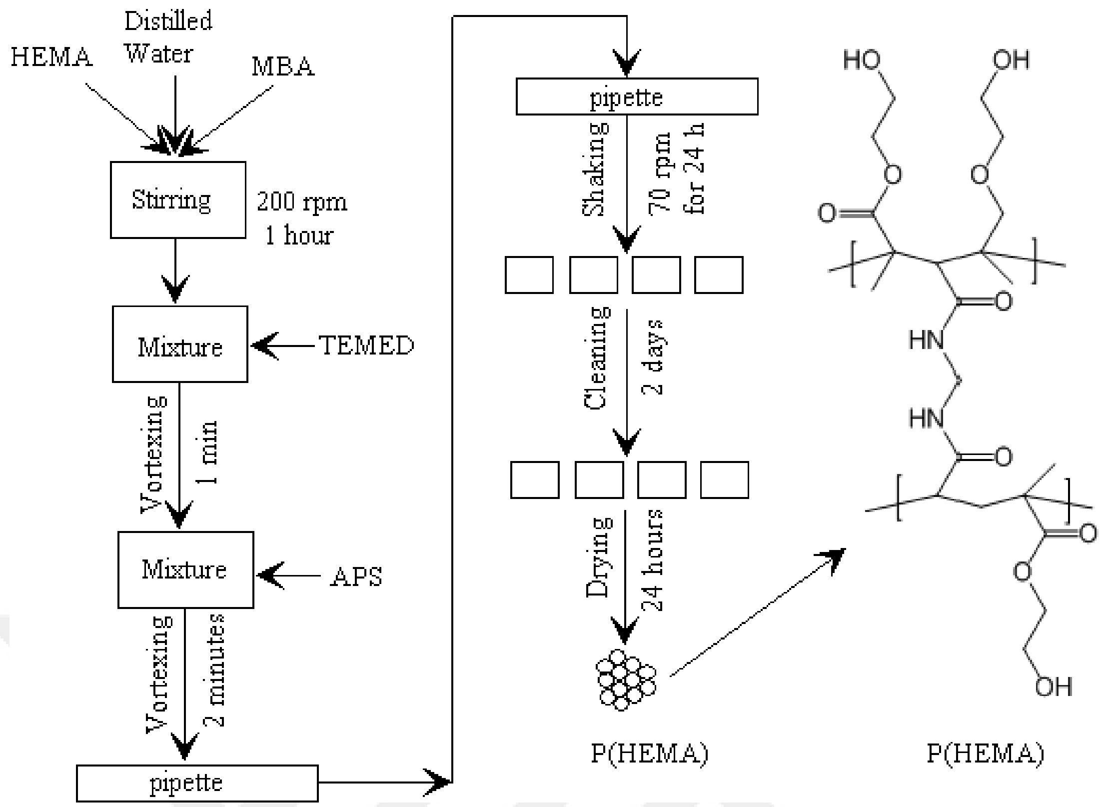

Figure 3.2 Schematic representation of the synthesis of PHEMA hydrogel.

3.3 Synthesis of Poly (N-hidroksietilmetakrilat) Hydrogel, P(N-HEA)

P(N-HEA) hydrogel is obtained by connecting N-NEHA monomers to each other with MBA cross-linker. First, 5 g N-HEA, 66 mg MBA and 5 mL distilled water were placed in a vortex tube and this mixture was mixed with a magnetic stirrer at 200 rpm for 1 hour at room temperature. Then, 30 μL TEMED was added to the mixture and then vortexed for 1 minute. 147 mg APS was added to this vortexed mixture and vortexed again for another 2 minutes. This last mixture was transferred to a plastic pipette with a diameter of 6 mm and one end closed, and after the transfer process, the other end of the pipette was also closed. The pipette tube was placed in the shaker and the gelation reaction was allowed to occur by shaking at 70 rpm for 24 hours at room temperature. The pipette containing the gel was cut to a length of 1 cm, the gels inside were taken out and washed with distilled water for 2 days. Finally, the gels were dried in the fume hood for 24 hours to take their final form (Figure 3.3).

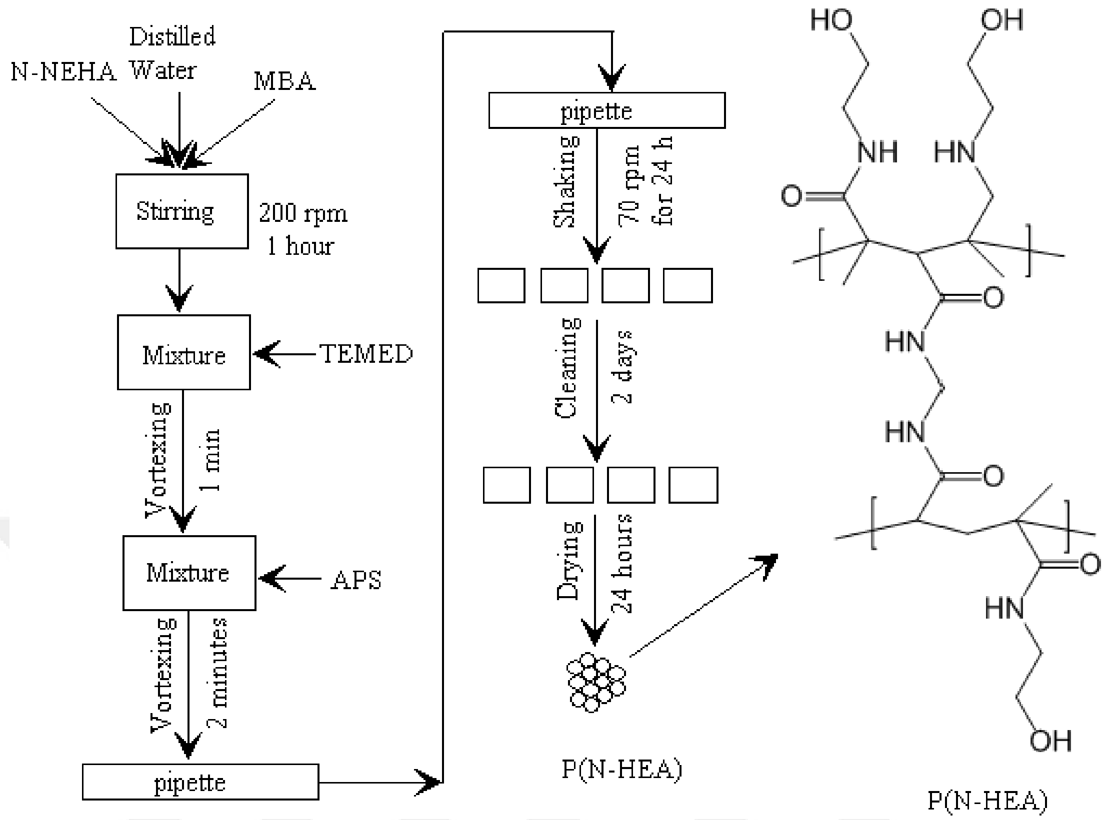

Figure 3.3 Schematic representation of the synthesis of P (N-HEA) hydrogel.

3.4 Synthesis of Poly (2-acrylamido-2-methylpropane sulfonic acid) Hydrogel, P(AMPSA)

P(AMPSA) hydrogel is obtained by connecting AMPSA monomers to each other with MBA cross-linker. First, 5 g AMPSA, 715 µl MBA and 4.25 mL distilled water were placed in a vortex tube and this mixture was mixed with a magnetic stirrer at 200 rpm for 1 hour at room temperature. Then, 30 µL TEMED was added to the mixture and then vortexed for 1 minute. 82.5 mg APS was added to this vortexed mixture and vortexed again for another 2 minutes. This last mixture was transferred to a plastic pipette with a diameter of 6 mm and one end closed, and after the transfer process, the other end of the pipette was also closed. The pipette tube was placed in the shaker and the gelation reaction was allowed to occur by shaking at 70 rpm for 24 hours at room temperature. The pipette containing the gel was cut to a length of 1 cm, the gels inside were taken out and washed with distilled water for 2 days.

Finally, the gels were dried in the fume hood for 24 hours to take their final form (Figure 3.4).

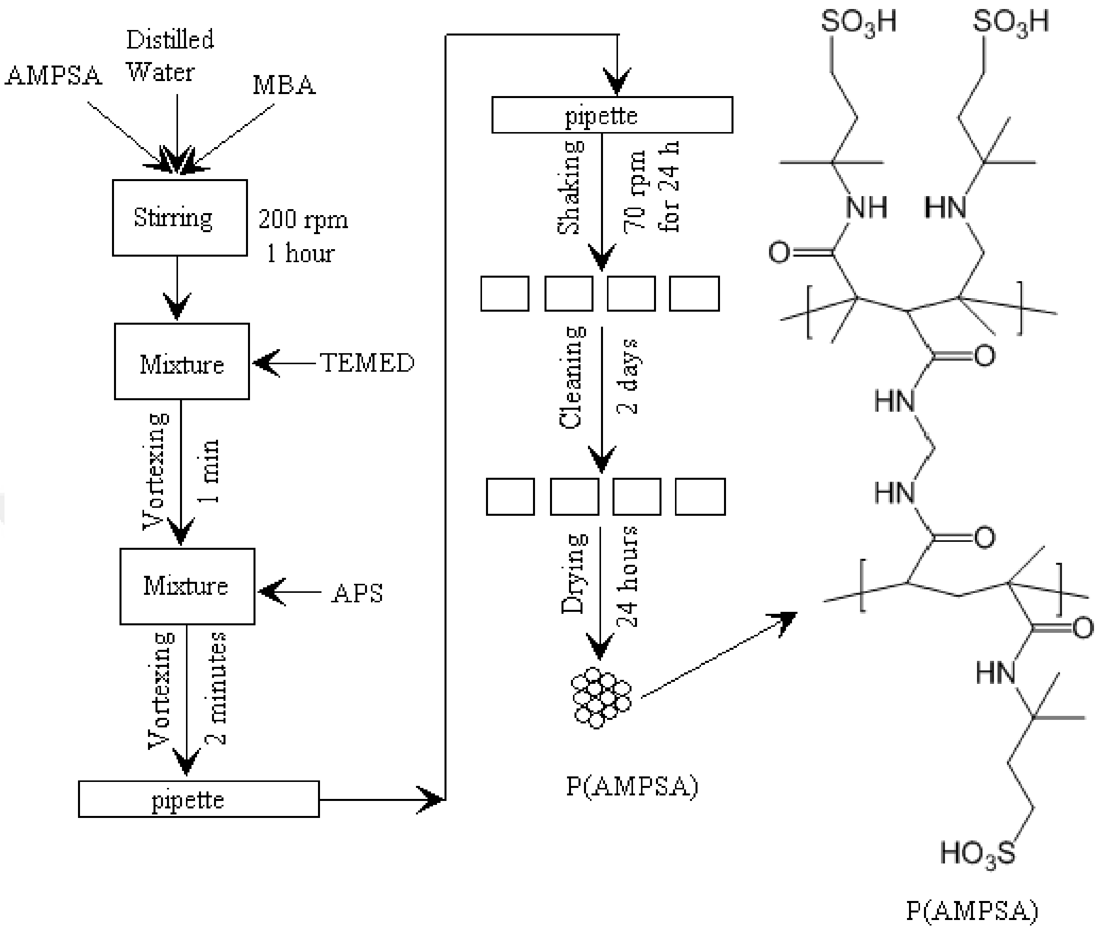

Figure 3.4 Schematic representation of the synthesis of P(AMPSA) hydrogel.

3.5 Synthesis of Poly (3-Sulfopropyl methacrylate potassium salt) Hydrogel, P(3-SPMP)

P (3-SPMP) hydrogel is obtained by connecting 3-SPMP monomers to each other with MBA cross-linker. First, 4.5 g 3-SPMP, 28 mg MBA and 4.5 mL distilled water were placed in a vortex tube and this mixture was mixed with a magnetic stirrer at 200 rpm for 1 hour at room temperature. Then, 20 μL TEMED was added to the mixture and then vortexed for 1 minute. 62.5 mg APS was added to this vortexed mixture and vortexed again for another 2 minutes. This last mixture was transferred to a plastic pipette with a diameter of 6 mm and one end closed, and after the transfer process, the other end of the pipette was also closed. The pipette tube was placed in the shaker and the gelation reaction was allowed to occur by shaking at 70 rpm for 24 hours at room temperature. The pipette containing the gel was cut to a length of 1 cm, the gels inside were taken out and washed with distilled water for 2 days. Finally, the gels were dried in the fume hood for 24 hours to take their final form (Figure 3.5).

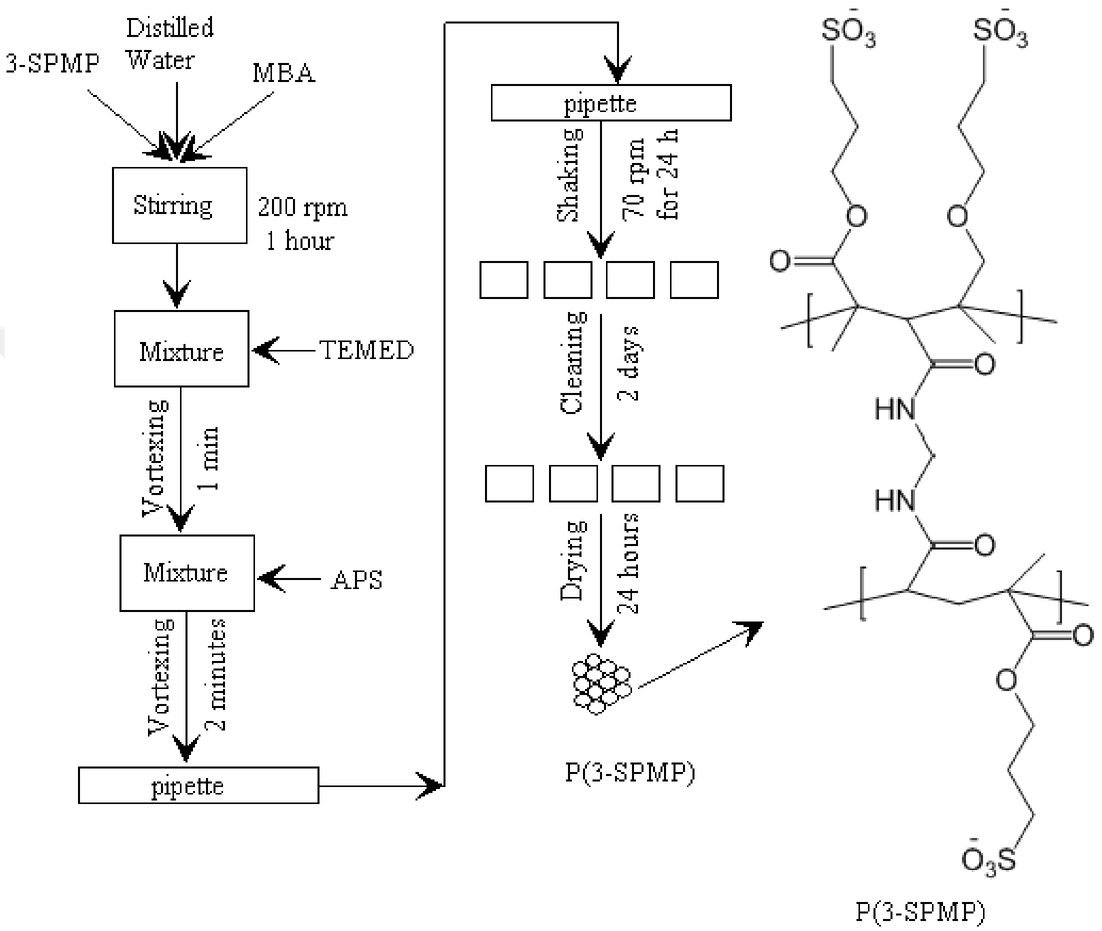

Figure 3.5 Schematic representation of the synthesis of P(3-SPMP) hydrogel.

3.6 Synthesis of Poly (Acrylic acid) Hydrogel, P(AAc)

P(AAc) hydrogel is obtained by connecting AAc monomers to each other with MBA cross-linker. First, 5 mL AAC, 112 mg MBA and 5 mL distilled water were placed in a vortex tube and this mixture was mixed with a magnetic stirrer at 200 rpm for 1 hour at room temperature. 24.96 mg APS was added to this mixture and vortexed for 2 minutes. This last mixture was transferred to a plastic pipette with a diameter of 6 mm and one end closed, and after the transfer process, the other end of the pipette was also closed. The pipette tube was placed in the shaker and the gelation reaction was allowed to occur by shaking at 70 rpm for 24 hours at room temperature. The pipette containing the gel was cut to a length of 1 cm, the gels inside were taken out and washed with distilled water for 2 days. Finally, the gels were dried in the fume hood for 24 hours to take their final form (Figure 3.6).

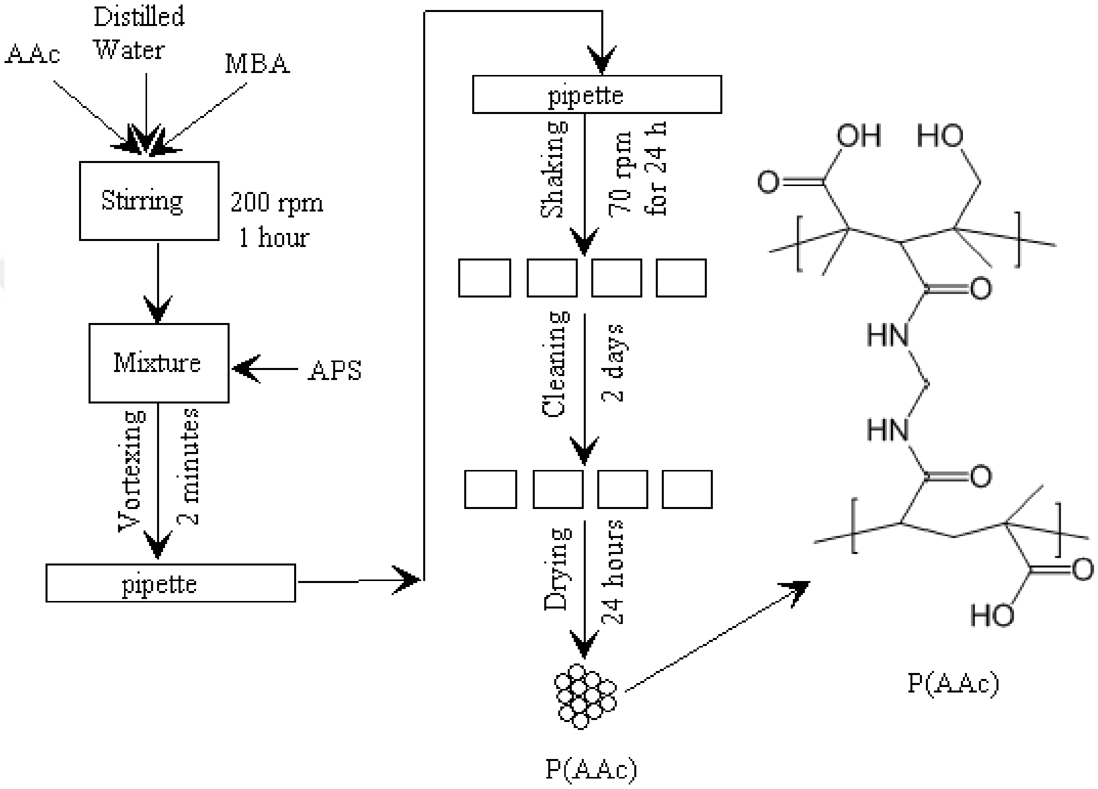

Figure 3.6 Schematic representation of the synthesis of P(AAc) hydrogel.

3.7 Modification of Hydrogels Using Amines

The hydrogels prepared above were modified using DETA and EOA for CO_2 adsorption. 0.2 g of amine was added to 5 g of hydrogel and it was allowed to absorb the amine for 12 hours. The amine-impregnated hydrogel was washed with pure water for 15 minutes and then frozen with liquid nitrogen. Frozen modified hydrogels were dried with a lyophilizer and stored in a desiccator to be used in CO_2 adsorption. In this study, when the DETA:hydrogel ratio was used as 20%, it was called DETA-1, while when the DETA:hydrogel ratio was 30%, it was called DETA

3.8 Characterization of Amin-Modified Hydrogels

3.8.1 SEM Imaging

The most common method used to characterize the microarchitectural structure of hydrogels is imaging the hydrogel with a scanning electron microscope (SEM). SEM imaging was applied to reveal the morphological structure of the produced hydrogels. The morphological structures of modified hydrogels were performed with Jeol JSM-7001 F (USA) brand SEM device (Figure 3.7).

Figure 3.7 SEM device.

3.8.2 TGA Analysis

Thermogravimetric analysis (TGA) is a technique used to determine the thermal stability of materials. In this method, the weight change of the material is detected as moisture and other volatile substances in the material structure are removed due to increasing temperature. Since the kinetics of thermal weight losses of the samples, that is the degradation state, were determined generally with the TGA technique, the degradation state of the hydrogels produced for CO_2 adsorption were tried to be determined by TGA (SDT Q600, TA Instruments, USA) (Figure 3.8). For this purpose, 5 mg of hydrogel was placed in the aluminum sample container of the TGA and the weight loss was determined in a nitrogen gas atmosphere with a temperature increase rate of 10 ^oC from room temperature to 1000 ^oC.

Figure 3.8 TGA device

3.8.3 FTIR Analysis

Using infrared light to scan the sample, this analyzer helps us observe the chemical properties of the sample as each molecule or chemical structure produces a unique spectral fingerprint. Hydrogel samples were placed on the diamond of the FTIR (Tensor 27, Bruker, USA) (Figure 3.9) device and spectra were obtained in the range of 4000 cm^{-1} and 400 cm^{-1} and with a resolution of 1 cm^{-1} at 30% nitrogen gas pressure.

Figure 3.9 FTIR device.

3.9 Gas Adsorption

Gas adsorption experiments were carried out at room temperature (293±2 K) using an adsorption cell operating with the constant volume varying pressure method (Figure 3-10 and 11). The internal pressure was measured using a pressure transducer (Enelsan, Turkiye) connected on the cylindrical of GSC made of brass and the GSC was kept closed with a screw closure cap on which there was a sample point for injecting and taking gas samples. A rubber septum was housed inside the sample point and this septum was tightened with a hole-nut. It was determined by the preliminary test whether there was any gas leakage from the GSC. N_2 gas was filled into the GSC at the maximum internal gas pressure to be used in the experiments, and the presence of leakage was checked with a pressure transducer for 24 hours.

For CO_2 adsorption, 0.25 g of hydrogel was weighed using a microbalance (Figure 3.12) (Model: AS 220. R2, RADWAG, Germany) and filled into a sample container

(SC), the SC was placed in the GSC and the screw closure cap of the GSC was closed. The inner atmosphere of the GSC was evacuated with a vacuum pump (Vacuubrand, Germany) (Figure 3.13) and then pure N_2 gas (99.99%) filled into the GSC at atmospheric pressure. If the internal pressure of the GSC filled with N_2 gas was above the atmospheric pressure, the internal pressure is reduced to atmospheric pressure with a syringe needle. After the adsorbents were prepared, they were kept in a desiccator in a normal atmosphere, so whether they adsorb N_2 gas was not tested. CO_2 gas was injected into the GSC, which contained N_2 gas, through the rubber septum with a syringe to provide the desired CO_2 concentration.

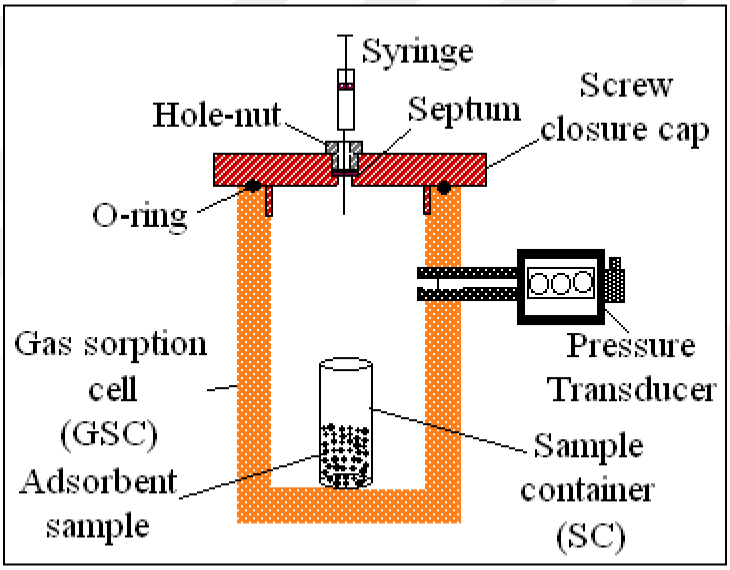

Figure 3.10 Schmatic drawing of gas adsorption cell (GSC).

Figure 3.11 GSC used for gas adsorption.

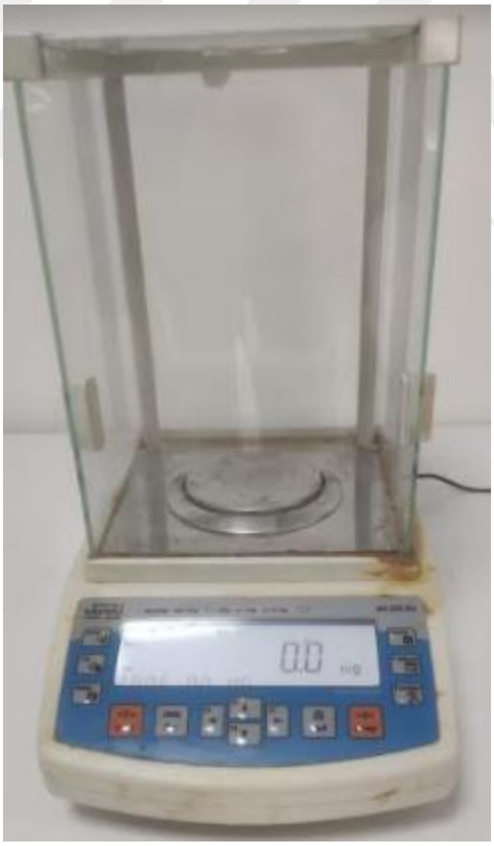

Figure 3.12 Microbalance.

Figure 3.13 Vacuum pump.

The amount of adsorbed CO_2 gas was determined using the previously prepared calibration chart (Figure 3.14). The calibration chart was obtained by injecting known amounts of CO_2 gas into the GSC, which already contains CO_2 gas at atmospheric pressure but no adsorbent. The graph is plotted against the amount of CO_2 gas injected into the GSC versus the value read on the transducer. In the equation y=999.634 +10.33062X in the (Figure 3.14), y- is the value read on the pressure transducer and X- is the volume of CO_2 injected into the GSC.

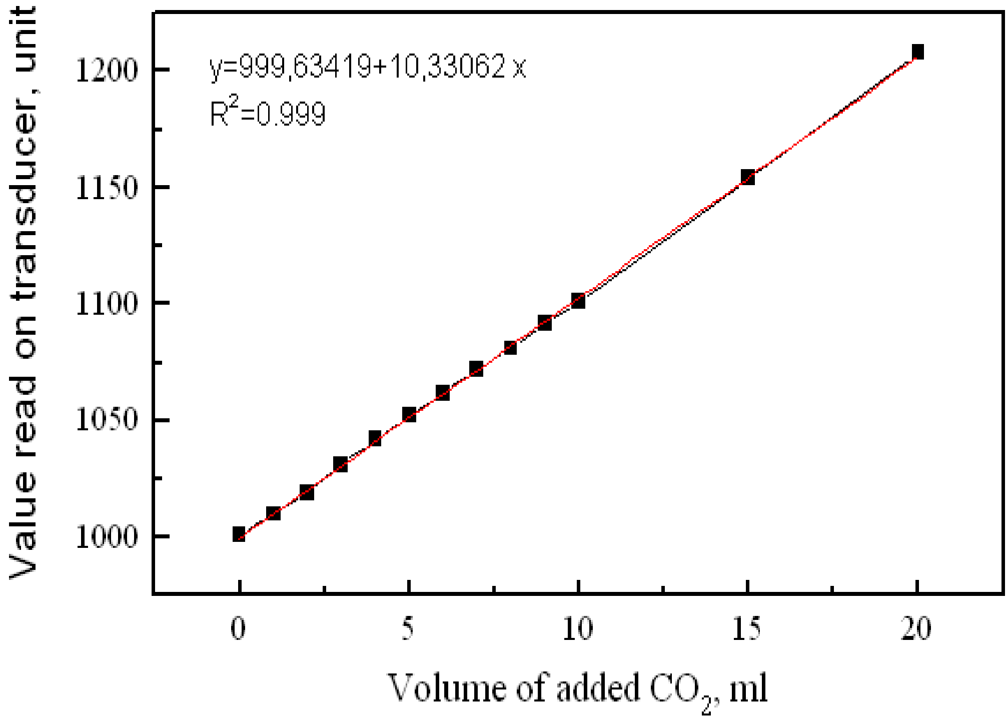

Figure 3.14 Pressure calibration for GSC.

When determining the adsorption capacity of an adsorbent at different CO_2 pressures, the adsorbent in the GSC was not changed and the gas was not evacuated. A certain amount of CO_2 gas was injected again onto the unadsorbed CO_2/N_2 mixture in the GSC when the adsorption ended with a pressure. The amounts of adsorbed and unadsorbed CO_2 were calculated using the calibration curve. In this way, different CO_2 partial pressures were tested without changing the adsorbent in the GSC.

4. RESULTS AND DISCUSSION

Hydrogels, which are used in various applications, were used to capture carbon dioxide in this study. Five different synthesized hydrogel structures were modified by loading monoethanol amine (MEA) and diethylenetriamine (DETA) and their CO_2 capture capacities were examined.

4.1 Characterization of Adsorbents

Hydrogels impregnated with MEA and DETA were characterized by SEM, TGA and FTIR analyses.

4.1.1 Scanning Electron Microscopy (SEM) Analysis

The morphologies of hydrogels synthesized for CO_2 adsorption and impregnated with MEA and DETA, examined using scanning electron microscopy (SEM), are shown in Figures 4.1-5. As can be seen from the figures, a homogeneous surface condition is not observed in any of the synthesized hydrogels. In SEM images, it is seen that the synthesized hydrogels do not have a smooth surface and the surfaces contain roughness and indentations. This type of structural state increases the surface area of hydrogels.

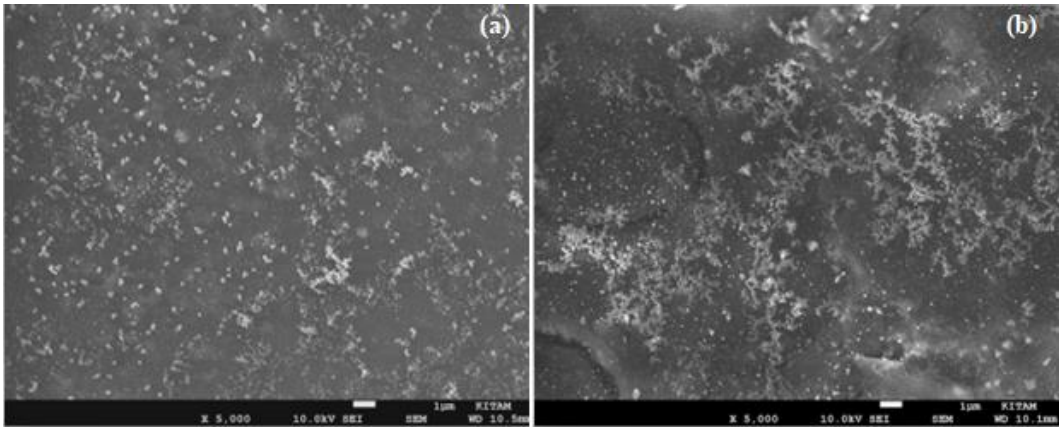

P(HEMA)-MEA b) P(HEMA)-DETA

Figure 4.1 SEM pictures of P(HEMA)

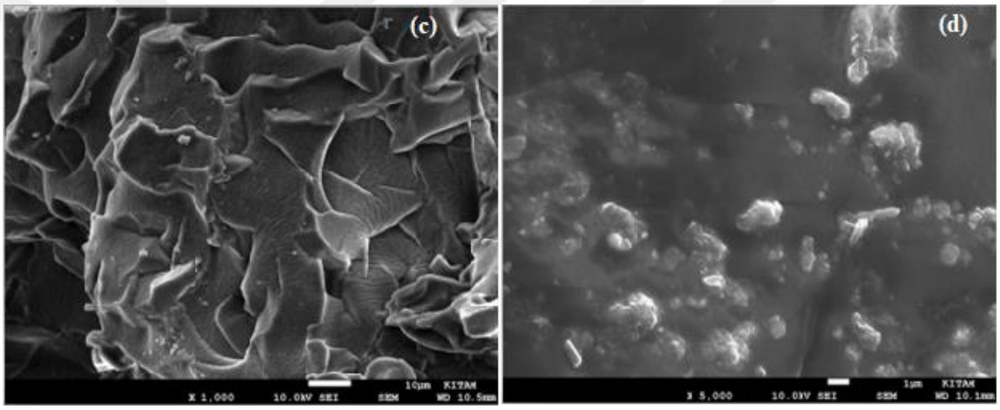

c) P(N-HEA)-MEA d) P(N-HEA)-DETA

Figure 4.2 SEM pictures of P(N-HEA).

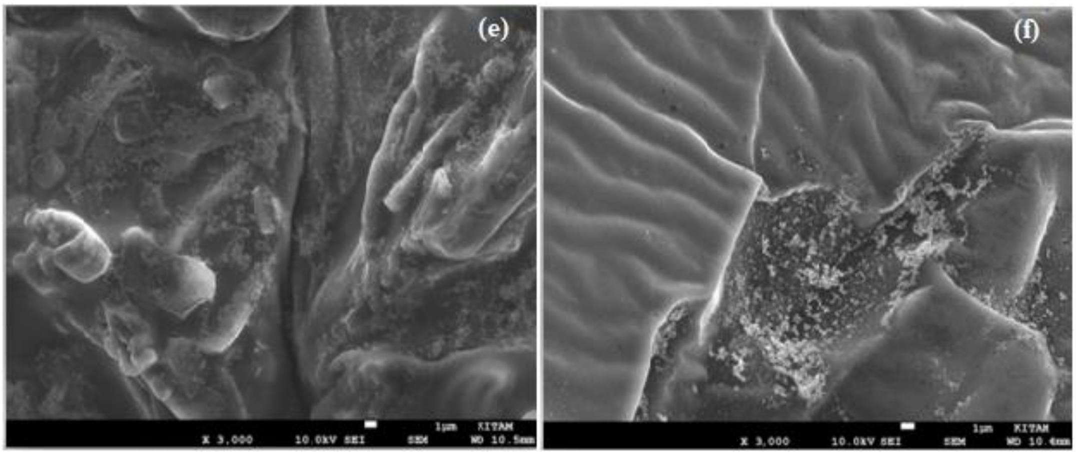

e) P(AAc)-MEA f) P(AAc)-DETA

Figure 4.3 SEM pictures of P(AAc)

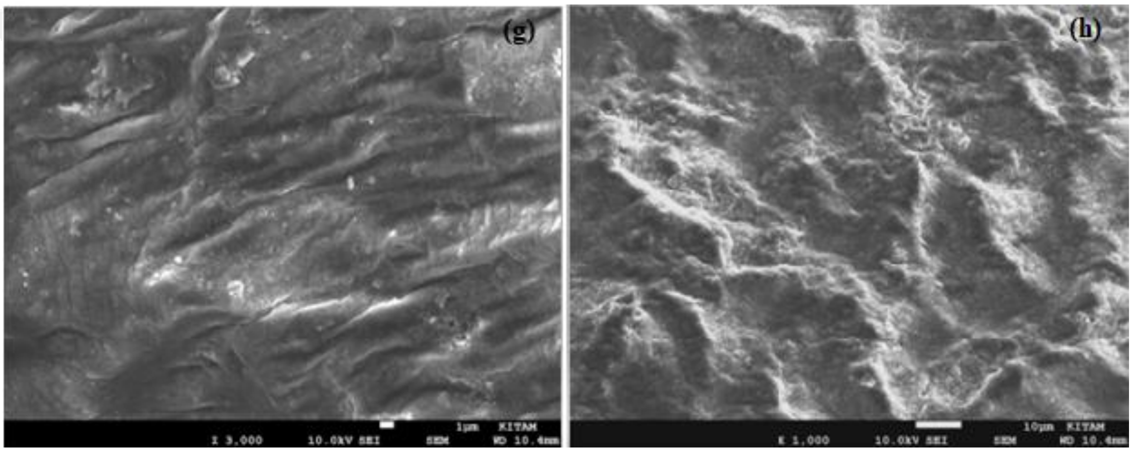

g) P(3-SPMP)-MEA h) P(3-SPMP)-DETA

Figure 4.4 SEM pictures of P(3-SPMP).

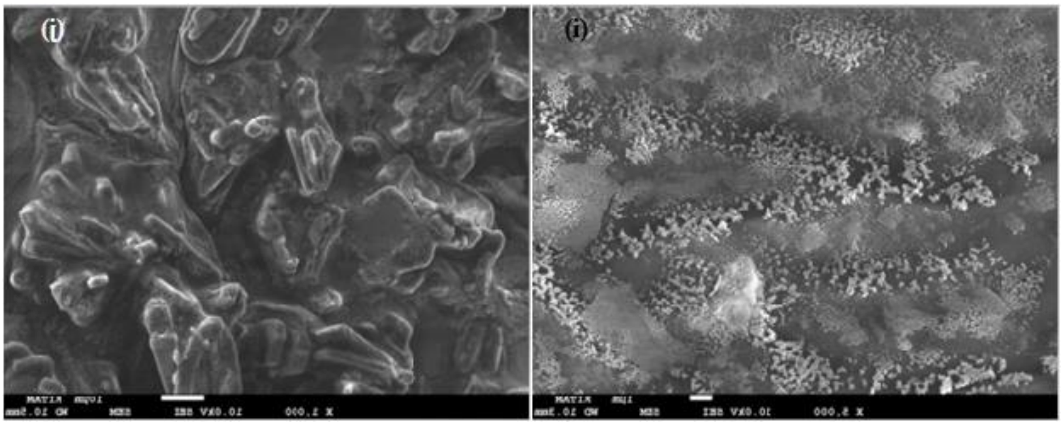

i) P(AMPSA)-MEA j) P(AMPSA)-DETA

Figure 4.5 SEM pictures of P(AMPSA).

4.1.2 Thermogravimetric Analysis (TGA)

TGA was used to assess the temperature effect on weight loss of the adsorbent. Between 0-100 ^oC temperature high volatile chemicals and water were removed from the adsorbent (Figure 4.6). Since MEA and DETA have high boiling points such as 170 ^oC and 207 ^oC, their removal from the hydrogel structure during heat treatment occurred between 120 ^oC and 300 ^oC. This demonstrates the temperature range that should be applied to control mass loss during the regeneration of saturated adsorbents by thermal treatment, whereas the regeneration of CO_2-saturated amines is generally carried out between 100-120 ^oC (Zhang et al., 2023). In the TGA graph, the changes in mass of hydrogels with an organic structure due to heat treatment were compared with sepiolite, which has an inorganic structure. As can be seen from the figure, since sepiolite is a natural inorganic material and not much amine can be impregnated into its structure, no sharp weight decreases were observed in the TGA curve.

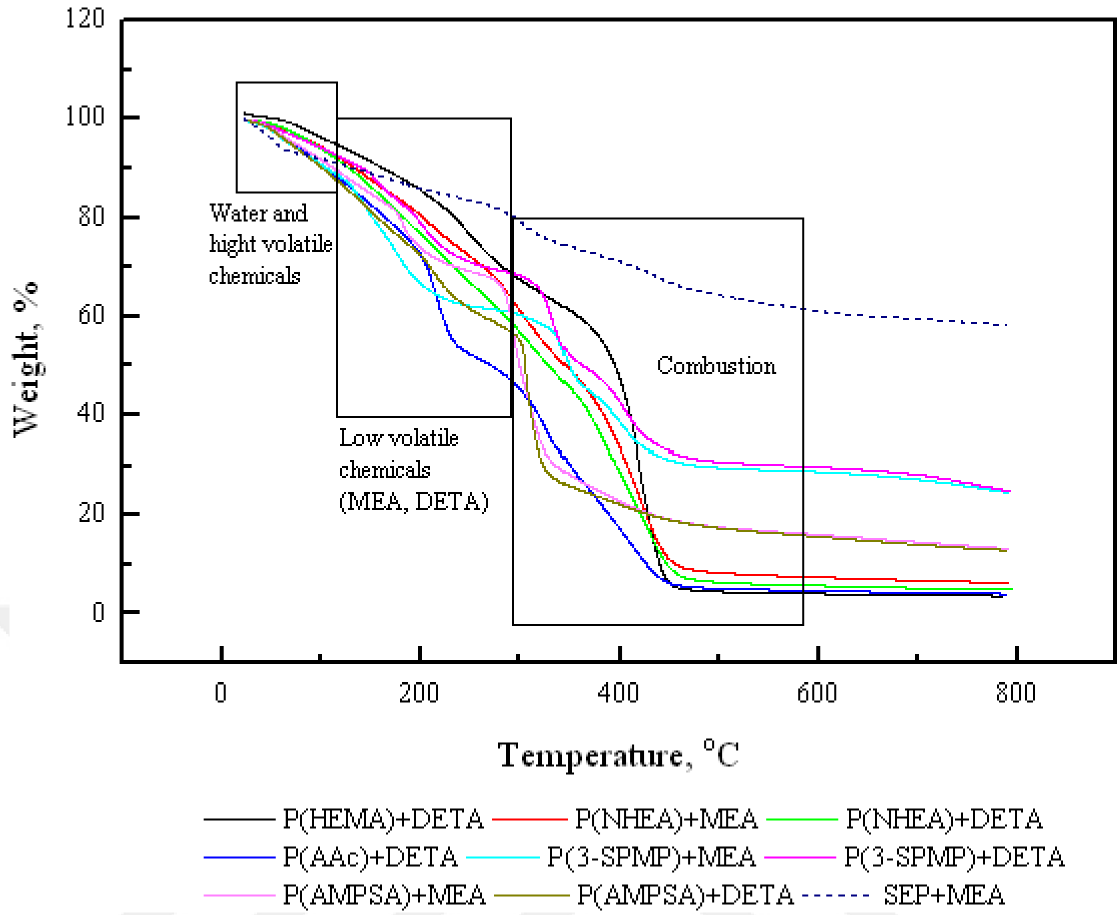

Figure 4.6 TGA curves of hydrogels impregnated with MEA and DETA.

4.1.3 Fourier Transform Infrared Spectroscopy

FTIR spectroscopy enables the identification of functional groups within the substance molecule in question as a result of irradiation of organic and, in some cases, inorganic materials with infra-red (IR) rays at certain wavelengths. When the substance is irradiated with the IR beam, the functional groups within the substance vibrate (either through stretching or bending in various ways). In FTIR spectroscopy, these vibrations and their intensity (% transmission) are plotted against the frequency of light (cm^{-1}). The peaks in the spectrum are the fingerprints of the substance being examined.

Hydrogels synthesized in this study and impregnated with amine (MEA or DETA) generally contain C-H, N-H, C=O, C-N and C-O functional groups. Figure 4.7 shows the functional groups in the P(HEMA) structure loaded with DETA. In the FTIR spectrum, O-H and C-H stretching are in the 3000-3400 cm-1 and 2800-3000 cm-1 bands, respectively, C=O stretching at 1650 cm-1, typical N-H bending of primary and secondary amines at 1500-1600 cm-1, C-N bending at 1400-1500 cm-1 and C-O stretching is seen at 900-1100 cm-1.

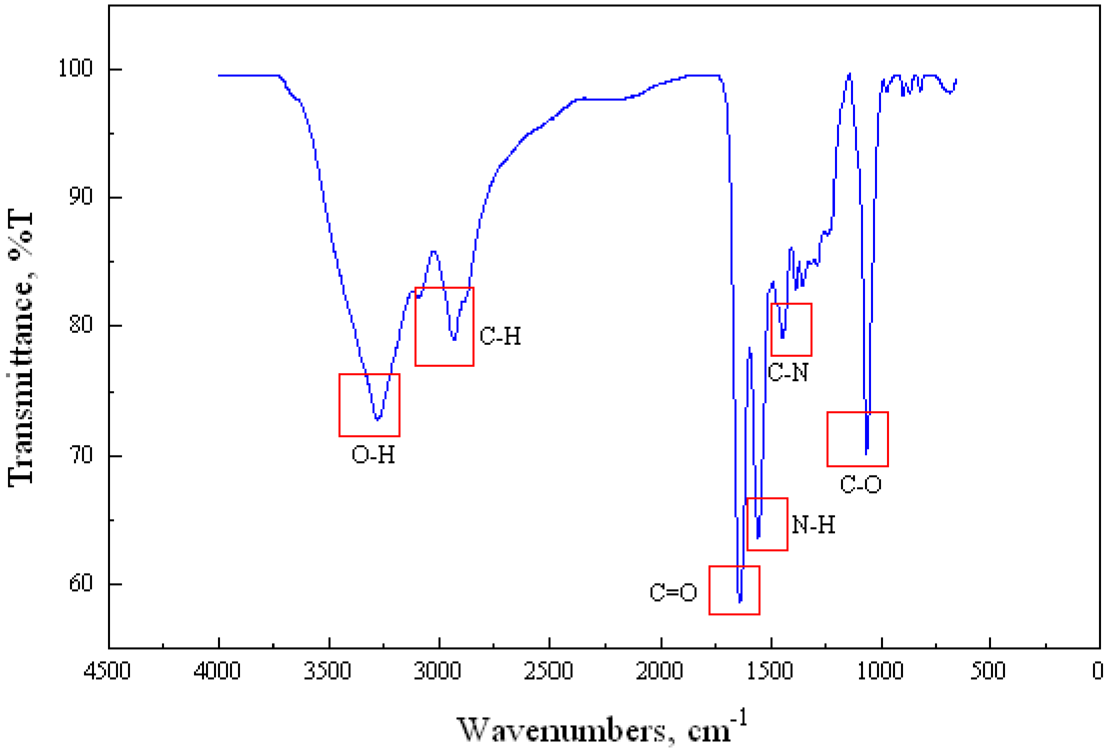

Figure 4.7 FTIR spectrum of P(HEMA) loaded with DETA.

In the FTIR spectrum of P(NHEA) loaded with DETA, there are O-H and C-H stretching in the 3250-3400 cm^{-1} and 2800-3000 cm^{-1} bands, respectively; also C=O stretching at 1750 cm^{-1}, N-H bending at 1500 cm^{-1}, C-N bending at 1200 cm^{-1} and C-H bending at 1050 cm^{-1} is seen in Figure (4.8)

Figure (4.7) shows the functional groups in the P(HEMA) structure loaded with DETA. In the FTIR spectrum, O-H and C-H stretching are in the 3000-3400 cm^{-1} and 2800-3000 cm^{-1} bands, respectively, C=O stretching at 1650 cm^{-1}, typical N-H bending of primary and secondary amines at 1500-1600 cm^{-1}, C-O-H bending at 1300 cm^{-1} and -C=C- stretching is observed at 900-1100 cm^{-1}.

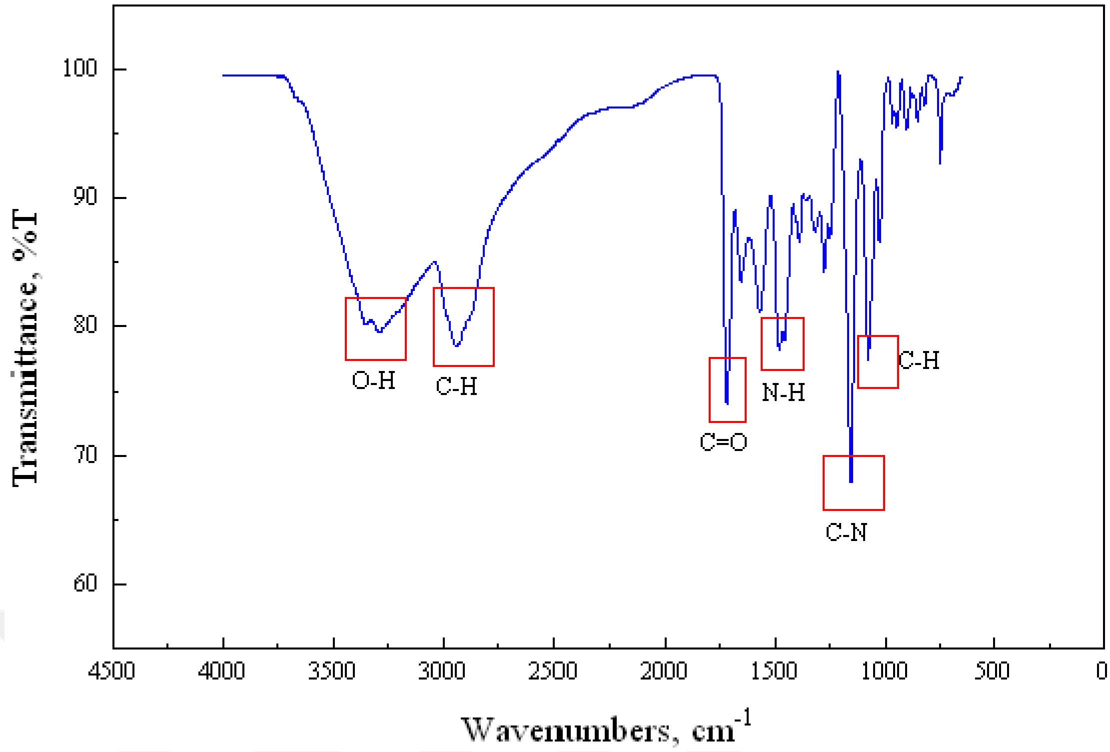

Figure 4.8 FTIR spectrum of P(NHEA) loaded with DETA.

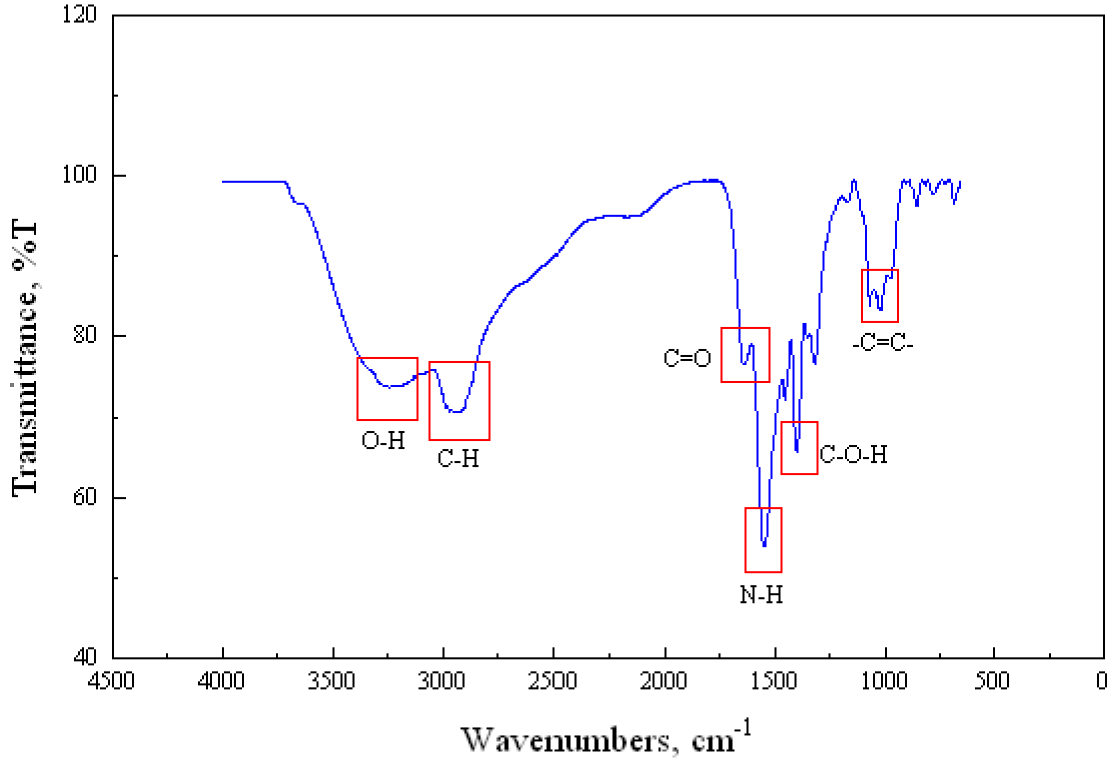

Figure 4.9 FTIR spectrum of P(AAc) loaded with DETA.

The FTIR spectrum of the hydrogel containing sulfonic acid in its structure and impregnated with MEA is seen in Figure (4.10). As can be seen from the figure, the peaks of conventional O-H and C-H stretching vibrations are located in the bands of 3000-3400 cm^{-1} and 2800-3000 cm^{-1}, respectively. The stretching of the carboxylic group (C=O) in the hydrogel structure is at 1600-1750 cm^{-1}, the N-H stretching coming from the amine is at 1500 cm^{-1}, and the bending of C-O, stretching of SO_3H and bending of C-S in the hydrogel structure are at 1240 cm^{-1}, 1100 cm^{-1} and 500-750 cm^{-1}, respectively.

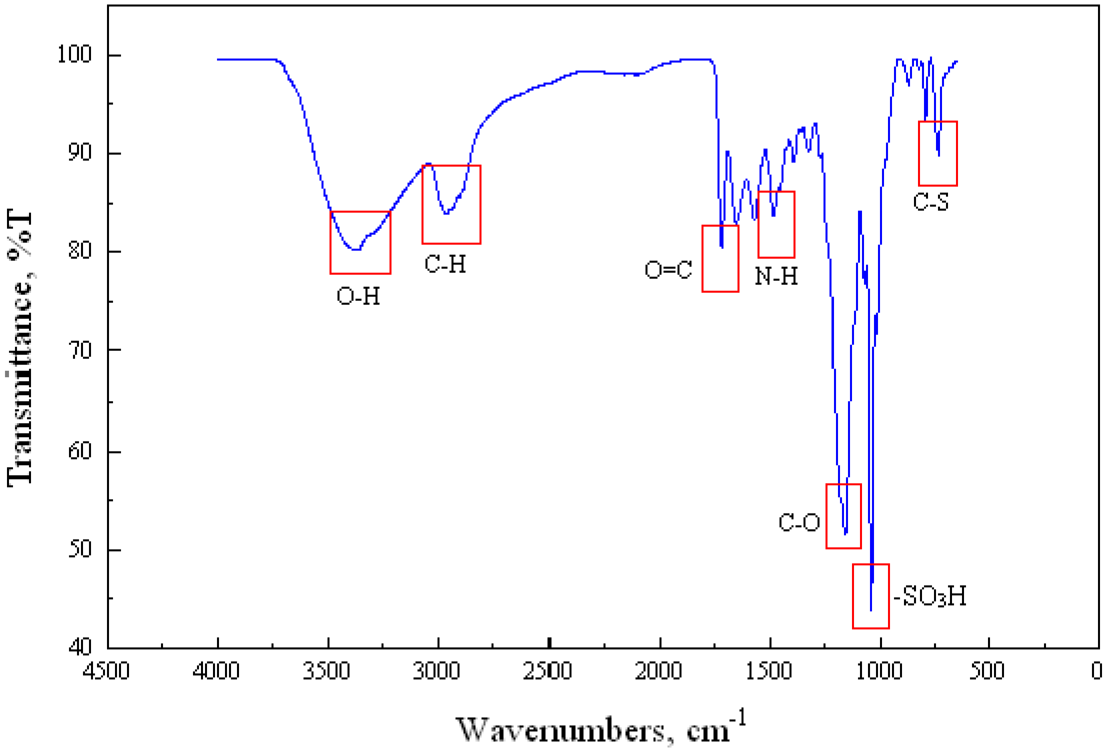

Figure 4.10 FTIR spectrum of P(3-SPMP) loaded with MEA.

It can be seen that the FTIR spectra of MEA and DETA impregnated P(AMPSA) in Figures (4.11 and 4.12), respectively, are almost identical to each other. P(AMPSA) is also structurally similar to P(3-SPMP). The difference between the two is that the C-N group in the P(3-SPMP) structure shows bending at 1150 cm-1, while the C-N group in the P(AMPSA) structure shows bending at 1200 cm-1. As in other amine loaded hydrogels, the N-H group in MEA and DETA loaded P(AMPSA) showed its characteristic peak at 1500 cm-1.

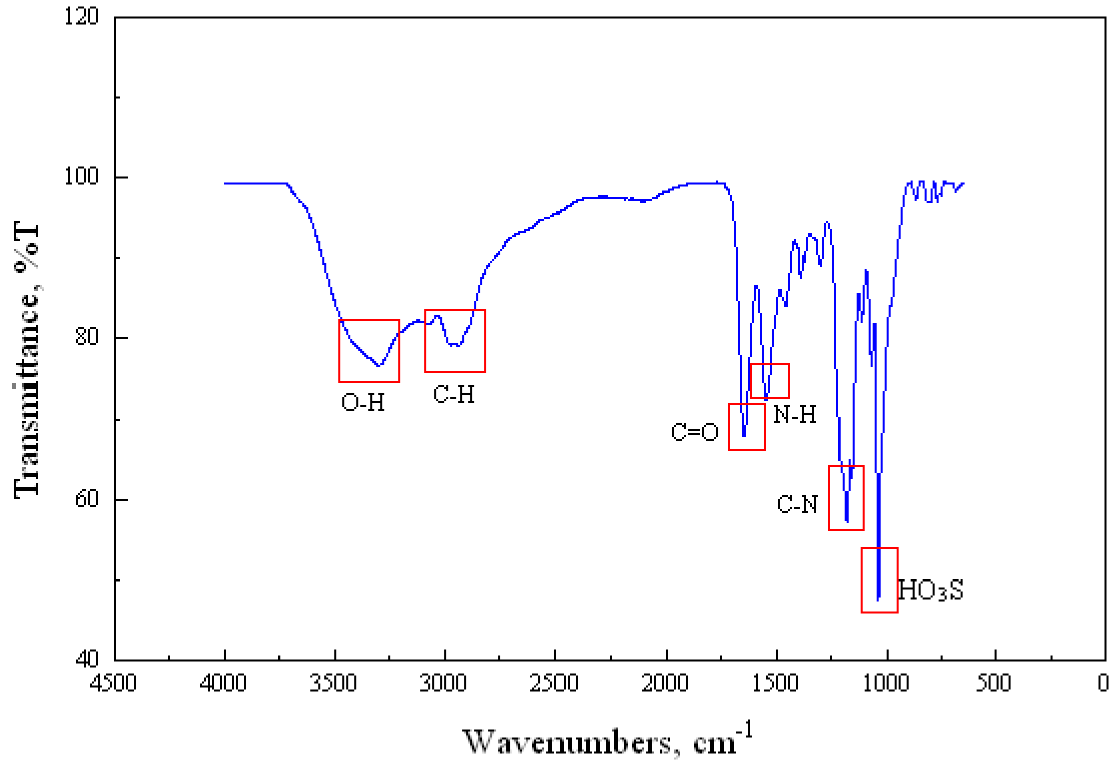

Figure 4.11 FTIR spectrum of P(AMPSA) loaded with MEA.

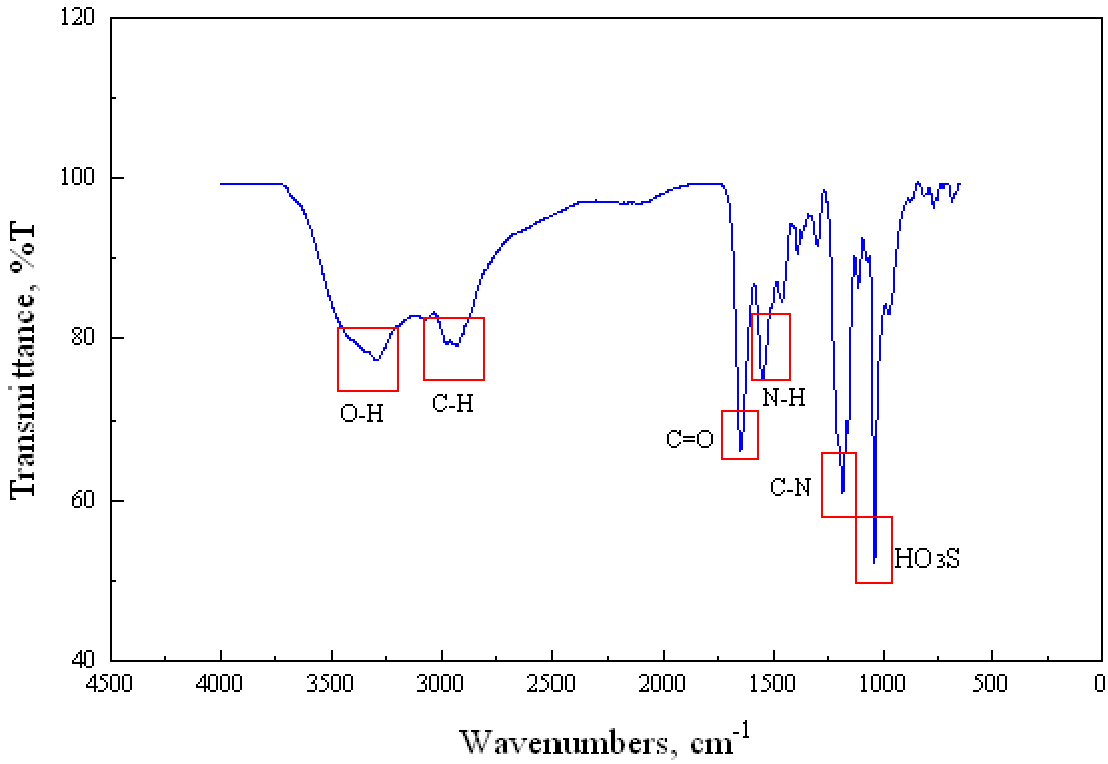

Figure 4.12 FTIR spectrum of P(AMPSA) loaded with DETA.

4.2 CO_2 Adsorption on Hydrogels

To determine the gas adsorption capacity of an adsorbent, the first step is to extract the isotherm, which graphically represents the equilibrium of the adsorption process in question. After a while during the adsorption process, the adsorbent reaches saturation and cannot adsorb any more CO_2. In this case, the adsorption isotherms obtained were evaluated by plotting the amount of CO_2 adsorbed on per unit mass of adsorbent (mg CO_2/g-adsorbent) versus the partial pressure of the CO_2 remaining unadsorbed in the CO_2/N_2 mixture. From these isotherms, information can be obtained about what the appropriate initial CO_2 concentration should be, depending on the amount of adsorbent used. In order to reveal what kind of relationship there is between adsorbent and adsorbate, it is necessary to find out which adsorption isotherm the adsorption in question is suitable for. For this, it is necessary to examine whether the experimental data are compatible with the Langmuir, Freundlich or BET models.

4.2.1 CO_2 Adsorption on P(HEMA)

Figure (4.13) shows the isotherm of the adsorption of CO_2 onto P(HEMA) at room temperature (293±2 K). It can be clearly seen from the figure that the adsorbed amount of CO_2 increases as the partial pressure of CO_2 in the CO_2/N_2 mixture increases, and this increase is greater for P(HEMA) impregnated with DETA. As can be seen in Figure (4.13), DETA impregnated P(HEMA) adsorbed 8 mg CO_2 at a CO_2 partial pressure of 10 kPa, while MEA impregnated adsorbed 5.4 mg CO_2 at the same partial pressure. This difference between the CO_2 capture capacities of amine-impregnated hydrogels is due to their different affinity for CO_2 and physical feature the related amine. According to MEA, the fact that DETA has more amino groups to react with CO_2 causes it to have a higher reaction rate and therefore more CO_2 capture capacity (Hartono et al., 2009; Gao et al., 2017). As can be seen from Equations 4.1 and 4.2, while 1 mol MEA reacts with 1 mol CO_2, 1 mole DETA reacts with 3 mol CO_2, it means that DETA captures three times more CO_2. The mass transfer of CO_2 adhesion to the amine-impregnated hydrogel also depends on the viscosity of the amine. Low viscosity amine promotes the diffusion of both CO_2 and the CO_2 amine reaction product (carbamate) into the bulk amine (Öztürk et al., 2022). Therefore, high viscosity DETA (7.16 cP at 293 K) retained more CO_2 than high viscosity MEA (24.09 cP at 293 K) (Sheng et al.,2018). tried to remove CO_2 from simulated flue gas in a rotating packed bed using DETA and MEA solutions, and as a result, they stated that DETA solution showed a higher CO_2 capture performance than MEA.

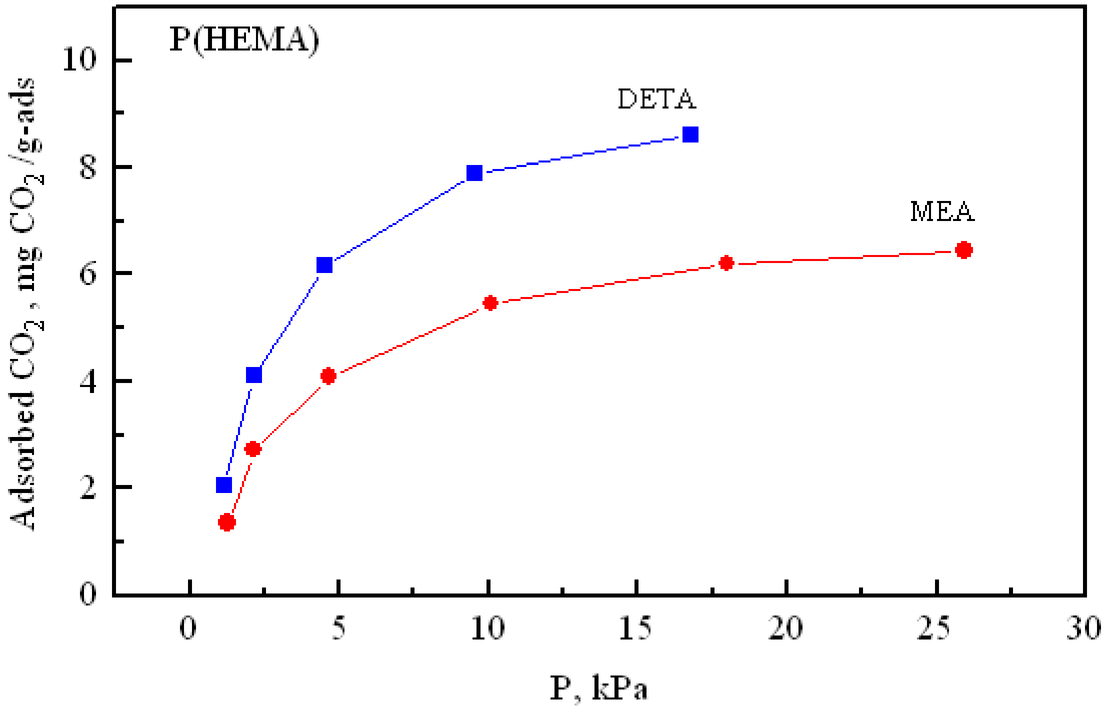

Figure 4.13 Adsorption isotherms for CO_2 adsorption onto P(HEMA) impregnated with MEA and DETA.

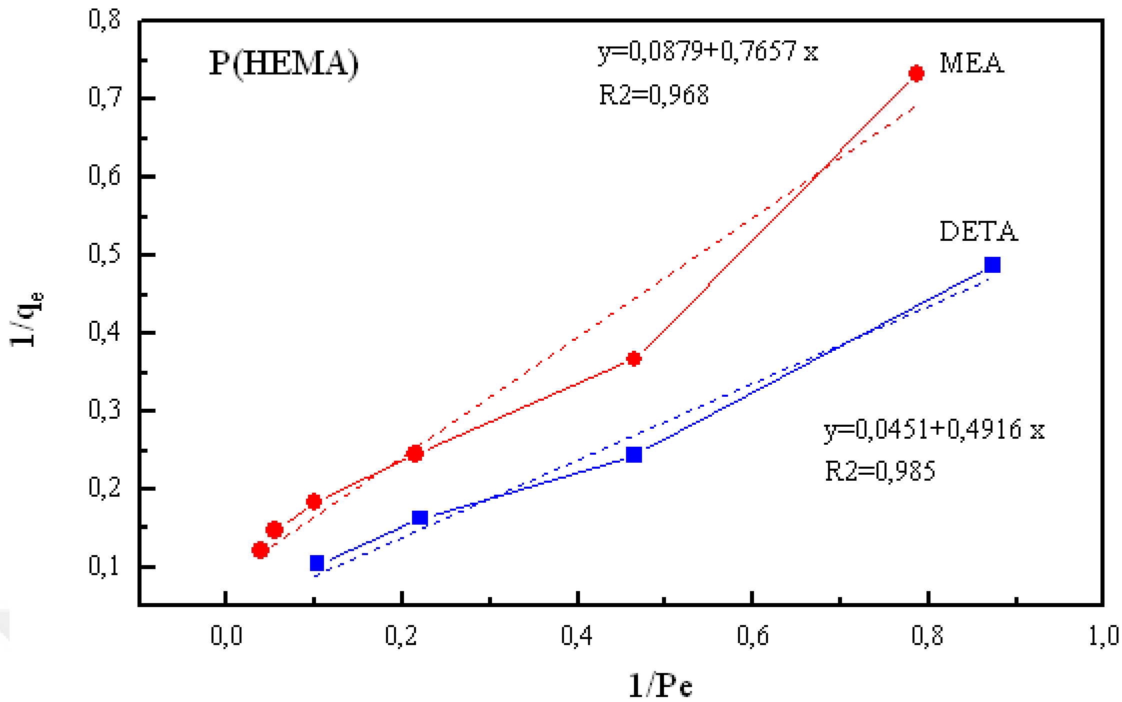

Figure 4.14 Langmuir plot of CO_2 adsorption on MEA and DETA impregnated P(HEMA).

When the relationship between adsorbent and adsorbate was examined, it was seen that the adsorption of CO_2 on MEA and DETA impregnated P(HEMA) conformed to the Langmuir model. The maximum adsorption capacity (q_m) and the Langmuir adsorption constant (K_L) related to the energy of the adsorption were determined from the intercept and slope of the curve seen in Figure (4.14), respectively, and their values are given in Table (4.1). The maximum adsorption capacities (q_m) of P(HEMA) impregnated with MEA and DETA were found as 11.38 mg CO_2/g-adsorbent and 22.2 mg CO_2/g-adsorbent, respectively, which indicates that DETA impregnated P(HEMA) adsorbed more CO_2. The more amino groups and low viscosity of DETA compared to the MEA resulted in the more CO_2 capture (Gao et al., 2017). Indicated that DETA has a faster CO_2 absorption rate and a higher CO_2 cyclic capacity than MEA solvent. And to strip the same amount of CO_2, DETA needed less regeneration energy than MEA solvent. The Langmuir adsorption coefficients (K_L) of P(HEMA) impregnated with MEA and DETA were 0.11 1/kPa and 0.09 1/kPa, respectively. Since a high K_L value indicates that there is a strong interaction between the adsorbent and the adsorbate, it indicates that more energy must be spent to regenerate the amine impregnated adsorbent in question (Gao et al., 2017).

$$CO_2 + \frac{2HOC_2H_4NH_2}{MEA} \leftrightarrow HOC_2H_4NH_3^+ + \frac{HOC_2H_4NHCOO^-}{carbamate}$$

(4.1)

$$3CO_2 + \frac{2(NH_2)(CH_2)_4NH}{DETA} \leftrightarrow (CH_2)_4NH(NH_3^+)_2$$

$$+ \frac{NHCOO^-(CH_2)_2NCOO^-CHCH_2NHCOO^-}{carbamate}$$

(4.2)

As can be seen in Figure (4.15), DETA impregnated P(NHEA) captured more CO_2 than MEA impregnated one. The difference between the adsorption capacities of adsorbents is caused by the differences in the properties of the adsorbents. General adsorbent properties that affect adsorption are the surface area of the adsorbent, its porosity, pore diameter, tortuosity, the degree of adsorbent-adsorbate interaction, and the physical and chemical properties and adsorbed amount of the adsorbed amine. In this study, approximately equal amounts of amine were generally loaded on per unit hydrogel mass. Since hydrogels are flexible polymeric materials, they do not have a fixed surface area, porosity, pore diameter and tortuosity. Therefore, the most important reasons for the difference between the CO_2 capture capacities of amine-impregnated P(HEMA) and P(NHEA) are due to the difference in the chemical structures of the hydrogels and the impregnated amines.

As explained above, according to MEA, DETA reacts quickly with CO_2 and has a high CO_2 capture capacity. The structures of P(HEMA) and P(NHEA) hydrogels are very similar to each other. The difference between them is that instead of O=C-O in the structure of P(HEMA), there is O=C-NH in the structure of P(NHEA). This O=C-NH in the P(NHEA) structure enabled it to capture more CO_2.

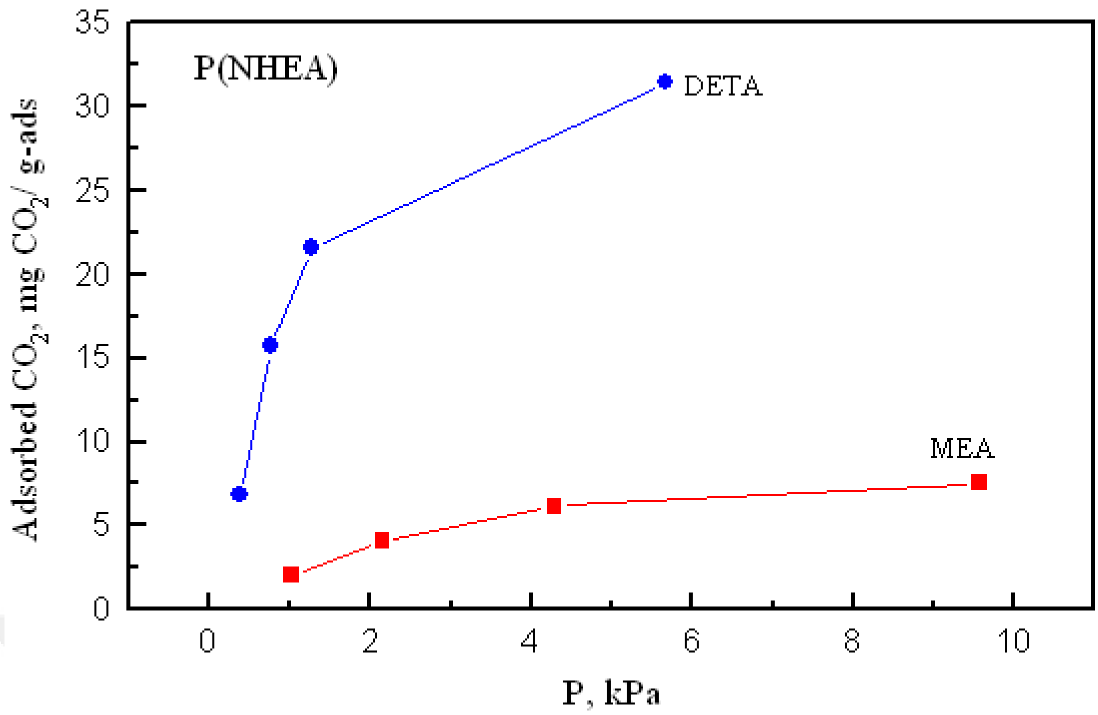

Figure 4.15 Adsorption isotherms for CO_2 adsorption onto P(NHEA) impregnated with MEA and DETA.

Since the CO_2 adsorption of MEA and DETA impregnated P(NHEA) complies with the Langmuir isotherm, the maximum CO_2 retention capacity (q_m) and Langmuir coefficient (K_L) of the adsorbent in question were found from the linearized Langmuir adsorption isotherm in Figure (4.16) and were given in Table 4.1. As can be seen from the Table 4.1, the q_m and K_L values of DETA impregnated P(NHEA) are higher than those impregnated with MEA. Compared to P(HEMA), the KL value of DETA impregnated P(NHEA) was found to be higher. The reason for this is that CO_2 may have formed a strong bond with -NH in the P(NHEA) structure.

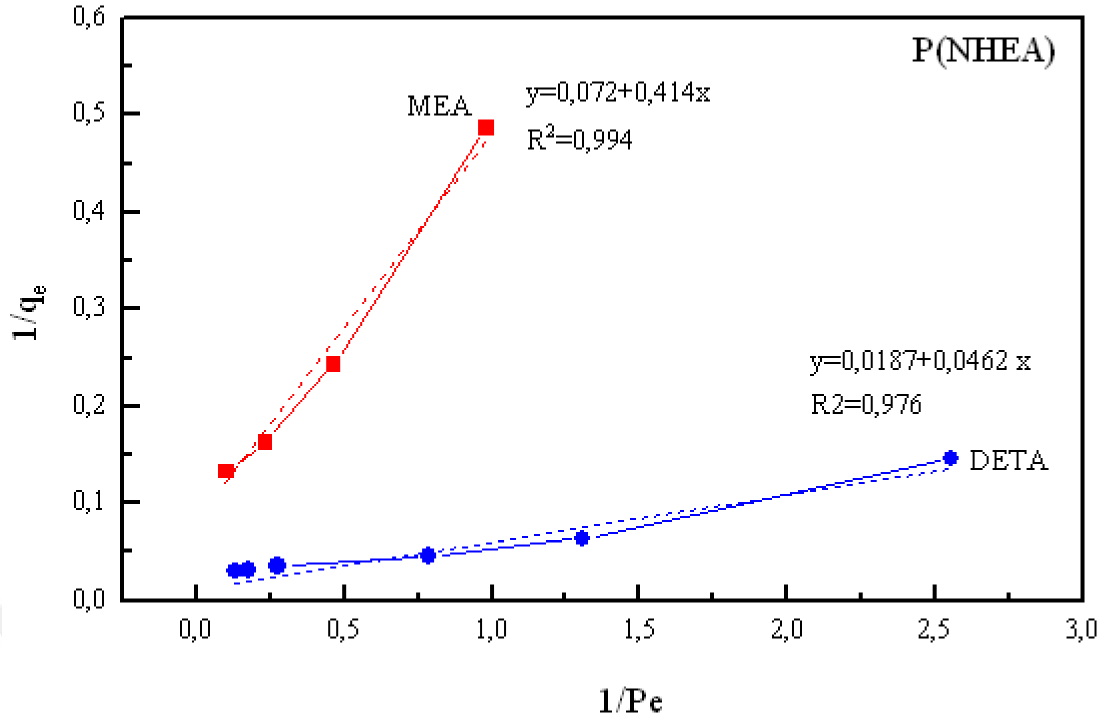

Figure 4.16 Langmuir plot of CO_2 adsorption on MEA and DETA impregnated P(NHEA).

Figure (4.17) shows the adsorption isotherm of amine impregnated P(AAC). MEA and DETA impregnated P(AAC) samples captured almost the same amount of CO_2 at low CO_2 partial pressures, and the difference between their CO_2 capture capacities increased at high partial pressures. Since the effect of pressure is the same for both amine-impregnated P(AAc), increasing pressure may have accelerated the diffusion of CO_2 into the adsorbent. However, in this case, DETA impregnated P(AAc) retained more CO_2 compared to MEA. The maximum CO_2 capture capacity (q_m) and K_L values of DETA impregnated P(AAc) were 87.72 mg CO_2/g-adsorbent and 0.244 1/kPa, respectively, while those of MEA impregnated P(AAc) were 47.62 mg CO_2/g-adsorbent and 0.465 1/kPa, respectively (Figure 4.18). The fact that MEA impregnated P(AAc) has a high K_L value means that it will be more difficult to strip CO_2 from it than DETA impregnated one.

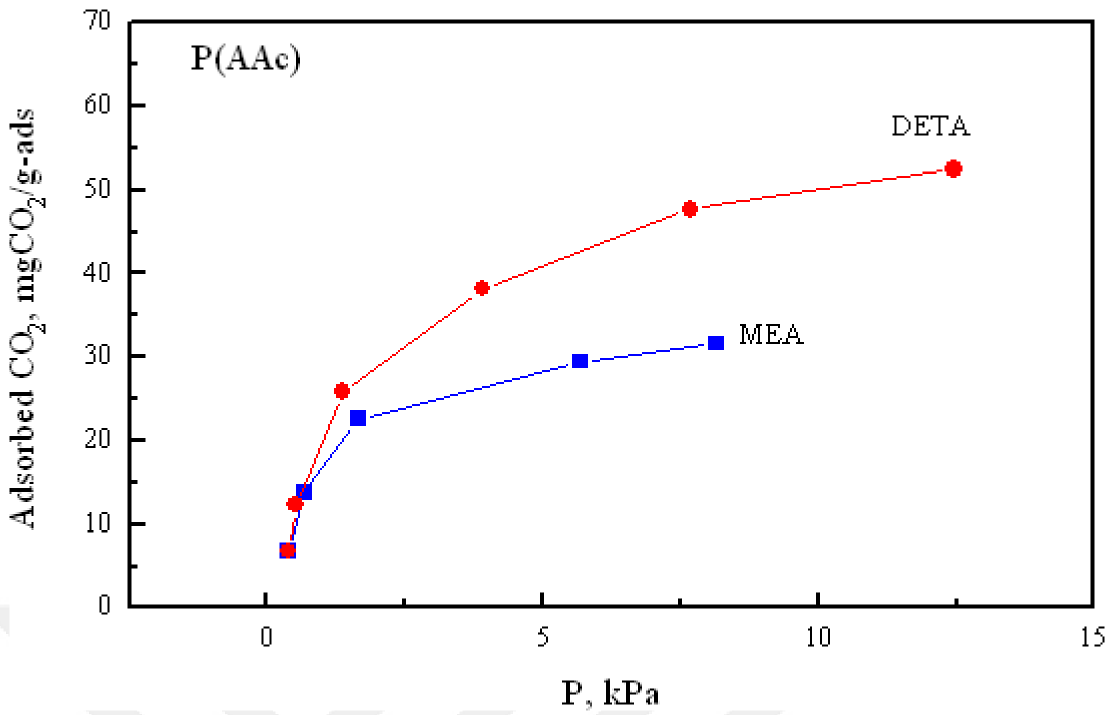

Figure 4.17 Adsorption isotherms for CO_2 adsorption onto P(AAc) impregnated with MEA and DETA.

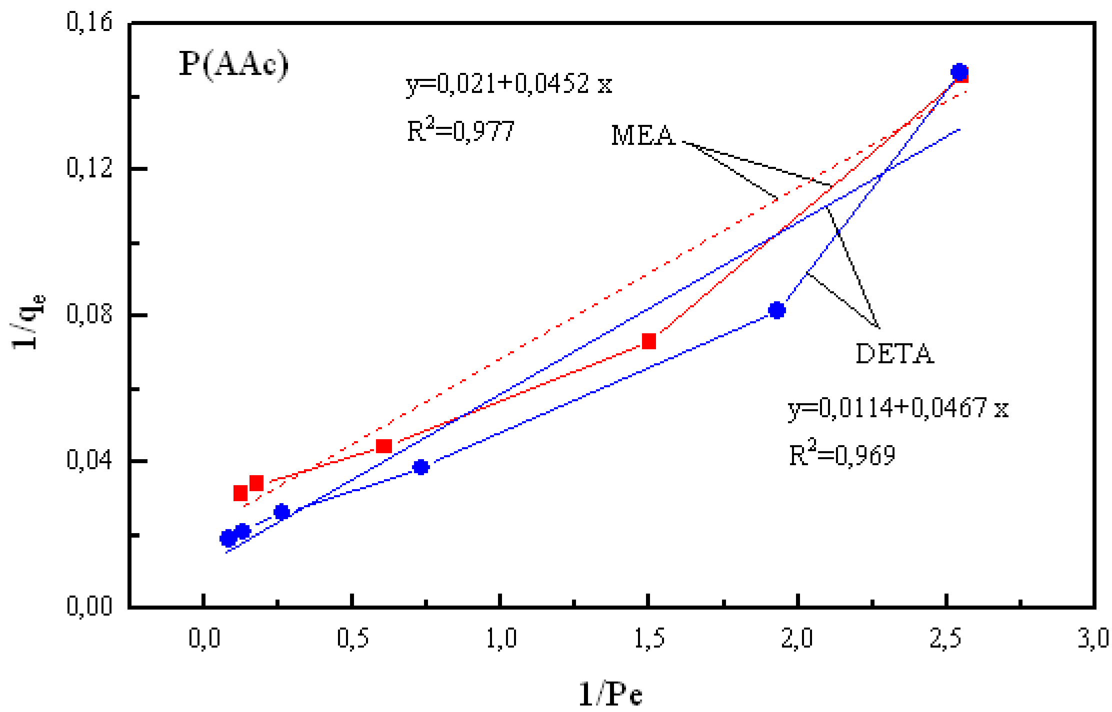

Figure 4.18 Langmuir plot of CO_2 adsorption on MEA and DETA impregnated P(AAc).

When the CO_2 retention properties of P(3-SPMP) and P(AMPSA), which have similar chemical structures, are compared, it can be said that P(AMPSA) retains more CO_2, and this is due to the -NH group in the structure of P(AMPSA) (Figures 4.19 and 4.20). Among the adsorbents used in this study, DETA impregnated P(AMPSA) retained the most CO_2 (Figure 4.19 and Table 4.1).

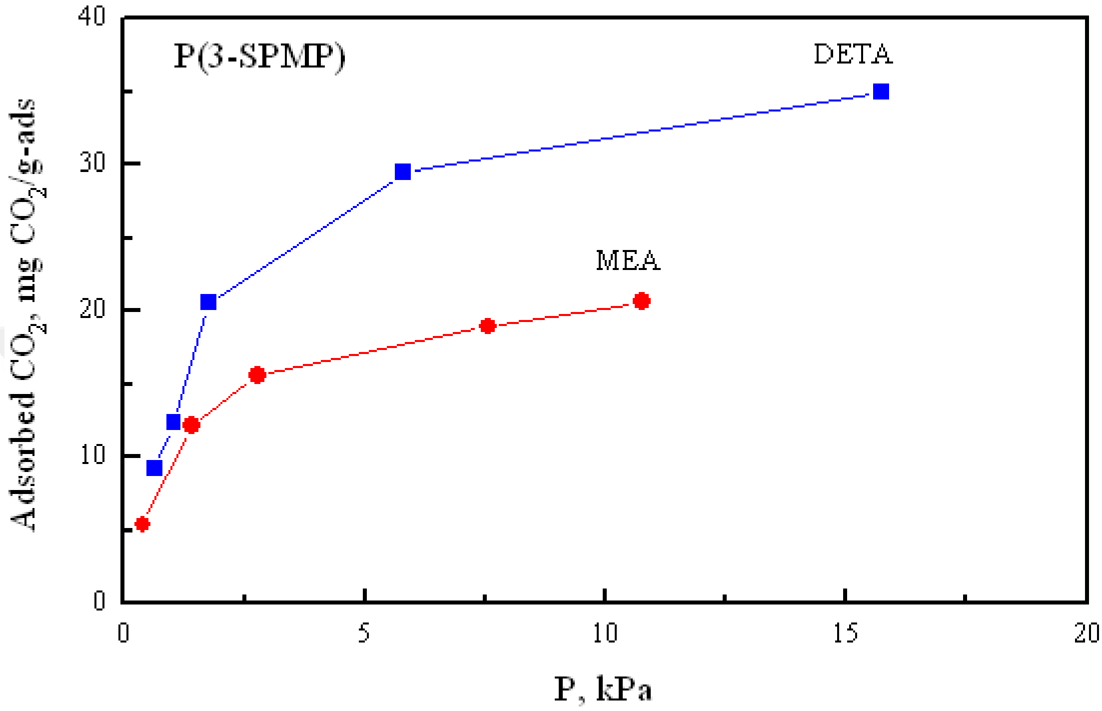

Figure 4.19 Adsorption isotherms for CO_2 adsorption onto P(3-SPMP) impregnated with MEA and DETA.

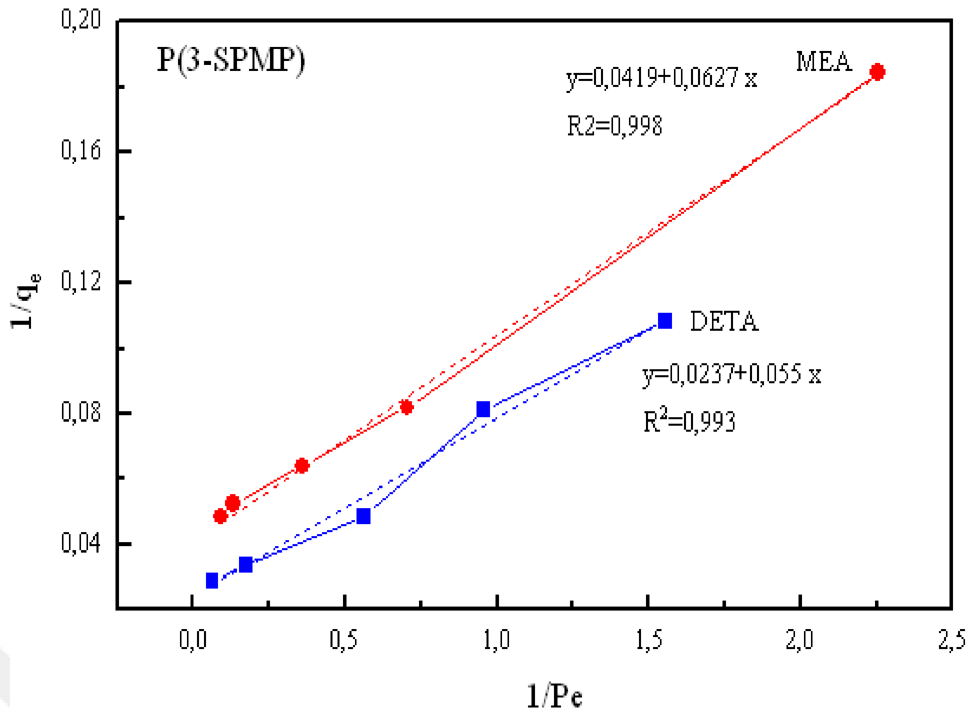

Figure 4.20 Langmuir plot of CO_2 adsorption on MEA and DETA impregnated P(3-SPMP)

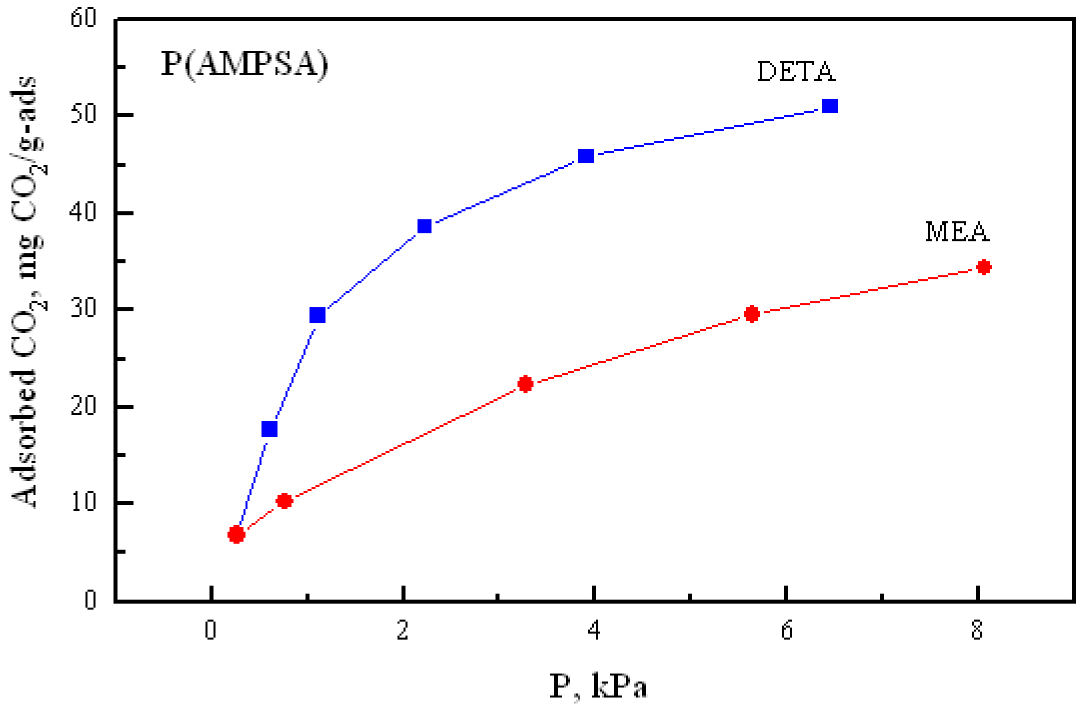

Figure 4.21 Adsorption isotherms for CO_2 adsorption onto P(AMPSA) impregnated with MEA and DETA.

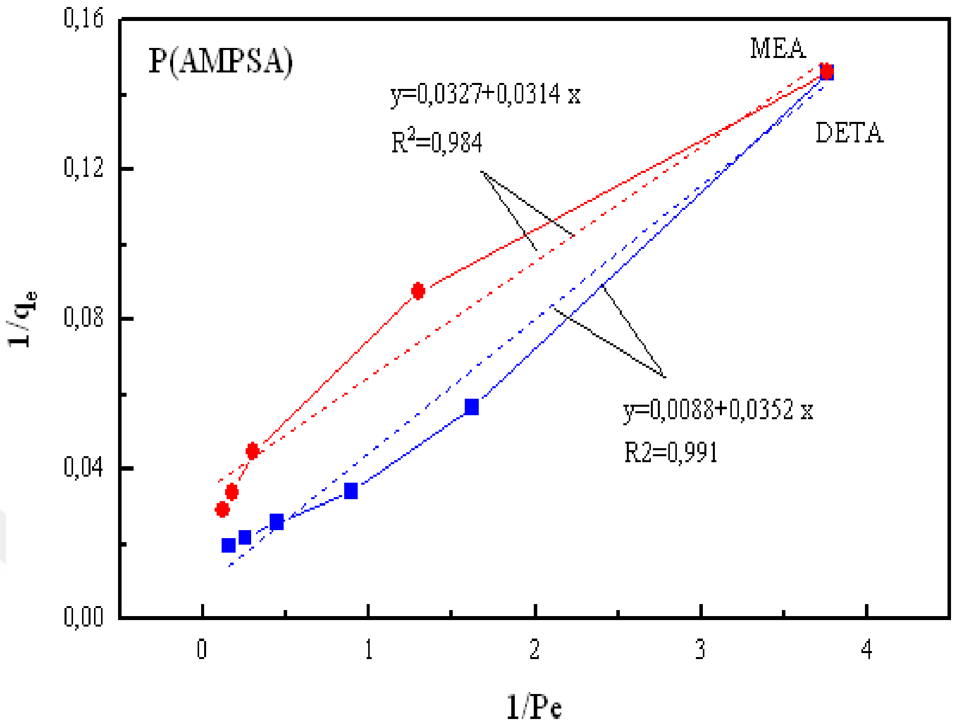

Figure 4.22 Langmuir plot of CO_2 adsorption on MEA and DETA impregnated P(AMPSA)

Among the adsorbents used in this study, amine impregnated P(NHEA), P(AAc) and P(AMPSA) captured high amount of CO_2 compared to the P(HEMA) and P(3-SPMP). The reason for this is that, unlike P(HEMA) and P(3-SPMP), the -NH group in the structure of P(NHEA), P(AAC) and P(AMPSA) may retain the amine containing NH_2 in their structure more, according to the principle of like dissolves like.

Table 4.1 Langmuir constants for adsorption of amine impregnated hydrogels.

Hydrogel	Impregnated amine	K_L, 1/kPa	q_m, mg CO_2/g-ads.
P(HEMA)	MEA	0.115	11.38
	DETA	0.09	22.20
P(NHEA)	MEA	0.174	13.89
	DETA	0.405	53.50
P(AAc)	MEA	0.465	47.62
	DETA	0.244	87.72
P(3-SPMP)	MEA	0.67	23.87
	DETA	0.43	42.20
P(AMPSA)	MEA	1.04	30.58
	DETA	0.25	113.64

5. CONCLUSION

In this study, the CO_2 capture capacities of P(HEMA), P(NHEA), P(AAc), P(3-SPMP) and P(AMPSA) impregnated with MEA and DETA were examined. From the results obtained;

1. DETA impregnated hydrogel captured more CO_2 than MEA impregnated one. It can be said that the reason for this is that amines have different affinities towards CO_2 and that the viscosity of the amine in question is effective in the diffusion of CO_2 into the amine loaded the hydrogel.
2. Hydrogel with -NH group in its structure retained more CO_2. The reason for this is that, according to the principle of like dissolves like, the amine containing NH_2 in its structure may be more loaded on the hydrogel with the -NH group in its structure.
3. The adsorption of CO_2 onto amine-impregnated hydrogels complies with the Langmuir adsorption isotherm, therefore the adsorbed CO_2 adheres to the adsorbent in a monolayer form. Considering that amine has a chemical reaction with CO_2, the CO_2 adhering to the amine-impregnated hydrogel has reaction products (such as cabamate) unlike adhesion to a solid surface, and these reaction products diffuse from the surface into the amine, causing the adsorption to occur in the form of monolayer adsorption.
4. As a continuation of this study, amine impregnation and CO_2 adsorption can be better explained by better examining the textural properties of the hydrogel. The state of the adsorbent and the amine impregnated with it can be examined by studying the adsorption-desorption cycle.

REFERENCES

Abbasi, A., Nasef, M. M., Babadi, F. E., Faridi-Majidi, R., Takeshi, M., Abouzari-Lotf, E. and Kheawhom, S. (2019). Carbon dioxide adsorption on grafted nanofibrous adsorbents functionalized using different amines. Frontiers in Energy Research, 7, 145.

Abbasi, A., Nasef, M. M., Kheawhom, S., Faridi-Majidi, R., Takeshi, M., Abouzari-Lotf, E., and Choong, T. (2019). Amine functionalized radiation induced grafted polyolefin nanofibers for CO_2 adsorption. Radiation Physics and Chemistry, 156, 58-66.

Abid, H. R., Rada, Z. H., Duan, X., Sun, H., and Wang, S. (2017). Enhanced CO_2 adsorption and selectivity of CO_2/N_2 on amino-MIL-53 (Al) synthesized by polar co-solvents. Energy and Fuels, 32(4), 4502-4510.

Abuelnoor, N., AlHajaj, A., Khaleel, M., Vega, L. F., and Abu-Zahra, M. R. (2021). Activated carbons from biomass-based sources for CO_2 capture applications. Chemosphere, 282, 131111.

Adelodun, A. A., Ngila, J. C., Kim, D. G., and Jo, Y. M. (2016). Isotherm, thermodynamic and kinetic studies of selective CO_2 adsorption on chemically modified carbon surfaces. Aerosol and Air Quality Research, 16(12), 3312-3329.

Agrawala, S. (1998). Context and early origins of the Intergovernmental Panel on Climate Change. Climatic Change, 39(4), 605-620.

Ahmed Ali, K., Ahmad, M. I., and Yusup, Y. (2020). Issues, impacts, and mitigations of carbon dioxide emissions in the building sector. Sustainability, 12(18), 7427.

Ahmed, S., Ramli, A., and Yusup, S. (2016). CO_2 adsorption study on primary, secondary and tertiary amine functionalized Si-MCM-41. International Journal of Greenhouse Gas Control, 51, 230-238.

Akeeb, O., Wang, L., Xie, W., Davis, R., Alkasrawi, M., and Toan, S. (2022). Post-combustion CO_2 capture via a variety of temperature ranges and material adsorption process: A review. Journal of Environmental Management, 313, 115026.

Al-Ghussain, L. (2019). Global warming: review on driving forces and mitigation Environ Prog and Sust Energy, 38(1), 13-21.

Ammendola, P., Raganati, F., and Chirone, R. (2017). CO_2 adsorption on a fine activated carbon in a sound assisted fluidized bed: Thermodynamics and kinetics. Chemical Engineering Journal, 322, 302-313.

Anbia, M., and Hoseini, V. (2012). Development of MWCNT@ MIL-101 hybrid composite with enhanced adsorption capacity for carbon dioxide. Chemical Engineering Journal, 191, 326-330.

Anderson, B., Bartlett, K. B., Frolking, S., Hayhoe, K., Jenkins, J. C., and Salas, W. A. (2010). Methane and nitrous oxide emissions from natural sources. EPA.430-R-10-001.

Andirova, D., Lei, Y., Zhao, X., and Choi, S. (2015). Functionalization of metal–organic frameworks for enhanced stability under humid carbon dioxide capture conditions. ChemSusChem, 8(20), 3405-3409.

Anomohanra, O. (2011). Estimating the greenhouse gas emission from petroleum product combustion in Nigeria. Journal of applied sciences, 11(17), 3209-3214.

Aragón-Pérez, A. (2021). The influence of the 1992 Earth Summit on the 1992 Olympic Games in Barcelona: Awakening of the Olympic environmental dimension. In New Dimensions of Sport in Modern Europe (pp. 122-144). Routledge.

Ares, E., Bennett, O., and Bolton, P. (2009). Climate change: the Copenhagen conference. Economic indicators, 3, 09.

Ayinla, R. T., Dennis, J. O., Zaid, H. M., Sanusi, Y. K., Usman, F., and Adebayo, L. L. (2019). A review of technical advances of recent palm bio-waste conversion to activated carbon for energy storage. Journal of cleaner production, 229, 1427-1442.

Aziz, B., Hedin, N., and Bacsik, Z. (2012). Quantification of chemisorption and physisorption of carbon dioxide on porous silica modified by propylamines: Effect of amine density. Microporous and Mesoporous Materials, 159, 42-49.

Bae, J. Y. (2017). CO_2 Capture by amine-functionalized mesoporous hollow silica. Journal of Nanoscience and Nanotechnology, 17(10), 7418-7422.

Baena-Moreno, F. M., Rodríguez-Galán, M., Vega, F., Alonso-Fariñas, B., Vilches Arenas, L. F., and Navarrete, B. (2019). Carbon capture and utilization technologies: a literature review and recent advances. Energy Sources, Part A: Recovery, Utilization, and Environmental Effects, 41(12), 1403-1433.

Bai, B. C., Kim, E. A., Lee, C. W., Lee, Y. S., and Im, J. S. (2015). Effects of surface chemical properties of activated carbon fibers modified by liquid oxidation for CO_2 adsorption. Applied Surface Science, 353, 158-164.

Batten, S. R., Champness, N. R., Chen, X. M., Garcia-Martinez, J., Kitagawa, S., Öhrström, L. and Reedijk, J. (2013). Terminology of metal–organic frameworks and coordination polymers (IUPAC Recommendations 2013). Pure and Applied Chemistry, 85(8), 1715-1724.

Benhelal, E., Zahedi, G., Shamsaei, E., and Bahadori, A. (2013). Global strategies and potentials to curb CO_2 emissions in cement industry. Journal of cleaner production, 51, 142-161.

Ben-Mansour, R., Habib, M. A., Bamidele, O. E., Basha, M., Qasem, N. A. A., Peedikakkal, A. B. D. U. L. M. A. L. I. K., and Ali, M. J. A. E. (2016). Carbon capture by physical adsorption: materials, experimental investigations and numerical modeling and simulations–a review. Applied Energy, 161, 225-255.

Benson, S. M., Bennaceur, K., Cook, P., Davison, J., de Coninck, H., Farhat, K. and Wright, I. (2012). Chapter 13: Carbon capture and storage. Global energy assessment-Toward a sustainable future, 993.

Bernhardsen, I. M., and Knuutila, H. K. (2017). A review of potential amine solvents for CO_2 absorption process: Absorption capacity, cyclic capacity and pKa. International Journal of Greenhouse Gas Control, 61, 27-48.

Bezerra, D. P., Oliveira, R. S., Vieira, R. S., Cavalcante, C. L., and Azevedo, D. C. (2011). Adsorption of CO_2 on nitrogen-enriched activated carbon and zeolite 13X. Adsorption, 17, 235-246.

Bhullar, G. S., Edwards, P. J., and Olde Venterink, H. (2014). Influence of different plant species on methane emissions from soil in a restored Swiss wetland. PLoS One, 9(2), e89588..

Bien, C. E., Chen, K. K., Chien, S. C., Reiner, B. R., Lin, L. C., Wade, C. R., and Ho, W. W. (2018). Bioinspired metal–organic framework for trace CO_2capture. Journal of the American Chemical Society, 140(40), 12662-12666.

Borhan, A., Yusup, S., Lim, J. W., and Show, P. L. (2019). Characterization and modelling studies of activated carbon produced from rubber-seed shell using KOH for CO_2adsorption. Processes, 7(11), 855.

Budzianowski, W. M. (2016). Explorative analysis of advanced solvent processes for energy efficient carbon dioxide capture by gas–liquid absorption. International Journal of Greenhouse Gas Control, 49, 108-120.

Calleja, G., Sanz, R., Arencibia, A., and Sanz-Pérez, E. S. (2011). Influence of drying conditions on amine-functionalized SBA-15 as adsorbent of CO_2. Topics in Catalysis, 54, 135-145.

Cecilia, J. A., Vilarrasa-García, E., Morales-Ospino, R., Bastos-Neto, M., Azevedo, D. C., and Rodríguez-Castellón, E. (2020). Insights into CO_2 adsorption in amino-functionalized SBA-15 synthesized at different aging temperature. Adsorption, 26, 225-240.

Cen, Q., Fang, M., Wang, T., Majchrzak-Kucęba, I., Wawrzyńczak, D., and Luo, Z. (2016). Thermodynamics and regeneration studies of CO_2 adsorption on activated carbon. Greenhouse Gases: Science and Technology, 6(6), 787-796.

Chai, S. Y. W., Ngu, L. H., and How, B. S. (2022). Review of carbon capture absorbents for CO_2 utilization. Greenhouse Gases: Science and Technology, 12(3), 394-427.

Chaikittisilp, W., Kim, H. J., and Jones, C. W. (2011). Mesoporous alumina-supported amines as potential steam-stable adsorbents for capturing CO_2 from simulated flue gas and ambient air. Energy and Fuels, 25(11), 5528-5537.

Chen, B., Tan, J., Wang, W., Dai, W., Ao, M., and Chen, C. (2023). Tomographic Reconstruction of Water Vapor Density Fields from the Integration of GNSS Observations and Fengyun-4A Products. IEEE Transactions on Geoscience and Remote Sensing, 61, 1-12.

Chen, C., and Bhattacharjee, S. (2017). Trimodal nanoporous silica as a support for amine-based CO_2 adsorbents: Improvement in adsorption capacity and kinetics. Applied Surface Science, 396, 1515-1519.

Chen, C., Kim, S. S., Cho, W. S., and Ahn, W. S. (2015). Polyethylenimine-incorporated zeolite 13X with mesoporosity for post-combustion CO_2 capture. Applied Surface Science, 332, 167-171.

Chen, Z., Deng, S., Wei, H., Wang, B., Huang, J., and Yu, G. (2013). Polyethylenimine-impregnated resin for high CO_2 adsorption: an efficient adsorbent for CO_2 capture from simulated flue gas and ambient air. ACS applied materials and interfaces, 5(15), 6937-6945.

Chiang, Y. C., Chen, Y. J., and Wu, C. Y. (2017). Effect of relative humidity on adsorption breakthrough of CO_2 on activated carbon fibers. Materials, 10(11), 1296.

Chiang, Y. C., Yeh, C. Y., and Weng, C. H. (2019). Carbon dioxide adsorption on porous and functionalized activated carbon fibers. Applied sciences, 9(10), 1977.

Conrad, R. (2009). The global methane cycle: recent advances in understanding the microbial processes involved. Environmental microbiology reports, 1(5), 285-292.

Dangal, S. R., Tian, H., Xu, R., Chang, J., Canadell, J. G., Ciais, P and Zhang, B. (2019). Global nitrous oxide emissions from pasturelands and rangelands: magnitude, spatiotemporal patterns, and attribution. Global Biogeochemical Cycles, 33(2), 200-222.

Das, U., Das, A., and Das, A. K. (2023). Confinement of ozone hole mainly in the Antarctic stratosphere to protect the living kingdom on the earth: chemistry behind this Nature's unique gift. Chemistry Teacher International, 5(1), 91-105.

Davini, P. (2002). Flue gas treatment by activated carbon obtained from oil-fired fly ash. Carbon, 40(11), 1973-1979.

Deng, J., Liu, Z., Du, Z., Zou, W., and Zhang, C. (2019). Fabrication of PEI-grafted porous polymer foam for CO_2 capture. Journal of Applied Polymer Science, 136(32), 47844.

Deng, M., and Park, H. G. (2019). Spacer-assisted amine-coiled carbon nanotubes for CO_2capture. Langmuir, 35(13), 4453-4459.

Depledge, J. (2008). Crafting the Copenhagen consensus: some reflections. Review of European Community and International Environmental Law, 17(2), 154-165.

Eroglu, N., Emekci, M., and Athanassiou, C. G. (2017). Applications of natural zeolites on agriculture and food production. Journal of the Science of Food and Agriculture, 97(11), 3487-3499.

Ewing, J. J. (2011). Cancun and Climate Security: New Approaches, Mixed Results. Non-Traditional Security (NTS) Studies in Asia (NTS-Asia).

Gerhard, D.P., Llewellyn, P. (2011). Opportunities for MOFs in CO_2 Capture from Flue Gases, Natural Gas, and Syngas by Adsorption, In Metal-organic frameworks: applications from catalysis to gas storage. 99-119. Ed. Farrusseng, D., John Wiley and Sons.

Fatemi, S., Vesali-Naseh, M., Cyrus, M., and Hashemi, J. (2011). Improving CO_2/CH_4 adsorptive selectivity of carbon nanotubes by functionalization with nitrogen-containing groups. Chemical engineering research and design, 89(9), 1669-1675.

Fatıma, S.S., Borhan, A., Ayoub, M. and Abd Ghani, N. (2022). CO_2 Adsorption Performance on Surface-Functionalized Activated Carbon Impregnated with Pyrrolidinium-Based Ionic Liquid, Processes, 10, 2372.

Feng, X. X., Xie, J., Hu, G. S., Jia, A. P., Xie, G. Q., and Luo, M. F. (2013). Preparation of pentaethylenehexamine-functionalized mesocellular silica foams and their application for CO2 adsorption. Acta Physico-Chimica Sinica, 29(6), 1266-1272.

Feng, X., Hu, G., Hu, X., Xie, G., Xie, Y., Lu, J., and Luo, M. (2013). Tetraethylenepentamine-modified siliceous mesocellular foam (MCF) for CO_2capture. Industrial and Engineering Chemistry Research, 52(11), 4221-4228.

Franchi, R. S., Harlick, P. J., and Sayari, A. (2005). Applications of pore-expanded mesoporous silica. 2. Development of a high-capacity, water-tolerant adsorbent for CO_2. Industrial and Engineering Chemistry Research, 44(21), 8007-8013.

Fuhr, L., Schalatek, L., Omari, K., Chagutah, T., and Nord, A. (2011). COP 17 in Durban: A largely empty package. Berlin: Heinrich Böll Stiftung.

Fujiki, J., Yamada, H., and Yogo, K. (2015). Enhanced adsorption of carbon dioxide on surface-modified mesoporous silica-supported tetraethylenepentamine: role of surface chemical structure. Microporous and Mesoporous Materials, 215, 76-83.

Fusco, C., Casiello, M., Catucci, L., Comparelli, R., Cotugno, P., Falcicchio, A. and Nacci, A. (2018). TiO2@ PEI-grafted-MWCNTs hybrids nanocomposites catalysts for CO_2 photoreduction. Materials, 11(2), 307.

Gao, Y., Gao, X., and Zhang, X. (2017). The 2 ^oC global temperature target and the evolution of the long-term goal of addressing climate change—from the United Nations framework convention on climate change to the Paris agreement. Engineering, 3(2), 272-278.

Gaurina-Međimurec, N., Novak-Mavar, K., and Majić, M. (2018). Carbon capture and storage (CCS): Technology, projects and monitoring review. Rudarsko-Geolosko-Naftni Zbornik, 33(2), 1-15.

Gautam, A., and Mondal, M. K. (2023). Review of recent trends and various techniques for CO_2 capture: Special emphasis on biphasic amine solvents. Fuel, 334, 126616.

Ge, L., Zhao, C., Chen, S., Li, Q., Zhou, T., Jiang, H., Li, X., Wang, Y., and Xu, C. (2022). An analysis of the carbonization process and volatile-release characteristics of coal-based activated carbon. Energy, 257, 124779.

Ge,L., Zhao,C., Zhou,T., Chen,S., Li, Q., Wang, X., Shen,D., Wang,Y., Xu,C. (2023). An analysis of the carbonization process of coal-based activated carbon at different heating rates. Energy, 267, 126557.

Gebald C, Wurzbacher J A, Stenfeld A, inventors; ETH Zurich . (2010). Amine containing fibrous structure for adsorption of CO_2 from atmospheric air. Patent No:WO 201009 1831 A1.

George, A., Shen, B., Craven, M., Wang, Y., Kang, D., Wu, C., and Tu, X. (2021). A Review of Non-Thermal Plasma Technology: A novel solution for CO_2 conversion and utilization. Renewable and Sustainable Energy Reviews, 135, 109702.

Ghanbari, T., Abnisa, F., and Daud, W. M. A. W. (2020). A review on production of metal organic frameworks (MOF) for CO_2 adsorption. Science of The Total Environment, 707, 135090.

Ghasemi, Z., Sourinejad, I., Kazemian, H., and Rohani, S. (2018). Application of zeolites in aquaculture industry: a review. Reviews in Aquaculture, 10(1), 75-95.

Gholidoust, A., Atkinson, J. D., and Hashisho, Z. (2017). Enhancing CO_2 adsorption via amine-impregnated activated carbon from oil sands coke. Energy and Fuels, 31(2), 1756-1763.

Gómez-Pozuelo, G., Sanz-Pérez, E. S., Arencibia, A., Pizarro, P., Sanz, R., and Serrano, D. P. (2019). CO_2 adsorption on amine-functionalized clays. Microporous and mesoporous Materials, 282, 38-47.

Gui, M. M., Yap, Y. X., Chai, S. P., and Mohamed, A. R. (2013). Multi-walled carbon nanotubes modified with (3-aminopropyl) triethoxysilane for effective carbon dioxide adsorption. International Journal of Greenhouse Gas Control, 14, 65-73.

Gunawardene, O. H., Gunathilake, C. A., Vikrant, K., and Amaraweera, S. M. (2022). Carbon Dioxide capture through physical and chemical adsorption using porous carbon materials: A review. Atmosphere, 13(3), 397.

Guo, L., Yang, J., Hu, G., Hu, X., Da Costa, H., and Fan, M. (2016). CO_2 removal from flue gas with amine-impregnated titanate nanotubes. Nano Energy, 25, 1-8.

Guo, Y., Tan, C., Wang, P., Sun, J., Yan, J., Li, W., Zhao, C., and Lu, P. (2019). Kinetic study on CO_2 adsorption behaviors of amine-modified co-firing fly ash. Journal of the Taiwan Institute of Chemical Engineers, 96, 374-381..

Gür, T. M. (2022). Carbon dioxide emissions, capture, storage and utilization: Review of materials, processes and technologies. Progress in Energy and Combustion Science, 89, 100965.

Han, Y., Hwang, G., Kim, H., Haznedaroglu, B. Z., and Lee, B. (2015). Amine-impregnated millimeter-sized spherical silica foams with hierarchical mesoporous–macroporous structure for CO_2 capture. Chemical Engineering Journal, 259, 653-662.

Hanif, A., Dasgupta, S., Divekar, S., Arya, A., Garg, M. O., and Nanoti, A. (2014). A study on high temperature CO_2 capture by improved hydrotalcite sorbents. Chemical Engineering Journal, 236, 91-99.

Haque, E., Islam, M. M., Pourazadi, E., Sarkar, S., Harris, A. T., Minett, A. I., Yanmaz E., Alshehri, S.M.,Ide, Y., Wu, K.C-W., Kaneti, Y.V., Yamauchi, Y., and Hossain, Md. S. A. (2017). Boron-functionalized graphene oxide-organic frameworks for highly efficient CO_2 capture. Chemistry–An Asian Journal, 12(3), 283-288.

Hartono Ardi, Svendsen Hallward F. 2009. Kinetics reaction of Primary and Secondary Amine Group in Aqueous Solution of Diethylenetriamine (DETA) with Carbon Dioxide. Energy Proc., 1:853-859.

Hashmi, R., and Alam, K. (2019). Dynamic relationship among environmental regulation, innovation, CO_2 emissions, population, and economic growth in OECD countries: A panel investigation. Journal of cleaner production, 231, 1100-1109.

Hatta, N. S. M., Hussin, F., Gew, L. T., and Aroua, M. K. (2023). Enhancing surface functionalization of activated carbon using amino acids from natural source for CO_2 capture. Separation and Purification Technology, 313, 123468.

Heo, Y. J., and Park, S. J. (2016). Investigation of carbon dioxide adsorption by nitrogen-doped carbons synthesized from cubic MCM-48 mesoporous silica. Carbon letters, 18(1), 62-66.

Heydari-Gorji, A., and Sayari, A. (2011). CO_2 capture on polyethylenimine-impregnated hydrophobic mesoporous silica: Experimental and kinetic modeling. Chemical Engineering Journal, 173(1), 72-79.

Heydari-Gorji, A., Belmabkhout, Y., and Sayari, A. (2011). Polyethylenimine-impregnated mesoporous silica: effect of amine loading and surface alkyl chains on CO_2 adsorption. Langmuir, 27(20), 12411-12416.

Heydari-Gorji, A., Belmabkhout, Y., and Sayari, A. (2011). Polyethylenimine-impregnated mesoporous silica: effect of amine loading and surface alkyl chains on CO_2 adsorption. Langmuir, 27(20), 12411-12416.

Heydari-Gorji, A., Yang, Y., and Sayari, A. (2011). Effect of the pore length on CO_2adsorption over amine-modified mesoporous silicas. Energy and Fuels, 25(9), 4206-4210.

Hong, S. M., Kim, S. H., and Lee, K. B. (2013). Adsorption of carbon dioxide on 3-aminopropyl-triethoxysilane modified graphite oxide. Energy and Fuels, 27(6), 3358-3363.

Huang, H. Y., Yang, R. T., Chinn, D., and Munson, C. L. (2003). Amine-grafted MCM-48 and silica xerogel as superior sorbents for acidic gas removal from natural gas. Industrial and Engineering Chemistry Research, 42(12), 2427-2433.

IEA (2021), Methane Tracker 2021, IEA, Paris https://www.iea.org/reports/methane-tracker-2021

Irani, M., Fan, M., Ismail, H., Tuwati, A., Dutcher, B., and Russell, A. G. (2015). Modified nanosepiolite as an inexpensive support of tetraethylenepentamine for CO_2 sorption. Nano Energy, 11, 235-246

Jain, P.C., (1993) Greenhouse effect and climate change: scientific basis and overview. Renewable Energy, 3(4-5), 403-420.

Ji, C., Huang, X., Li, L., Xiao, F., Zhao, N., and Wei, W. (2016). Pentaethylenehexamine-loaded hierarchically porous silica for CO_2 adsorption. Materials, 9(10), 835.

Jiang, N., Shang, R., Heijman, S. G., and Rietveld, L. C. (2020). Adsorption of triclosan, trichlorophenol and phenol by high-silica zeolites: Adsorption efficiencies and mechanisms. Separation and purification technology, 235, 116152.

Jiang, Y., Zong, P., Tian, B., Xu, F., Tian, Y., Qiao, Y., and Zhang, J. (2019). Pyrolysis behaviors and product distribution of Shenmu coal at high heating rate: A study using TG-FTIR and Py-GC/MS. Energy Conversion and Management, 179, 72-80.

Jiao, J., Cao, J., Xia, Y., and Zhao, L. (2016). Improvement of adsorbent materials for CO_2 capture by amine functionalized mesoporous silica with worm-hole framework structure. Chemical Engineering Journal, 306, 9-16.

Jiao, J., Lv, P., Wang, L., Dan, S., Qi, L., and Cui, Y. (2014). CO_2 capture of amino functionalized three-dimensional worm-hole mesostructured MSU-J silica. Journal of Porous Materials, 21, 775-781.

Jie, G., Yin, J., Zhu, F., Chen, X., Tong, M., Kang, W., Zhou, Y., and Lu, J. (2017). Postcombustion CO_2 capture using diethylenetriamine (DETA) solvent in a pilot-plant test bed compared to monoethanolamine (MEA) solvent. Environ. Progress and Sust. Energy, 36(4):1131-1138.

Jing, Y., Wei, L., Wang, Y., and Yu, Y. (2014). Synthesis, characterization and CO_2 capture of mesoporous SBA-15 adsorbents functionalized with melamine-based and acrylate-based amine dendrimers. Microporous and Mesoporous Materials, 183, 124-133.

Jo, D. H., Lee, C. H., Jung, H., Jeon, S., and Kim, S. H. (2015). Effect of amine surface density on CO_2 adsorption behaviors of amine-functionalized polystyrene. Bulletin of the Chemical Society of Japan, 88(9), 1317-1322.

Jung, H., Jeon, S., Jo, D. H., Huh, J., and Kim, S. H. (2017). Effect of crosslinking on the CO_2 adsorption of polyethyleneimine-impregnated sorbents. Chemical Engineering Journal, 307, 836-844.

Kapica-Kozar, J., Piróg, E., Kusiak-Nejman, E., Wrobel, R. J., Gęsikiewicz-Puchalska, A., Morawski, A. W., Narkiewicz, U., and Michalkiewicz, B. (2017). Titanium dioxide modified with various amines used as sorbents of carbon dioxide. New Journal of Chemistry, 41(4), 1549-1557.

Karka, S., Kodukula, S., Nandury, S. V., and Pal, U. (2019). Polyethylenimine-modified zeolite 13X for CO_2 capture: adsorption and kinetic studies. ACS omega, 4(15), 16441-16449.

Kasikamphaiboon, P., and Khunjan, U. (2018). CO_2 adsorption from biogas using amine-functionalized MgO. International Journal of Chemical Engineering, 2018, 1-8.

Khalili, S., Ghoreyshi, A. A., and Jahanshahi, M. (2013). Carbon dioxide captured by multiwalled carbon nanotube and activated charcoal: A comparative study. Chemical Industry and Chemical Engineering Quarterly/CICEQ, 19(1), 153-164.

Kim, C., Cho, H. S., Chang, S., Cho, S. J., and Choi, M. (2016). An ethylenediamine-grafted Y zeolite: a highly regenerable carbon dioxide adsorbent via temperature swing adsorption without urea formation. Energy and Environmental Science, 9(5), 1803-1811.

Kim, D. H., and Ko, Y. S. (2018). Effect of various aminosilanes functionalized inside nanoporous silica on CO_2 adsorption performance. Research on Chemical Intermediates, 44, 3661-3672.

Kim, S. N., Son, W. J., Choi, J. S., and Ahn, W. S. (2008). CO_2 adsorption using amine-functionalized mesoporous silica prepared via anionic surfactant-mediated synthesis. Microporous and Mesoporous Materials, 115(3), 497-503.

Kishor, R., and Ghoshal, A. K. (2016). High molecular weight polyethyleneimine functionalized three dimensional mesoporous silica for regenerable CO_2 separation. Chemical Engineering Journal, 300, 236-244.

Kleszyk, P., Ratajczak, P., Skowron, P., Jagiello, J., Abbas, Q., Frąckowiak, E., and Béguin, F. (2015). Carbons with narrow pore size distribution prepared by simultaneous carbonization and self-activation of tobacco stems and their application to supercapacitors. Carbon, 81, 148-157.

Knowles, G. P., and Chaffee, A. L. (2016). Aminopropyl-functionalized silica CO_2 adsorbents via sonochemical methods. Journal of Chemistry, 2016.

Knowles, G. P., Graham, J. V., Delaney, S. W., and Chaffee, A. L. (2005). Aminopropyl-functionalized mesoporous silicas as CO_2 adsorbents. Fuel Processing Technology, 86(14-15), 1435-1448.

Knutson, T., Kossin, J., Mears, C., Perlwitz, J., and Wehner, M. (2017). Detection and attribution of climate change. In: Climate Science Special Report: Fourth National Climate Assessment, Volume I. Climate Science Special Report. Washington, DC, USA, pp. 114-132.

Kommalapati, R. R., Du, H., Stewart, M. L., Shen, X., and Huque, Z. (2020). The effects of synthesis conditions on the carbon capture capacity of polyethylenimine impregnated protonated titanate nanotubes. Science of Advanced Materials, 12(2), 228-236.

Kong, X., Li, S., Strømme, M., and Xu, C. (2019). Synthesis of porous organic polymers with tunable amine loadings for CO_2 capture: balanced physisorption and chemisorption. Nanomaterials, 9(7), 1020.

Kong, Y., Jiang, G., Wu, Y., Cui, S., and Shen, X. (2016). Amine hybrid aerogel for high-efficiency CO_2 capture: Effect of amine loading and CO_2 concentration. Chemical Engineering Journal, 306, 362-368.

Koohestanian, E., Shahraki, F. (2021). Review on principles, recent progress, and future challenges for oxy-fuel combustion CO_2 capture using compression and purification unit. Journal of Environmental Chemical Engineering, 9(4), 105777.

Koornneef, J., Van Harmelen, T., Van Horssen, A., and Ramirez, A. (2011). Carbon Dioxide Capture and Air Quality. Chemistry, Emission Control, Radioactive Pollution and Indoor Air Quality, IntechOpen Book, 2011.

Köne, A. Ç., and Büke, T. (2010). Forecasting of CO_2 emissions from fuel combustion using trend analysis. Renewable and Sustainable Energy Reviews, 14(9), 2906-2915.

Krady, M., and abd, L. (2018). Global warming phenomena it's harms and causes and previntations method. Journal of Northern Europe Academy for Studies and Research, 1(1), 101-113.

Kumar, S., Himanshu, S.K., and Gupta. K.K., (2012). Effect of Global Warming on Mankind. Int. Res. J. Environment Sci. 1(4), 56-59.

Kumar, P. M., and Pooja, R. (2020). Global warming, impacts and mitigation measures: An overview. Disaster Adv, 13(5), 82-96.

Kweku, D. W., Bismark, O., Maxwell, A., Desmond, K. A., Danso, K. B., Oti-Mensah, E. A., and Adormaa, B. B. (2018). Greenhouse effect: greenhouse gases and their impact on global warming. Journal of Scientific research and reports, 17(6), 1-9.

Lai, N., Zhu, Q., Qiao, D., Chen, K., Tang, L., Wang, D., He W., Chen, Y. and Yu, T. (2020). CO_2 Capture with Absorbents of Tertiary Amine Functionalized Nano–SiO2. Frontiers in Chemistry, 8, 146.

Le, M. U. T., Lee, S. Y., and Park, S. J. (2014). Preparation and characterization of PEI-loaded MCM-41 for CO_2 capture. International journal of hydrogen energy, 39(23), 12340-12346.

Le, M. U. T., Lee, S. Y., and Park, S. J. (2014). Preparation and characterization of PEI-loaded MCM-41 for CO_2 capture. International journal of hydrogen energy, 39(23), 12340-12346.

Le, Y., Guo, D., Cheng, B., and Yu, J. (2013). Amine-functionalized monodispersed porous silica microspheres with enhanced CO_2 adsorption performance and good cyclic stability. Journal of colloid and interface science, 408, 173-180.

Lee, B. S., Bullister, J. L., Murray, J. W., and Sonnerup, R. E. (2002). Anthropogenic chlorofluorocarbons in the Black Sea and the Sea of Marmara. Deep Sea Research Part I: Oceanographic Research Papers, 49(5), 895-913.

Lee, C. H., Hyeon, D. H., Jung, H., Chung, W., Jo, D. H., Shin, D. K., and Kim, S. H. (2015). Effects of pore structure and PEI impregnation on carbon dioxide adsorption by ZSM-5 zeolites. Journal of Industrial and Engineering Chemistry, 23, 251-256.

Lee, C. S., Ong, Y. L., Aroua, M. K., and Daud, W. W. (2013). Impregnation of palm shell-based activated carbon with sterically hindered amines for CO_2 adsorption. Chemical engineering journal, 219, 558-564.

Lee, S. C., Hsieh, C. C., Chen, C. H., and Chen, Y. S. (2013). CO_2 adsorption by Y-type zeolite impregnated with amines in indoor air. Aerosol and Air Quality Research, 13(1), 360-366.

Leemans, R., and Vellinga, P. (2017). The scientific motivation of the internationally agreed 'well below 2 C'climate protection target: a historical perspective. Current Opinion in Environmental Sustainability, 26, 134-142.

Leggett, J. A. (2020). The united nations framework convention on climate change, the Kyoto protocol, and the Paris agreement: a summary. UNFCC, New York, 2.

Leung, D. Y., Caramanna, G., and Maroto-Valer, M. M. (2014). An overview of current status of carbon dioxide capture and storage technologies. Renewable and sustainable energy reviews, 39, 426-443.

Lewicka, K. (2017). Activated carbons prepared from hazelnut shells, walnut shells and peanut shells for high CO_2 adsorption. Polish Journal of Chemical Technology, 19(2), 38-43.

Li, H., Wang, K., Feng, D., Chen, Y. P., Verdegaal, W., and Zhou, H. C. (2016). Incorporation of alkylamine into metal–organic frameworks through a Brønsted acid–base reaction for CO_2capture. ChemSusChem, 9(19), 2832-2840.

Li, H., Wang, K., Hu, Z., Chen, Y. P., Verdegaal, W., Zhao, D., and Zhou, H. C. (2019). Harnessing solvent effects to integrate alkylamine into metal–organic frameworks for exceptionally high CO_2 uptake. Journal of Materials Chemistry A, 7(13), 7867-7874.

Lima, M. G. B., and Gupta, J. (2013). Studying global environmental meetings. Global Environmental Politics, 13(August), 46-64.

Lin, Y., Yan, Q., Kong, C., and Chen, L. (2013). Polyethyleneimine incorporated metal-organic frameworks adsorbent for highly selective CO_2 capture. Scientific reports, 3(1), 1859.

Lin, Z., Wei, J., Geng, L., Mei, D., and Liao, L. (2017). Adsorption of carbon dioxide by a novel amine impregnated ZSM-5/KIT-6 composite. RSC advances, 7(86), 54422-54430.

Linneen, N. N., Pfeffer, R., and Lin, Y. S. (2013). Amine distribution and carbon dioxide sorption performance of amine coated silica aerogel sorbents: Effect of synthesis methods. Industrial and Engineering Chemistry Research, 52(41), 14671-14679.

Linneen, N., Pfeffer, R., and Lin, Y. S. (2013). CO_2 capture using particulate silica aerogel immobilized with tetraethylenepentamine. Microporous and Mesoporous Materials, 176, 123-131.

Liu, F. L., Chen, S. X., and Fu, W. H. (2018). Synthesis and CO_2 adsorption behavior of amine-functionalized porous polyacrylonitrile resin. Acta Polym. Sin, 7, 886-892.

Liu, F., Chen, S., Gao, Y., and Xie, Y. (2017). Synthesis and CO_2 adsorption behavior of amine-functionalized porous polystyrene adsorbent. Journal of Applied Polymer Science, 134(28), 45046.

Liu, L., Chen, H., Shiko, E., Fan, X., Zhou, Y., Zhang, G. and Hu, X. E. (2018). Low-cost DETA impregnation of acid-activated sepiolite for CO_2 capture. Chemical Engineering Journal, 353, 940-948.

Liu, Q., Shi, Y., Zheng, S., Ning, L., Ye, Q., Tao, M., and He, Y. (2014). Amine-functionalized low-cost industrial grade multi-walled carbon nanotubes for the capture of carbon dioxide. Journal of Energy Chemistry, 23(1), 111-118.

Liu, S. H., and Sie, W. H. (2016). CO_2 Capture on Mesocellular Silica Foam Supported Amino Acid-Functionalized Ionic Liquids. Water, Air, and Soil Pollution, 227, 1-8.

Liu, S. H., Hsiao, W. C., and Chiang, C. C. (2013). Synthesis of Stable tetraethylenepentamine-functionalized mesocellular silica foams for CO_2 adsorption. Journal of Chemistry, 2013.

Liu, S. H., Wu, C. H., Lee, H. K., and Liu, S. B. (2010). Highly stable amine-modified mesoporous silica materials for efficient CO_2 capture. Topics in Catalysis, 53, 210-217.

Liu, X., Zhai, X., Liu, D., and Sun, Y. (2017). Different CO_2 absorbents-modified SBA-15 sorbent for highly selective CO_2 capture. Chemical Physics Letters, 676, 53-57.

Liu, Y., Lin, X., Wu, X., Liu, M., Shi, R., and Yu, X. (2017). Pentaethylenehexamine loaded SBA-16 for CO_2 capture from simulated flue gas. Powder technology, 318, 186-192.

Liu, Y., Lin, X., Wu, X., Liu, M., Shi, R., and Yu, X. (2017). Pentaethylenehexamine loaded SBA-16 for CO_2 capture from simulated flue gas. Powder technology, 318, 186-192.

Liu, Z., Pudasainee, D., Liu, Q., and Gupta, R. (2015). Post-combustion CO_2 capture using polyethyleneimine impregnated mesoporous cellular foams. Separation and Purification Technology, 156, 259-268.

Liu, Z., Teng, Y., Zhang, K., Chen, H., and Yang, Y. (2015). CO_2 adsorption performance of different amine-based siliceous MCM-41 materials. Journal of Energy Chemistry, 24(3), 322-330.

Lloret,J.O., Vega,L.F., Llovell,F. (2017). A consistent and transferable thermodynamic model to accurately describe CO_2 capture with monoethanolamine, J.CO_2 Utilization, 21, 521-533.

Lua, A. C., and Guo, J. (2001). Preparation and characterization of activated carbons from oil-palm stones for gas-phase adsorption. Colloids and Surfaces A: Physicochemical and Engineering Aspects, 179(2-3), 151-162.

Ma, J., Liu, Q., Chen, D., Wen, S., and Wang, T. (2014). CO_2 adsorption on amine-modified mesoporous silicas. Journal of Porous Materials, 21, 859-867.

Ma, J., Liu, Q., Chen, D., Zhou, Y., and Wen, S. (2014). Carbon dioxide adsorption using amine-functionalized mesocellular siliceous foams. Journal of Materials Science, 49, 7585-7596.

Ma, L., Bai, R., Hu, G., Chen, R., Hu, X., Dai, W and Fan, M. (2013). Capturing CO_2 with amine-impregnated titanium oxides. Energy and fuels, 27(9), 5433-5439.

Ma, R., Hu, P., Xu, L., Fan, J., Wang, Y., Niu, M., and Tao, S. (2017). Nanostructured polyethylenimine decorated palygorskite for reversible CO_2 capture. Materials express, 7(4), 253-260.

Magner, N. S., Lavin, J. F., Valle, M. A., and Hardy, N. (2020). The volatility forecasting power of financial network analysis. Complexity, 2020, 1-17.

Magner, N. S., Lavin, J. F., Valle, M. A., and Hardy, N. (2020). The volatility forecasting power of financial network analysis. Complexity, 2020, 1-17.

Mahurin, S. M., Górka, J., Nelson, K. M., Mayes, R. T., and Dai, S. (2014). Enhanced CO_2/N_2 selectivity in amidoxime-modified porous carbon. Carbon, 67, 457-464.

Mamonov N.A., Mikhailov S.A., Dzhungurova G.E., Bessudnov A.E., Grigor'ev D.A., Bedrina I.M., Mikhailov M.N. (2018). Investigation of CO_2 adsorption on amine-functionalized silicas and metal-organic polymers. Russian Chem. Bullet, 67(9): 1595-1600

Manabe, S. (2019). Role of greenhouse gas in climate change. Tellus A: Dynamic Meteorology and Oceanography, 71(1), 1620078.

Mane, S., Li, Y. X., Xue, D. M., Liu, X. Q., and Sun, L. B. (2018). Rational design and fabrication of nitrogen-enriched and hierarchical porous polymers targeted for selective carbon capture. Industrial and Engineering Chemistry Research, 57(38), 12926-12934.

Maresz, K., Ciemięga, A., Malinowski, J. J., and Mrowiec-Białoń, J. (2020). Effect of support structure and polyamine type on CO_2 capture in hierarchically structured monolithic sorbents. Chemical Engineering Journal, 383, 123175.

Martin, C. F., Sweatman, M. B., Brandani, S., and Fan, X. (2016). Wet impregnation of a commercial low cost silica using DETA for a fast post-combustion CO_2 capture process. Applied Energy, 183, 1705-1721.

Martínez, F., Sanz, R., Orcajo, G., Briones, D., and Yángüez, V. (2016). Amino-impregnated MOF materials for CO_2 capture at post-combustion conditions. Chemical Engineering Science, 142, 55-61.

Martins, V. S., Lyapustin, A., Wang, Y., Giles, D. M., Smirnov, A., Slutsker, I., and Korkin, S. (2019). Global validation of columnar water vapor derived from EOS MODIS-MAIAC algorithm against the ground-based AERONET observations. Atmospheric Research, 225, 181-192.

Mello, M. R., Phanon, D., Silveira, G. Q., Llewellyn, P. L., and Ronconi, C. M. (2011). Amine-modified MCM-41 mesoporous silica for carbon dioxide capture. Microporous and Mesoporous Materials, 143(1), 174-179.

Miaopeng Sheng , Chenxia Xie, Xiaofei Zeng, Baochang Sun, Liangliang Zhang, Guangwen Chu, Yong Luo, Jian-Feng Chen, Haikui Zou. 2018. Intensification of CO_2capture using aqueous diethylenetriamine (DETA) solution from simulated flue gas in a rotating packed bed. Fuel, 234:1518-1527.

Middleton, R. S., Yaw, S. P., Hoover, B. A., and Ellett, K. M. (2020). SimCCS: An open-source tool for optimizing CO_2 capture, transport, and storage infrastructure. Environmental Modelling and Software, 124, 104560.

Mikhaylov, A., Moiseev, N., Aleshin, K., and Burkhardt, T. (2020). Global climate change and greenhouse effect. Entrepreneurship and Sustainability Issues, 7(4), 2897.

Min, J., Yan, G., Abed, A. M., Elattar, S., Khadimallah, M. A., Jan, A., and Ali, H. E. (2022). The effect of carbon dioxide emissions on the building energy efficiency. Fuel, 326, 124842.

Mon, M., Bruno, R., Ferrando-Soria, J., Armentano, D., and Pardo, E. (2018). Metal–organic framework technologies for water remediation: towards a sustainable ecosystem. Journal of materials chemistry A, 6(12), 4912-4947.

Montagnaro, F., Silvestre-Albero, A., Silvestre-Albero, J., Rodríguez-Reinoso, F., Erto, A., Lancia, A., and Balsamo, M. (2015). Post-combustion CO_2 adsorption on activated carbons with different textural properties. Microporous and Mesoporous Materials, 209, 157-164.

Morel, R., Leguet, B., and Bellassen, V. (2013). International climate negotiations at COP 18: the art of the Doha-ble (Doctoral dissertation, auto-saisine).

Mukherjee, A., Okolie, J. A., Abdelrasoul, A., Niu, C., and Dalai, A. K. (2019). Review of post-combustion carbon dioxide capture technologies using activated carbon. Journal of Environmental Sciences, 83, 46-63.

Neira, M., Campbell-Lendrum, D., Maiero, M., Dora, C., and Bustreo, F. (2014). Health and climate change: the end of the beginning?. The Lancet, 384(9960), 2085-2086.

Nie, L., Mu, Y., Jin, J., Chen, J., and Mi, J. (2018). Recent developments and consideration issues in solid adsorbents for CO_2 capture from flue gas. Chinese Journal of Chemical Engineering, 26(11), 2303-2317.

Nigar, H., Garcia-Baños, B., Peñaranda-Foix, F. L., Catalá-Civera, J. M., Mallada, R., and Santamaría, J. (2016). Amine-functionalized mesoporous silica: A material capable of CO_2 adsorption and fast regeneration by microwave heating. AIChE Journal, 62(2), 547-555.

Obergassel, W., Arens, C., Hermwille, L., Kreibich, N., Mersmann, F., Ott, H. E., and Wang-Helmreich, H. (2018). The calm before the storm: an assessment of the 23rd Climate Change Conference (COP 23) in Bonn.

Ogungbenro, A. E., Quang, D. V., Al-Ali, K., and Abu-Zahra, M. R. (2017). Activated carbon from date seeds for CO_2 capture applications. Energy Procedia, 114, 2313-2321.

Ohashi, Y., Ogawa, T., and Egami, N. (2011). Development of carbon dioxide removal system from the flue gas of coal fired power plant. Energy Procedia, 4: 29-34.

Olabi, A. G., Obaideen, K., Elsaid, K., Wilberforce, T., Sayed, E. T., Maghrabie, H. M., and Abdelkareem, M. A. (2022). Assessment of the pre-combustion carbon capture contribution into sustainable development goals SDGs using novel indicators. Renewable and Sustainable Energy Reviews, 153, 111710.

Olajire, A. A. (2010). CO_2 capture and separation technologies for end-of-pipe applications–A review. Energy, 35(6), 2610-2628.

Ooi, Z. L., Tan, P. Y., Tan, L. S., and Yeap, S. P. (2020). Amine-based solvent for CO_2absorption and its impact on carbon steel corrosion: A perspective review. Chinese Journal of Chemical Engineering, 28(5), 1357-1367.

Öztürk B., Demiral Ş. and Aykaç Özen H., 2022. Adsorptive capture of CO_2 by amine-impregnated activated carbon, pumice, and zeolite 4A. Greehouses Gases Sci.Technol. 12:602-615.

Panda, D., Kumar, E. A., and Singh, S. K. (2019). Amine modification of binder-containing zeolite 4A bodies for post-combustion CO_2 capture. Industrial and Engineering Chemistry Research, 58(13), 5301-5313.

Park, S., Choi, K., Yu, H. J., Won, Y., Kim, C., Choi, M., Cho, S., Lee, J., Lee, S. Y., and Lee, J. S. (2018). Thermal stability-enhanced tetraethylenepentamine / silica adsorbents for high performance CO_2 capture. Ind. Eng. Chem.Res. 57(13), 4632-4639.

Patel, H. A., Byun, J., and Yavuz, C. T. (2017). Carbon dioxide capture adsorbents: chemistry and methods. ChemSusChem, 10(7), 1303-1317.

Prokopiou, M., Sapart, C. J., Rosen, J., Sperlich, P., Blunier, T., Brook, E and Röckmann, T. (2018). Changes in the isotopic signature of atmospheric nitrous oxide and its global average source during the last three millennia. Journal of Geophysical Research: Atmospheres, 123(18), 10-757.

Radu, D. R., Pizzi, N. A., and Lai, C. Y. (2016). Functionalized stellate macroporous silica nanospheres for CO_2 mitigation. Journal of Materials Science, 51, 10632-10640.

Raftery, A. E., Zimmer, A., Frierson, D. M., Startz, R., and Liu, P. (2017). Less than 2 C warming by 2100 unlikely. Nature climate change, 7(9), 637-641.

Raganati, F., Miccio, F., and Ammendola, P. (2021). Adsorption of carbon dioxide for post-combustion capture: A review. energy and fuels, 35(16), 12845-12868.

Raghuvanshi, S. P., Chandra, A., and Raghav, A. K. (2006). Carbon dioxide emissions from coal based power generation in India. Energy Conversion and Management, 47(4), 427-441.

Ramentol, E., Grimm, S., Stinzendörfer, M., and Wagner, A. (2023). Short-Term Air Pollution Forecasting Using Embeddings in Neural Networks. Atmosphere, 14(2), 298.

Rao, N., Wang, M., Shang, Z., Hou, Y., Fan, G., and Li, J. (2018). CO_2 adsorption by amine-functionalized MCM-41: a comparison between impregnation and grafting modification methods. Energy and fuels, 32(1), 670-677.

Rubin, E. S. (2012). Understanding the pitfalls of CCS cost estimates. International Journal of Greenhouse Gas Control, 10, 181-190.

Sakpal, T., Kumar, A., Kamble, S., and Kumar, R. (2012). Carbon dioxide capture using amine functionalized silica gel.

Samanta, A., Zhao, A., Shimizu, G. K., Sarkar, P., and Gupta, R. (2012). Post-combustion CO_2capture using solid sorbents: a review. Industrial and Engineering Chemistry Research, 51(4), 1438-1463.

Sanz, R., Calleja, G., Arencibia, A., and Sanz-Pérez, E. S. (2015). CO_2 capture with pore-expanded MCM-41 silica modified with amino groups by double functionalization. Microporous and Mesoporous Materials, 209, 165-171.

Sanz-Pérez, E. S., Arencibia, A., Calleja, G., and Sanz, R. (2018). Tuning the textural properties of HMS mesoporous silica. Functionalization towards CO_2 adsorption. Microporous and Mesoporous Materials, 260, 235-244.

Sanz-Pérez, E. S., Arencibia, A., Sanz, R., and Calleja, G. (2016). New developments on carbon dioxide capture using amine-impregnated silicas. Adsorption, 22, 609-619.

Sanz-Pérez, E. S., Olivares-Marín, M., Arencibia, A., Sanz, R., Calleja, G., and Maroto-Valer, M. M. (2013). CO_2 adsorption performance of amino-functionalized SBA-15 under post-combustion conditions. International Journal of Greenhouse Gas Control, 17, 366-375.

Sanz-Pérez, E. S., Rodríguez-Jardón, L., Arencibia, A., Sanz, R., Iglesias, M., and Maya, E. M. (2019). Bromine pre-functionalized porous polyphenylenes: New platforms for one-step grafting and applications in reversible CO_2 capture. Journal of CO_2Utilization, 30, 183-192.

Saravanan, A., Vo, D. V. N., Jeevanantham, S., Bhuvaneswari, V., Narayanan, V. A., Yaashikaa, P. R., Reshma, B. (2021). A comprehensive review on different approaches for CO_2utilization and conversion pathways. Chemical Engineering Science, 236, 116515.

Sarmah, M., Baruah, B. P., and Khare, P. (2013). A comparison between CO_2 capturing capacities of fly ash based composites of MEA/DMA and DEA/DMA. Fuel processing technology, 106, 490-497.

Saunois, M., Jackson, R. B., Bousquet, P., Poulter, B., and Canadell, J. G. (2016). The growing role of methane in anthropogenic climate change. Environmental Research Letters, 11(12), 120207

Sayari, A., Belmabkhout, Y., and Serna-Guerrero, R. (2011). Flue gas treatment via CO_2adsorption. Chemical Engineering Journal, 171(3), 760-774.

Schneider, T., O'Gorman, P. A., and Levine, X. J. (2010). Water vapor and the dynamics of climate changes. Reviews of Geophysics, 48(3).

Sethia, G., and Sayari, A. (2015). Comprehensive study of ultra-microporous nitrogen-doped activated carbon for CO_2 capture. Carbon, 93, 68-80.

Shafeeyan, M. S., Daud, W. M. A. W., Houshmand, A., and Arami-Niya, A. (2011). Ammonia modification of activated carbon to enhance carbon dioxide adsorption: effect of pre-oxidation. Applied Surface Science, 257(9), 3936-3942.

Sher, F., Iqbal, S. Z., Albazzaz, S., Ali, U., Mortari, D. A., and Rashid, T. (2020). Development of biomass derived highly porous fast adsorbents for post-combustion CO_2 capture. Fuel, 282, 118506.

Song, C., Liu, Q., Deng, S., Li, H., and Kitamura, Y. (2019). Cryogenic-based CO_2 capture technologies: State-of-the-art developments and current challenges. Renewable and sustainable energy reviews, 101, 265-278.

Songolzadeh, M., Ravanchi, M. T., and Soleimani, M. (2012). Carbon dioxide capture and storage: a general review on adsorbents. International Journal of Chemical and Molecular Engineering, 6(10), 906-913.

Songolzadeh, M., Soleimani, M., Takht Ravanchi, M., and Songolzadeh, R. (2014). Carbon dioxide separation from flue gases: a technological review emphasizing reduction in greenhouse gas emissions. The Scientific World Journal, 2014.

Sreedhar, I., Nahar, T., Venugopal, A., and Srinivas, B. (2017). Carbon capture by absorption–Path covered and ahead. Renewable and sustainable energy reviews, 76, 1080-1107.

Stevens, L., Williams, K., Han, W. Y., Drage, T., Snape, C., Wood, J., and Wang, J. (2013). Preparation and CO_2 adsorption of diamine modified montmorillonite via exfoliation grafting route. Chemical Engineering Journal, 215, 699-708.

Su, F., Lu, C., Kuo, S. C., and Zeng, W. (2010). Adsorption of CO_2 on amine-functionalized Y-type zeolites. Energy and Fuels, 24(2), 1441-1448.

Sulukan, E., Baran, A., Kankaynar, M., Kızıltan, T., Bolat, İ., Yıldırım, S and Ceyhun, S. B. (2023). Global warming and glyphosate toxicity (II): Offspring zebrafish modelling with behavioral, morphological and immunohistochemical approaches. Science of the Total Environment, 856, 158903.

Sun, Y., Huang, H., Vardhan, H., Aguila, B., Zhong, C., Perman, J. A and Ma, S. (2018). Facile approach to graft ionic liquid into MOF for improving the efficiency of CO_2chemical fixation. ACS applied materials and interfaces, 10(32), 27124-27130.

Tang, Q., Jiang, W., and Hu, G. (2017). Effect of amine structure on CO_2 capture performance of amine-modified SBA-15. Chemical Research in Chinese Universities, 33, 666-671.

Tang, Z., Han, Z., Yang, G., and Yang, J. (2013). Polyethylenimine loaded nanoporous carbon with ultra-large pore volume for CO_2 capture. Applied surface science, 277, 47-52.

Teng, Y., Liu, Z., Xu, G., and Zhang, K. (2017). Desorption kinetics and mechanisms of CO2 on amine-based mesoporous silica materials. Energies, 10(1), 115.

Thakkar, H., Issa, A., Rownaghi, A. A., and Rezaei, F. (2017). CO_2 capture from air using amine-functionalized kaolin-based zeolites. Chemical Engineering and Technology, 40(11), 1999-2007.

Theo, W. L., Lim, J. S., Hashim, H., Mustaffa, A. A., and Ho, W. S. (2016). Review of pre-combustion capture and ionic liquid in carbon capture and storage. Applied energy, 183, 1633-1663.

Tian, H., Pan, J., Zhu, D., Guo, Z., Yang, C., Xue, Y., Li, S., and Wang, Y. (2021). Innovative one-step preparation of activated carbon from low-rank coals activated with oxidized pellets. Journal of Cleaner Production, 313, 127877.

Timilsina, A., Bizimana, F., Pandey, B., Yadav, R. K. P., Dong, W., and Hu, C. (2020). Nitrous oxide emissions from paddies: understanding the role of rice plants. Plants, 9(2), 180.

Tiwari, S., Singh, C., and Singh, J. S. (2020). Wetlands: A major natural source responsible for methane emission. In: Upadhyay, A., Singh, R., Singh, D. (eds) Restoration of Wetland Ecosystem: A Trajectory Towards a Sustainable Environment. 52-59, Springer, Singapore.

Trenberth, K. E. (2011). Changes in precipitation with climate change. Climate research, 47(1-2), 123-138.

Tseng, R. L., Wu, F. C., and Juang, R. S. (2015). Adsorption of CO_2 at atmospheric pressure on activated carbons prepared from melamine-modified phenol–formaldehyde resins. Separation and Purification Technology, 140, 53-60.

Ullah, R., Atilhan, M., Aparicio, S., Canlier, A., and Yavuz, C. T. (2015). Insights of CO_2 adsorption performance of amine impregnated mesoporous silica (SBA-15) at wide range pressure and temperature conditions. International Journal of Greenhouse Gas Control, 43, 22-32.

Ullah, S., Bustam, M. A., Assiri, M. A., Al-Sehemi, A. G., Kareem, F. A. A., Mukhtar, A., ... and Gonfa, G. (2019). Synthesis and characterization of iso-reticular metal-organic Framework-3 (IRMOF-3) for CO2/CH4 adsorption: Impact of post-synthetic aminomethyl propanol (AMP) functionalization. Journal of Natural Gas Science and Engineering, 72, 103014..

Usman.u A. (2012) Synopsis on the Effects of Anthropogenic Greenhouse Gases Emissions from Power Generation and Energy Consumption

Vieira, R. B., Moura, P. A., Vilarrasa-García, E., Azevedo, D. C., and Pastore, H. O. (2018). Polyamine-grafted magadiite: high CO_2 selectivity at capture from CO2/N2 and CO2/CH4 mixtures. Journal of CO_2 Utilization, 23, 29-41.

Vilarrasa-García, E., Cecilia, J. A., Azevedo, D. C. S., Cavalcante Jr, C. L., and Rodríguez-Castellón, E. (2017). Evaluation of porous clay heterostructures modified with amine species as adsorbent for the CO_2 capture. Microporous and mesoporous Materials, 249, 25-33.

Vilarrasa-García, E., Cecilia, J. A., Ortigosa Moya, E. M., Cavalcante Jr, C. L., Azevedo, D. C. S., and Rodríguez-Castellón, E. (2015). "Low cost" pore expanded SBA-15 functionalized with amine groups applied to CO_2 adsorption. Materials, 8(5), 2495-2513.

Vu, Q. T., Yamada, H., and Yogo, K. (2018). Exploring the role of imidazoles in amine-impregnated mesoporous silica for CO_2capture. Industrial and Engineering Chemistry Research, 57(7), 2638-2644.

Wallenius, A. J., Dalcin Martins, P., Slomp, C. P., and Jetten, M. S. (2021). Anthropogenic and environmental constraints on the microbial methane cycle in coastal sediments. Frontiers in Microbiology, 12, 631621.

Wang, D., Wang, X., and Song, C. (2017). Comparative Study of Molecular Basket Sorbents Consisting of Polyallylamine and Polyethylenimine Functionalized SBA-15 for CO_2Capture from Flue Gas. ChemPhysChem, 18(22), 3163-3173.

Wang, J., Chen, H., Zhou, H., Liu, X., Qiao, W., Long, D., and Ling, L. (2013). Carbon dioxide capture using polyethylenimine-loaded mesoporous carbons. Journal of Environmental Sciences, 25(1), 124-132..

Wang, K., Shang, H., Li, L., Yan, X., Yan, Z., Liu, C., and Zha, Q. (2012). Efficient CO_2 capture on low-cost silica gel modified by polyethyleneimine. Journal of Natural Gas Chemistry, 21(3), 319-323.

Wang, L., and Yang, R. T. (2011). Increasing selective CO_2 adsorption on amine-grafted SBA-15 by increasing silanol density. The Journal of Physical Chemistry C, 115(43), 21264-21272.

Wang, L., Yao, M., Hu, X., Hu, G., Lu, J., Luo, M., and Fan, M. (2015). Amine-modified ordered mesoporous silica: The effect of pore size on CO_2 capture performance. Applied Surface Science, 324, 286-292..

Wang, L., Zhang, J., Tan, Z., Jiang, H., and Xiong, C. (2015). Development of ionic liquids tethered to coconut shell activated carbon for biogas upgrading in a packed bed. Energy Technology, 3(5), 509-517.

Wang, P., Scott, J. R., Solomon, S., Marshall, J., Babbin, A. R., Lickley, M and Prinn, R. G. (2021). On the effects of the ocean on atmospheric CFC-11 lifetimes and emissions. Proceedings of the National Academy of Sciences, 118(12), e2021528118.

Wang, W., Xiao, J., Wei, X., Ding, J., Wang, X., and Song, C. (2014). Development of a new clay supported polyethylenimine composite for CO_2 capture. Applied energy, 113, 334-341.

Wang, X., and Guo, Q. (2016). CO_2 adsorption behavior of activated coal char modified with tetraethylenepentamine. Energy and Fuels, 30(4), 3281-3288.

Wang, X., Chen, L., and Guo, Q. (2015). Development of hybrid amine-functionalized MCM-41 sorbents for CO_2 capture. Chemical Engineering Journal, 260, 573-581.

Wang, X., Guo, Q., and Kong, T. (2015). Tetraethylenepentamine-modified MCM-41/silica gel with hierarchical mesoporous structure for CO_2 capture. Chemical Engineering Journal, 273, 472-480.

Wang, X., Zeng, W., Zhang, H., Li, D., Tian, H., Hu, X and Liu, W. (2019). The dynamic CO_2adsorption of polyethylene polyamine-loaded MCM-41 before and after methoxypolyethylene glycol codispersion. RSC advances, 9(46), 27050-27059.

Wang, Y., and Yang, R. T. (2019). Chemical liquid deposition modified 4A zeolite as a size-selective adsorbent for methane upgrading, CO_2 capture and air separation. ACS Sustainable Chemistry and Engineering, 7(3), 3301-3308.

Wang, Y., Du, T., Qiu, Z., Song, Y., Che, S., and Fang, X. (2018). CO_2 adsorption on polyethylenimine-modified ZSM-5 zeolite synthesized from rice husk ash. Materials Chemistry and Physics, 207, 105-113.

Watabe, T., Nishizaka, Y., Kazama, S., and Yogo, K. (2013). Development of amine-modified solid sorbents for postcombustion CO_2 capture. Energy Procedia, 37, 199-204.

Wei, J., Lin, Z., He, Z., Geng, L., and Liao, L. (2017). Bagasse activated carbon with TETA/TEPA modification and adsorption properties of CO_2. Water, Air, and Soil Pollution, 228, 1-11.

Wei, J., Shi, J., Pan, H., Zhao, W., Ye, Q., and Shi, Y. (2008). Adsorption of carbon dioxide on organically functionalized SBA-16. Microporous and Mesoporous Materials, 116(1-3), 394-399.

Wei, L., Gao, Z., and Wang, Y. (2017). Integrated two-stage adsorption for selective removal of CO2 and SO2 by amine-functionalized SBA-15. Asia-Pacific Journal of Chemical Engineering, 12(4), 660-670.

Wei, X., Manovic, V., and Hanak, D. P. (2020). Techno-economic assessment of coal-or biomass-fired oxy-combustion power plants with supercritical carbon dioxide cycle. Energy Conversion and Management, 221, 113143.

Wilberforce, T., Baroutaji, A., Soudan, B., Al-Alami, A. H., and Olabi, A. G. (2019). Outlook of carbon capture technology and challenges. Science of the total environment, 657, 56-72.

Wilberforce, T., Olabi, A. G., Sayed, E. T., Elsaid, K., and Abdelkareem, M. A. (2021). Progress in carbon capture technologies. Science of The Total Environment, 761, 143203.

Williams, S. J. (2013). Sea-level rise implications for coastal regions. Journal of Coastal Research, (63), 184-196.

Wilson, I. G., and Staffell, I. (2018). Rapid fuel switching from coal to natural gas through effective carbon pricing. Nature Energy, 3(5), 365-372.

Wu, X., Liu, M., Shi, R., Yu, X., and Liu, Y. (2018). CO_2 adsorption/regeneration kinetics and regeneration properties of amine functionalized SBA-16. Journal of Porous Materials, 25, 1219-1227.

Xu, C., and Hedin, N. (2014). Microporous adsorbents for CO_2 capture–a case for microporous polymers?. Materials Today, 17(8), 397-403.

Xu, X., Song, C., Andresen, J. M., Miller, B. G., and Scaroni, A. W. (2002). Novel polyethylenimine-modified mesoporous molecular sieve of MCM-41 type as high-capacity adsorbent for CO_2 capture. Energy and Fuels, 16(6), 1463-1469.

Xu, X., Song, C., Andrésen, J. M., Miller, B. G., and Scaroni, A. W. (2003). Preparation and characterization of novel CO_2"molecular basket" adsorbents based on polymer-modified mesoporous molecular sieve MCM-41. Microporous and mesoporous materials, 62(1-2), 29-45.

Xue, B., Yu, Y., Chen, J., Luo, X., and Wang, M. (2017). A comparative study of MEA and DEA for post-combustion CO_2 capture with different process configurations. International Journal of Coal Science and Technology, 4, 15-24.

Yan, X., Zhang, L., Zhang, Y., Qiao, K., Yan, Z., and Komarneni, S. (2011). Amine-modified mesocellular silica foams for CO2 capture. Chemical Engineering Journal, 168(2), 918-924.

Yan, X., Zhang, L., Zhang, Y., Yang, G., and Yan, Z. (2011). Amine-modified SBA-15: effect of pore structure on the performance for CO_2 capture. Industrial and Engineering Chemistry Research, 50(6), 3220-3226.

Yang, H., Li, W., Liu, J., Sun, Y., and Liu, W. (2019). Polyethylenimine-impregnated resins: The effect of support structures on selective adsorption for CO_2 from simulated biogas. Chemical Engineering Journal, 355, 822-829.

Yao, M., Dong, Y., Hu, X., Feng, X., Jia, A., Xie, G and Fan, M. (2013). Tetraethylenepentamine-modified silica nanotubes for low-temperature CO_2capture. Energy and fuels, 27(12), 7673-7680.

Yaumi, A. L., Bakar, M. A., and Hameed, B. H. (2018). Melamine-nitrogenated mesoporous activated carbon derived from rice husk for carbon dioxide adsorption in fixed-bed. Energy, 155, 46-55.

Yıldız, M. G., Davran-Candan, T., Günay, M. E., and Yıldırım, R. (2019). CO_2 capture over amine-functionalized MCM-41 and SBA-15: Exploratory analysis and decision tree classification of past data. Journal of CO_2 utilization, 31, 27-42.

Yin, F., Peng, P., Mo, W., Chen, S., and Xu, T. (2017). The preparation of a porous melamine–formaldehyde adsorbent grafted with polyethyleneimine and its CO_2 adsorption behavior. New Journal of Chemistry, 41(13), 5297-5304.

Yin, F., Zhuang, L., Luo, X., and Chen, S. (2018). Simple synthesis of nitrogen-rich polymer network and its further amination with PEI for CO_2 adsorption. Applied Surface Science, 434, 514-521.

Yoo, D. K., Khan, N. A., and Jhung, S. H. (2018). Polyaniline-loaded metal-organic framework MIL-101 (Cr): Promising adsorbent for CO_2 capture with increased capacity and selectivity by polyaniline introduction. Journal of CO2 Utilization, 28, 319-325.

Younas, M., Rezakazemi, M., Daud, M., Wazir, M. B., Ahmad, S., Ullah, N., and Ramakrishna, S. (2020). Recent progress and remaining challenges in post-combustion CO_2 capture using metal-organic frameworks (MOFs). Progress in Energy and Combustion Science, 80, 100849.

Yu, J., and Balbuena, P. B. (2015). How impurities affect CO_2 capture in metal–organic frameworks modified with different functional groups. Acs Sustainable Chemistry and Engineering, 3(1), 117-124.

Yurata, T., Lei, H., Tang, L., Lu, M., Patel, J., Lim, S., ... and Li, C. E. (2019). Feasibility and sustainability analyses of carbon dioxide–hydrogen separation via de-sublimation process in comparison with other processes. International Journal of Hydrogen Energy, 44(41), 23120-23134.

Zanganeh, K. E., Shafeen, A., and Salvador, C. (2009). CO_2 capture and development of an advanced pilot-scale cryogenic separation and compression unit. Energy Procedia, 1(1), 247-252.

Zelenak, V., Halamova, D., Gaberova, L., Bloch, E., and Llewellyn, P. (2008). Amine-modified SBA-12 mesoporous silica for carbon dioxide capture: Effect of amine basicity on sorption properties. Microporous and Mesoporous Materials, 116(1-3), 358-364.

Zeleňák, V., Skřínska, M., Zukal, A., and Čejka, J. (2018). Carbon dioxide adsorption over amine modified silica: effect of amine basicity and entropy factor on isosteric heats of adsorption. Chemical Engineering Journal, 348, 327-337.

Zhang F.F., Shang H., Yang J.F., Ouyang K., Li J.P. (2017) . Ethylenediamine modified light metal aluminum-metal-organic framework material for CO_2/CH_4 separation. Chinese J. Inorg. Chem, 33(9): 1611-1617

Zhang, G., Zhao, P., Hao, L., and Xu, Y. (2018). Amine-modified SBA-15 (P): A promising adsorbent for CO_2 capture. Journal of CO_2 Utilization, 24, 22-33.

Zhang, S., Chen, C., and Ahn, W. S. (2019). Recent progress on CO_2 capture using amine-functionalized silica. Current Opinion in Green and Sustainable Chemistry, 16, 26-32.

Zhang, S., Chen, C., and Ahn, W. S. (2019). Recent progress on CO_2 capture using amine-functionalized silica. Current Opinion in Green and Sustainable Chemistry, 16, 26-32.

Zhang, T., Zhang, Y., Jiang, H., and Wang, X. (2019). Aminosilane-grafted spherical cellulose nanocrystal aerogel with high CO_2adsorption capacity. Environmental Science and Pollution Research, 26, 16716-16726.

Zhang, W., and Zhou, T. (2020). Increasing impacts from extreme precipitation on population over China with global warming. Science Bulletin, 65(3), 243-252.

Zhang, X., Qin, H., Zheng, X., and Wu, W. (2013). Development of efficient amine-modified mesoporous silica SBA-15 for CO_2capture. Materials Research Bulletin, 48(10), 3981-3986.

Zhang, Z., Ma, X., Wang, D., Song, C., and Wang, Y. (2012). Development of silica-gel-supported polyethylenimine sorbents for CO_2 capture from flue gas. AIChE Journal, 58(8), 2495-2502.

Zhao, A., Samanta, A., Sarkar, P., and Gupta, R. (2013). Carbon dioxide adsorption on amine-impregnated mesoporous SBA-15 sorbents: experimental and kinetics study. Industrial and Engineering Chemistry Research, 52(19), 6480-6491.

Zhao, P., Zhang, G., Xu, Y., Lv, Y. K., Yang, Z., and Cheng, H. (2019). Development of amine-functionalized silica foams with hierarchical pore structure for CO_2 capture. Energy and Fuels, 33(4), 3357-3369.

Zhao, X., Cui, Q., Wang, B., Yan, X., Singh, S., Zhang, F., Gao, X., and Li, Y. (2018). Recent progress of amine modified sorbents for capturing CO_2 from flue gas. Chinese Journal of Chemical Engineering, 26(11), 2292–2302.

Zhao, Y., Ding, H., and Zhong, Q. (2012). Preparation and characterization of aminated graphite oxide for CO_2 capture. Applied Surface Science, 258(10), 4301-4307.

Zhu, J., Wu, L., Bu, Z., Jie, S., and Li, B. G. (2019). Polyethyleneimine-modified UiO-66-NH2 (Zr) metal–organic frameworks: preparation and enhanced CO_2 selective adsorption. ACS omega, 4(2), 3188-3197.

Zou, Y. H., Huang, Y. B., Si, D. H., Yin, Q., Wu, Q. J., Weng, Z., and Cao, R. (2021). Porous metal–organic framework liquids for enhanced CO_2 adsorption and catalytic conversion. Angewandte Chemie, 133(38), 21083-21088.

CURRICULUM VITEA

Huda Fahad Muttaır AL-BEHADILI, graduate of Al-Zawraa Secondary School in 2005-2006, after which She obtained a bachelor's degree from the Southern Technical University, Faculty of Technical Engineering Department of Environment in 2010-2011. Then she was accepted to attend Ondokuz Mayis University. Department of Environmental Engineering Master's Program (English) for the year 2021/September. she works in the Maysan Municipalities Directorate

she communicates in two languages: English and Arabic

Contact Information :

ORCID ID :0009-0006-9557-0293

Publications :

1.Huda. F.Muttaır, Bahtiyar ÖZTÜRK, Dr.Öğr. Üyesi. Hülya AYKAÇ ÖZEN (2023) Karbondioksit Giderimindeki Yeni Gelişmeler Ve AdsorpsiyonunÖnemi. JUNE 9 - 11, 2023.